Hsc70 mediated endocytosis regulates Fgf signaling in early zebrafish development

Zur Erlangung des akademischen Grades eines

DOKTORS DER NATURWISSENSCHAFTEN

(Dr. rer. nat.)

Fakultät für Chemie und Biowissenschaften

Karlsruher Institut für Technologie (KIT) - Universitätsbereich

genehmigte

DISSERTATION

von

Charanya Rengarajan

aus

Chennai, India.

Referent: KIT Associate Fellow Dr. Steffen Scholpp

Korreferent: Prof.Dr. Martin Bastmeyer

Korreferent: Priv.-Doz. Dr. Dietmar Gradl

Tag der mündlichen Prüfung: 20.12.13

PUBLICATION

Rengarajan C, Matzke A, Reiner L, Orian-Rousseau V, Scholpp S
Endocytosis of Fgf8 Is a Double-Stage Process and Regulates Spreading and Signaling.
PLOS ONE 2014.

INDEX

ABBREVIATIONS

Fgf	Fibroblast growth factor
CME	Clathrin Mediated Endocytosis
Hsc70	Heat shock cognate protein Hsc70
HSPGS	Heparan sulfate proteoglycans
DN	Dominant negative
AP	Anteroposterior
DV	Dorso ventral
MAPK	Regulate Mitogen Activated Protein Kinases
RTKs	Receptor tyrosine kinases
FCS	Fluorescent correlation spectroscopy
CCVs	Clathrin coated vesicles
MO	Morpholino oligomer

SUMMARY

Tightly controlled concentration gradients of morphogens provide positional information and thus regulate tissue differentiation and morphogenesis in multicellular organisms. However, how such morphogen gradients are formed and maintained remains debated. In this study I show that fibroblast growth factor 8 (Fgf8) morphogen gradients in zebrafish embryos are established and maintained by two essential mechanisms. Firstly, I show that the Fgf signaling range is altered during changes in the rate of clathrin mediated endocytosis (CME). Then I show that the localization of Fgf8 is also altered during changes in the rate of CME. After this I show that after endocytosis the routing of Fgf8 from the early endosome to the late endosome is required for the termination of Fgf8 signaling. Therefore, intracellular endocytic transport may regulate the intensity and duration of Fgf8 signaling. I show that internalization of Fgf8 into the early endosome and subsequent transport towards the late endosome are two independent processes. Finally I show that Fgf signaling activity is also regulated during alterations in CME. Therefore, I hypothesize that CME regulates the Fgf propagation width and the signaling activity of the morphogen.

ACKNOWLEDGEMENTS

I would like to thank Steffen Scholpp for giving me an opportunity to work on this project in his lab. His constant support and helpful discussions kept me motivated throughout my thesis work and I am very thankful for that!

A big thanks to all the people in my lab. They have been very kind and supportive throughout my PhD in KIT and I am happy to have met such wonderful people in my life.

Thanks to Daniela Peukert and Anja Hagemann for all the helpful discussions and advises.

Special thanks to Sabrina Weber for being a great support throughout my journey as a PhD student and also for helping me a lot during the 'thesis submission' period.

Thanks to Eliana Stanganello and Bernadett Bösze for helping me with the submission of my thesis.

Thanks to Alexandra Matzke for helping me with my immunoblot experiments. I really appreciate it.

Thanks to Prof.Martin Bastmeyer and Dr. Dietmar Gradl for reviewing my thesis.

Many thanks to all my friends for always being there for me and supporting me throughout my PhD.

Finally, I would like to thank my family for their endless love, kindness and support without which this work would have never been possible!

INTRODUCTION

Developmental Biology

Developmental biology is the study of processes involved during the formation of a complex animal with different cell types, tissues and body parts from a fertilized egg. This complex process can be divided into 5 different compartments: Regional specification, Cell differentiation, Morphogenesis, Growth and Time (Slack, 2001).

Regional specification is the process of formation of heterogenous patterns from relatively homogenous cell populations. Different regions of the body, such as the head, trunk, and tail are formed with the help of cells in different regions programmed for that purpose. Initially, within the fertilized eggs, regulatory molecules also known as determinants are deposited in particular regions. Later on, in each zone of cells, different combinations of developmental control genes are upregulated with the help of intercellular signaling events.

Cell differentiation is the process by which different types of cells are formed. The variety ranging from epidermis to lymphocyte, thyroid epithelium or a neuron, there are more than 200 cell types found in a vertebrate body. Specific genes code specific proteins that endow the cell types with their unique characters.

Morphogenesis is the formation of a shape of the developing organ or organism by the movements of cells and tissues. The mechanics of the visco-elastic properties of the cells as well as the dynamics of the cytoskeleton are important for this process.

Growth is the process where the proportions of the body parts of the organism are controlled and the overall size of the organism is increased.

Time refers to the coordinated time taken for the development of an organism. Different organisms develop at different rates; however the reason is unknown and still remains a mystery.

Morphogens

Many years ago, evidence was accumulated that cells acquire informations regarding their position that prompt their development in specific ways according to their positon within the tissue (Wolpert, 1969). Later on, it was found that morphogens were responsible for this positional information and they do so by forming signalling gradients. Morphogen is defined a signaling molecule that arises from a localized source and spreads through the surrounding tissue via a concetration gradient (Green and Smith, 1991). The concept of positional information was well described by Lewis Wolpert with the help of the french flag model (Wolpert, 1969). According to his model, cells closer to the source respond differently to different threshold concentrations and therefore differentiate independantly from one another. The cell's position is defined by the concentration of the morphogen. The positional value of the morphogen yields a particular pattern due to cellular differentiation. The concept of positional information therefore provided an attractive model by combining the development as well as regulation of various patterns.

Establishment of a morphogen gradient for embryonic development

Morphogens were discovered to play the main role for formation of developmental pattern forming stable gradients across tissues (Lander, 2013). In the present models, it is stated that a signal upon release form a localized source, spreads through the surrounding tissue thereby forming a concentration gradient as shown in Figure 1.

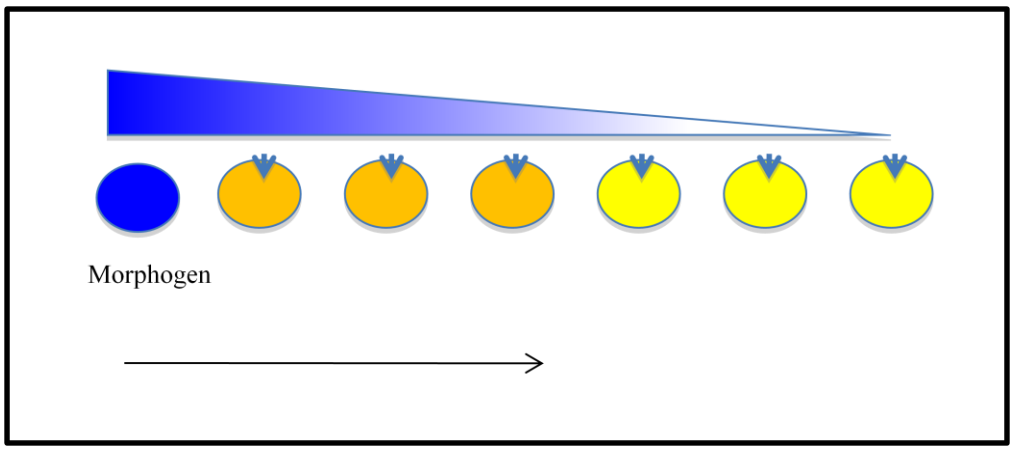

Figure 1: Morphogen gradient formation. Morphogen secreted from the source diffuses in a concentration dependent manner to the cells. The cells closer to the source receive a higher concentration and the ones further away receive lesser morphogen concentration.

The cells are acted upon by the graded signals thereby specifying changes in gene expression and cell fate decision in a concentration dependent fashion. Therefore the ligand concentration enables the cells to measure their positions with relation to the source of the signal in order to organize the pattern of cell differentiation. The signals play different roles ranging from cell identity specifications in certain tissues in Drosophila and vertebrates, to establishment of primary polarities in embryos (Ashe and Briscoe, 2006). Several signaling molecules such as Fgfs, Bone morphogenetic proteins (Bmps), Sonic hedgehog (Shh), Wnt, Transforming Growth Factor β (Tgf-β) may act as morphogens.

There are two facets to the functioning of a morphogen gradient.

1. **The formation of a concentration gradient**.

The formation of a concentration gradient depends on the morphogen identity, molecular nature and the absolute concentration of the gradient, the shape and absolute concentration as well as the maintenance of the gradient at various positions (Wolpert, 1969). Diffusion of morphogens was also shown to be responsible for the formation of a gradient. This process was shown to be influenced at various levels such as morphogen movement, signalling and trafficking by molecules such as Heparan sulfate proteoglycans (HSPGS), which are found in the extracellular space (Yan and Lin, 2009). Studies showed that for optimal functioning of a morphogen gradient, there is a requirement for a varying rate of decay. This rate of decay should be rapid at positions close to the morphogen source but significantly slower over the rest of the field. These variable decay rates were shown to be achieved when morphogens enhanced their own degradation via reciprocal interactions between the morphogen and its cellular receptor. Such a morphogen that generates its own decay is capable of generating a morphogen gradient that is not affected by inconsistancies in morphogen production at the source morphogens must be degraded (Eldar et al., 2003, Wartlick et al., 2009).

2. **Interpretation of a morphogen concentration by the cells.**

This depends on the cellular response to the different threshold concentrations of the morphogens through cell surface receptors, the transduction of the signal to the nucleus of the cell and the subsequent response at the genetic or the cellular level (Neumann and Cohen, 1997, Gurdon and Bourillot, 2001). The morphogen concentration is also interpreted by the cells through a concept known as positional information. Postional information refers to the informations the cell obtains from the local information source. This information is continously variable along an axis and on obtaining this, the cells interpret their position by developing in certain ways (Summerbell, 1979). Initial evidence in literature, on positional information, was obtained from studies on the development of the chick limb where models for positional specification along the two axes (proximo-distal and antero-posterior) were analyzed (Tickle et al., 1975). These were consistent with earlier results from positional specificational studies in Hydra and were corroborated by subsequent studies in insect limbs (Wolpert, 1971). The most significant evidence for positional signals in a developing system was seen in Drosophila embryo (Lawrence, 1992). Nüsslein-Volhard and Driever showed that a gradient in the protein Bicoid was established in Drosophila and this gradient was responsible for providing positonal information for early patterning. Above a particular threshold concentration of Bicoid, the gene *hunchback* gets activated. The activation of *hunchback* then forms a gradient thereby providing positional signals for other target genes. At high nuclear concentrations, other genes such as *snail* and *misi* are activated and they inturn play a role in the specification of the mesoderm. Positional signals have also been shown to be involved in the development of the insect wing and the vertebrate limb (D'Mello and Jazwinski, 1991). It was shown that in chick limb, patterning across the anteroposterior axis occurs due to a positional signal present at the polarizing region in the posterior margin, which specifies muscle differentiation as well as patterning of cartilage. During insect wing development, signals present at the boundary induce patterning along the anteroposterior axis, through division of the wing imaginal disc into anterior and posterior sections (Meinhardt, 1982). In vertebrate neural tube as well, positional signals were shown to pattern its stucture. Depending on the concentration, Sonic hedgehog acts on the ventral region and members of the TGF-β family act as positional signals on the dorsal region (Placzek and Furley, 1996).

There have been studies shown that cells can indeed accurately recognize certain morphogen concentrations. For example, it was shown that during the mesoderm development in Xenopus, activin played a role in the induction of mesoderm in the presumptive ectoderm. Increasing the concentrations of activin resulted in the induction of successive mesoderm tissues (Green et al., 1992). While the lowest concentration of activin resulted in the induction of haemopoietic tissue, the highest concentration gave rise to notochord. It was also shown that minor increases in the concentration of activin subsequently altered the cell's response. In the insect imaginal disc, the concentration of DPP was also shown to activate certain genes at threshold concentrations in a similar manner (Nellen et al., 1996, Lecuit et al., 1996). Although there have been some revelations on the topic of morphogen gradient formation, the exact understanding of the dynamic gradient behavior in relation to downstream interpretation resulting in the exact/correct positioning of gene expression, however, still remains as a major challenge. The morphogen concentration helps in tissue patterning through intracellular signal transductions that convert morphogen concentrations into activated transcriptional effectors.

The formation of a morphogen gradient and the subsequent signaling range has been shown to depend upon the mechanism of transportation of these morphogens (Muller et al., 2013). The following are the means through which morphogens are transported.

Morphogen Transport

There are different ways by which morphogens can be transported (Muller et al., 2013).

Free Diffusion

This refers to the dispersion of the molecules across the tissue. The movement of the morphogens is in a free manner. However this method of transportation of morphogens does not form a morphogen gradient as the morphogens are evenly spread. In order to have a gradient formed, there should be a "clearance" of morphogens, ie a rapid degradation.

Hindered diffusion

This refers to the diffusion of morphogens in a hindered manner. The hindrance maybe caused by their binding to morphogen receptors or components in the extracellular matrix (EM) (Lander et al., 2002, Baeg et al., 2004, Belenkaya et al., 2004, Han et al., 2004, Lin, 2004, Han et al., 2005, Callejo et al., 2006, Hufnagel et al., 2006, Thorne et al., 2008, Miura et al., 2009, Yan and Lin, 2009, Muller and Schier, 2011, Muller et al., 2012, Sawala et al., 2012). The hindrance may also be caused due to the dense packing of the cells in the tissue which makes the morphogens travel around them (Nicholson and Sykova, 1998, Rusakov and Kullmann, 1998, Tao and Nicholson, 2004, Thorne and Nicholson, 2006, Thorne et al., 2008).

Facilitated Diffusion

This refers to the act of mobilising an otherwise immobile morphogen by positive regulators. One such process is called shuttling. In this case, regulators called as shuttles are generated by the source that produces the morphogens. These shuttles bind to the morphogens and the complex is then diffused rapidly (Eldar et al., 2002, Mizutani et al., 2005, van der Zee et al., 2006, Ben-Zvi et al., 2011, Haskel-Ittah et al., 2012, Matsuda and Shimmi, 2012, Sawala et al., 2012).

Cytonemes

Morphogens have also been shown to be dispersed through directed delivery (Deuchar, 1970, Miller et al., 1995, Ramirez-Weber and Kornberg, 1999, Ramirez-Weber and Kornberg, 2000, Kerszberg and Wolpert, 2007, Kornberg and Guha, 2007, Wolpert, 2009, Roy and Kornberg, 2011, Kornberg, 2012). For example, filopodia (filopodial structures), have been shown to be involved in the transportation of morphogens apart from their other functions including signal detection and transport of information to the neighbouring cells (Gustafson and Wolpert, 1967, Karp and Solursh, 1985, Bentley and Toroian-Raymond, 1986, Locke, 1987, Miller et al., 1995, Jacinto et al., 2000, Vasioukhin et al., 2000, Milan et al., 2001, Renaud and Simpson, 2001, Sato and Kornberg, 2002, Wolf et al., 2002, De Joussineau et al., 2003, Gallo and Letourneau, 2004, Yuste and Bonhoeffer, 2004, Lehmann et al., 2005,

Demontis and Dahmann, 2007, Kress et al., 2007, Cohen et al., 2010, Swaney et al., 2010, Callejo et al., 2011, Cohen et al., 2011, Inaba et al., 2012, Peng et al., 2012, Rojas-Rios et al., 2012).

This patterning of a tissue can either directly correlate with the morphogen gradient or can also be altered due to mechanisms such as amplification/feedback as well as intracellular trafficking (Paulsen et al., 2011, Dessaud et al., 2010). Also for the maintanence of such a gradient, morphogens need to be degraded at a constant rate (Muller and Schier, 2011, Wartlick et al., 2009, Muller et al., 2013). This study intends to analyze the factors involved in the regulation of one such morphogen Fgf and the effect on its signaling range and activity. For this study I have used zebrafish as a model organism.

Zebrafish as a model organism

Zebrafish (Danio rerio), is a tropical fresh water fish that is typically found in the rivers of Bhutan, Nepal, northen Pakistan and northern India in Southern Asia. The species, belonging to the Cyprindae family, acquired its name due to the charecteristic stripes found along the fins and the body (Stephanie et al., 2006). Over the past decade, the use of zebrafish as a model organism has expedited due to its special characteristics.

Due to the evolutionarily conserved nature of gene programming and molecular processes, gene expression studies conducted in zebrafish can be reliably extrapolated to further vertebrates, thereby making zebrafish a very good model for these studies (Hill et al., 2005). Unlike other fish species, the adult zebrafish is approximately 3-5cm in length and therefore are easily managible in the laboratory even in large numbers (Kishi et al., 2003). The small larval and adult zebrafish size helps in cost reduction as this reduces husbandry costs as well as the housing space. The small size allows for easy statistical evaluation and validation of results as they can be analyzed using high throughput methods such as multi-well plates (Hill et al., 2005). Over the past decade, the use of zebrafish as a model organism has been expedited due to its special characteristics.

Zebrafish development is highly comparable to the embryonic development in other vertebrates such as humans. However, unlike mammals, the development of an adult zebrafish from a fertilized egg takes place outside the female. The embryos are transparent during the initial development taking place the first few days which makes analysis of zebrafish during development a much easier process (Wixon, 2000). Zebrafish embryonic development takes place at a fast rate. All major organs develop in the first 24 hours. Zebrafish are sexually mature and can produce new offsprings after three to four months. A single female lays around 200 eggs per week (Stern and Zon, 2003). As zebrafish achieves sexual maturity at around 100 days, they are also an attractive model for conducting transgenerational studies (Hill et al., 2005).

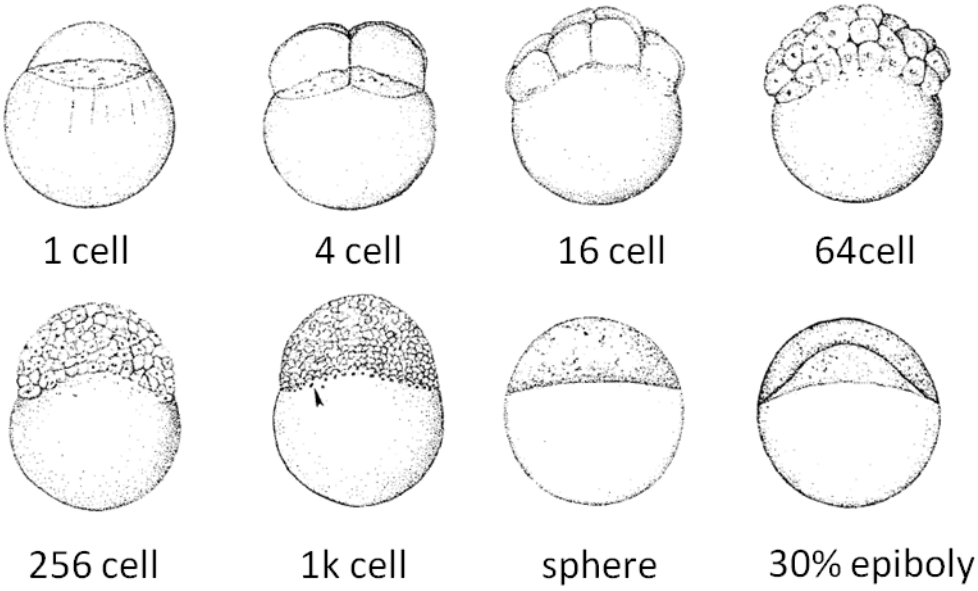
1 cell
4 cell
16 cell
64cell
256 cell
1k cell
sphere
30% epiboly

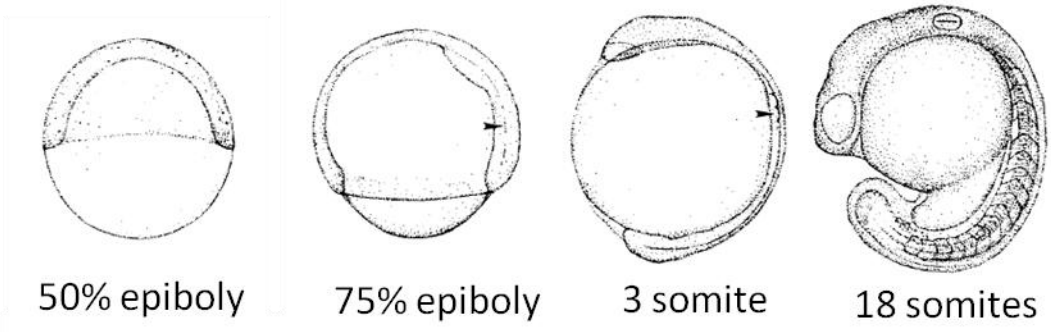
50% epiboly
75% epiboly
3 somite
18 somites

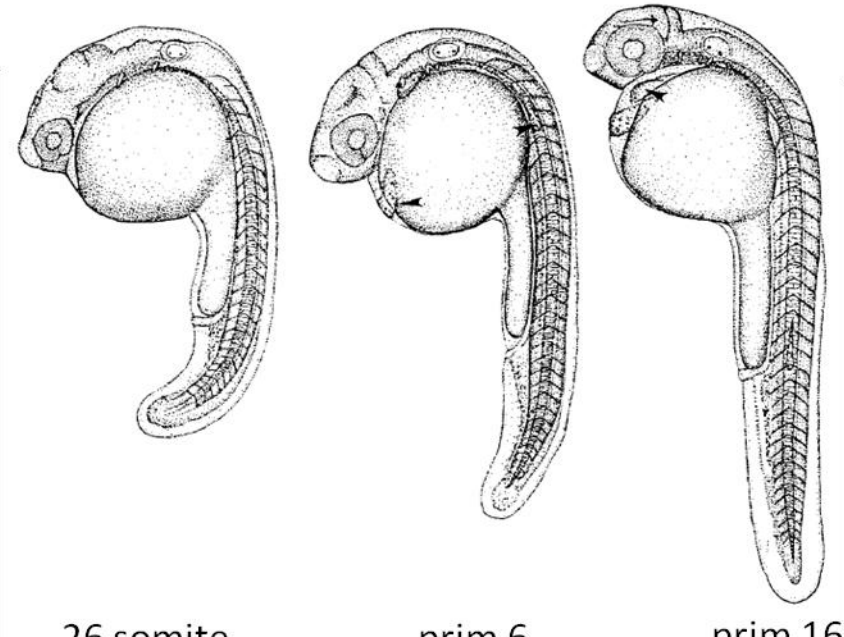
26 somite
prim 6
prim 16

Figure 2: Development of zebrafish at different stages. Kimmel et al., 1995, modified.

A morphological and histological description of embryonic development of zebrafish has been well established as shown in Figure 2 (Kimmel et al., 1995). The zebrafish eggs and the embryos are transparent during the first day. Pigmentation occurs at around 30-72 hours post fertilization. Morphological changes within the early stages of development can therefore be easily analysed under the microscope. Prevention of pigmentation is possible *in vivo*, by treating the embryos with 0.003% phenylthiourea (PTU). This further enables extended time for observation. Since the development takes place outside the body of the mother, it is also easy to follow the developmental stages. This is different from mammals where the embryos need to be harvested. Despite exhibiting organ dysfunction and major morphological changes, mutant zebrafish embryos are able to survive beyond the time at which the normal organs in healthy zebrafish are expected to start functioning. This characteristic is not usually noticed in other model organisms including rodents (Hill et al., 2005). Due to these special characteristics, zebrafish is now a popular model organism for studying the roles of specific genes and signaling pathways during development (Spitsbergen and Kent, 2003).

FGF signaling

One of the major signaling pathways in invertebrates and vertebrates is the Fgf signaling pathways.

Structure and signal transduction

The Fgf family of proteins in humans, comprises of 22 members that share a high-sequence homology within a central core domain of 120 amino acids and possess a high affinity for heparin (Ornitz and Itoh, 2001, Eriksson et al., 1991, Plotnikov et al., 2000). Their biological responses are induced when Fgfs bind and activate Fgfrs that belong to the family of receptor tyrosine kinases (RTKs). The Fgfr gene family in vertebrate contains four related genes, Fgfr1–4 (Johnson and Williams, 1993). The structure of Fgf protein comprises of a conserved core region containing receptor as well as HSPG binding sites. Fgf receptor consists of an acidic box, a heparin binding domain, Ig domains, CAM-homolgy domains (CHD), split tyrosine kinase domain and a transmembrane domain (Cotton et al., 2008).

Fgfr signal transduction

Fgfrs, after binding to the ligands, via tyrosine phophorylation transmit extracellular signals to several cytoplasmic signal transduction pathways. This tyrosine phosphorylation by receptors is a role similar to other RTKs.

Formation of the ligand receptor complex leads to the dimerization of the receptor which targets the activation of tyrosine kinase and subsequent autophosphorylation of the intracellular domain (McKeehan et al., 1998). Apart from controlling the protein tyrosine kinase activity, tyrosine phosphorylation of the receptor is also required for the assembly and recruitment of signaling complexes (Schlessinger, 2000). There are three main signaling pathways through which Fgf signal transduction could occur.

Ras/MAPK pathway

Mitogen Activated Protein Kinases (MAPK) pathway is the most common pathway through which Fgfs function.The first step involved in the MAPK pathway is the constitutive binding of the lipid anchored docking protein FRS2 to Fgfr1.This process of receptor protein binding could also occur without the receptor activation (Wang et al., 1996). Upon Fgfr activation, FRS2 undergoes tyrosine phosphorylation and this is then recognized and bound to by the growth receptor bound protein (Grb2) and the protein tyrosine phophatase (PTP) Shp2 (Kouhara et al., 1997, Hadari et al., 2001). Grb2 binds to guanine nucleotide exchange factor Son of Sevenless (SOS), through its SH3 domain. Grb2-SOS translocation to the plasma membrane upon binding to the phosphorylated FRS2 leads to the activation of Ras SOS through GTP exchange. The now active Ras, activates the MAPK signaling cascade by interacting with several effector proteins such as Raf. The activation of the MAPK signaling cascade leads to the phosphorylation of the target transcription factors such as members of the ETS family of transcription factors, AP1 and c-myc (Lee and McCubrey, 2002).

PI3 kinase/Akt pathway

Fgfrs activate PI3 kinase/Akt pathway via three separate routes. The indirect binding of Gab1 through Grb2 to FRS2 results in the activation of PI3/Akt pathway via PI3 kinase-regulatory subunit p85 (Hadari et al., 2001). Secondly, the pathway could be activated due to the binding of p85 to a phophorylated tyrosine residue of FGFR (Ryan et al., 1998). Thirdly, it could be triggered by activated Ras that can localize and activate the p110 catalytic subunit of PI3 kinase (Rodriguez-Viciana et al., 1994).

PLCγ/Ca2+ pathway

The PLCγ/Ca2+ pathway is triggered when PLC binds to the phosphorylated tyrosine 766 of Fgf receptor1 (Fgfr1) (Mohammadi et al., 1992). Activation of PLC leads to the hydrolysis of phosphatidylinositol-4, 5-diphos- phate to inositol-1, 4, 5-triphos- phate and diacylglycerol. The release of intracellular calcium is stimulated by inositol-1, 4, 5-triphosphate whereas protein kinase C is activated by diacylglycerol (Doherty and Walsh, 1996).

Function of Fgf signaling

Fgf signaling has been shown to be a crucial requirement for several biological processes. Their roles involve regulation of cell migration, differentiation and cell survival. Loss or gain of Fgf signaling leads to several diseases and defects related to embryonic development.

Role of Fgf in embryonic development

Regulation of embryonic development

Cell migration

The effect of Fgf on embryonic development is evolutionarily conserved. In mice, individual knock-outs of various Fgf ligands and Fgfrs, Fgf8, Fgf4, Fgfr1, Fgfr2 showed embryonic lethality. Fgf8 and Fgr1 knock-outs also showed defects in cell migration (Feldman et al., 1995, Goldin and Papaioannou, 2003, Meyers et al., 1998, Sun et al., 1999, Yamaguchi et al., 1994, Deng et al., 1994, Ciruna et al., 1997, Arman et al., 1998). Analysis of chimeric mice that contain DN-Fgfr1 cells displayed a characteristic inability to migrate away from the primitive streak (Ciruna et al., 1997). In Xenopus, expression of DN mutant of Fgfr4 showed blockage of anterior neural induction and repression of posterior neural induction (Hongo et al., 1999, Hardcastle et al., 2000). In sea urchin, the ligand FgfA and its receptor Fgfr2 play a critical role in the migration of the primary mesenchymal cells (Rottinger et al., 2008). This is also observed in Drosophila, where Fgfr2 gene heartless mutation lead to an impairment of mesodermal cell migration away from the midline during gastrulation (Beiman et al., 1996, Gisselbrecht et al., 1996). In mice, during gastrulation, mutant mouse for Fgfr1 and Fgf8 show critical impairements in cell migration (Deng et al., 1994, Sun et al., 1999, Yamaguchi et al., 1994). These results suggest that Fgf signaling is required for proper cell migration.

Gastrulation

Xenopus embryos over expressed with DN Fgfr1 showed failure in gastrulation movements (Amaya et al., 1991). Injection of Fgf8 morpholino disrupted the process of gastrulation (Fletcher et al., 2006).

Patterning

In zebrafish, injection of DN-Fgfr1 showed loss of trunk and tail as well as loss of no tail 1 (ntl1) expression (Griffin et al., 1995), whereas DN-Fgfr3 injection resulted in the loss of notochord as well anteroposterior (AP) patterning defects (Ota et al., 2009). Treatment with the antagonist of Fgf receptor, SU5402, showed a reduced expression of mesodermal markers. In these SU5402 treated embryos, axial and paraxial mesoderm were inhibited (Fletcher and Harland, 2008). In Xenopus, expression of DN-mutant of Fgfr1 leads to abnormal mesoderm specification as well as loss of trunk and tail (Amaya et al., 1991, Amaya et al., 1993). Fgf8 knockdown in zebrafish showed an inhibition in the formation of posterior neuronal tissue (Fletcher et al., 2006) and displayed defects in somitogenesis, midbrain-hindbrain boundary (MHB) maintenance and in left right (L/R) axis specification (Reifers et al., 1998, Albertson and Yelick, 2005). In addition to these symptoms, Fgf8 mutants also displayed loss of posterior mesoderm (Reifers et al., 1998). This suggests that Fgf signaling is required for the posteriorization of the tissue.

Axis specification

Anteroposterior (AP) patterning

Fgfs have been shown to be involved in the anteroposterior (AP) patterning in Xenopus, zebrafish, chick and mouse (Amaya et al., 1991, Christen and Slack, 1999, Davidson et al., 2000, Draper et al., 2003, Griffin et al., 1995, Isaacs et al., 1994, Isaacs et al., 1992, Ota et al., 2009, Partanen et al., 1998, Storey et al., 1998, Xu et al., 1999). At the time of the AP patterning of the neural plate, Fgfs were shown to act as strong factors for posteriorization. The anterior neural tissue could be transformed to more posterior neural cell types by the Fgfs (Lamb and Harland, 1995, Cox and Hemmati-Brivanlou, 1995).

In Xenopus, Fgf soaked beads that were placed in the anterior neural pate inhibited the expression of the anterior neural marker (Pownall et al., 1996). This was later on suggested to occur due to cross-talk with the Wnt signaling pathway (McGrew et al., 1997). The AP axis patterning by Fgf signaling was also shown to occur in all three germ layers (Cox and Hemmati-Brivanlou, 1995, Dessimoz et al., 2006, Lamb and Harland, 1995, Partanen et al., 1998, Pownall et al., 1996, Wells and Melton, 2000, Xu et al., 1999). In zebrafish, Fgf3 overexpression resulted in a similar expansion of the posterior neural tissue (Koshida et al., 2002). However, DN-Fgfr1 as well as DN Ras inhibited posterior neural marker induction (Ribisi et al., 2000, Holowacz and Sokol, 1999). The patterned expression of the Homeobox (*Hox*) genes, transcriptional regulators that control embryonic morphogenesis, across the AP axis of the embryo, was then associated with the patterning of the neuroectoderm and mesoderm was then associated with the patterned expression of Homeobox (*Hox*) genes across the AP axis of the embryo. Hox genes are transcriptional regulators that control embryonic morphogenesis (Krumlauf, 1994, Akin and Nazarali, 2005). Further studies showed that the early AP patterning in mouse, chick and Xenopus, was regulated by Fgf signaling through the regulation of *Hox* genes (Krumlauf, 1994). Overexpression of Fgfs showed an increase in the expression of the posterior members of the *Hox* family of genes (Pownall et al., 1996, Partanen et al., 1998). However, overexpression of DN Fgfr1 resulted in a suppressed expression of *Hox* gene (Pownall et al., 1996). In chick, Fgfs were shown to adopt a different mechanism of action as a posteriorizing agent. In the chick neural tube, Fgfs were found to moderate neural stem cell maintenance at Henson's node. Hence, it was suggested that Fgfs may promote the continuous development of the posterior nervous system by prolonging the average time to which the cells were exposed to other posteriorizing agents, like Wnts or retinoic acids (Mathis et al., 2001). The AP patterning of the embryo is not performed by Fgf signaling alone. The AP axis is established through cross talks between several signaling molecules, Wnts and retinoic acid (RA) (Bayha et al., 2009, Blumberg et al., 1997, Durston et al., 1989, Kiecker and Niehrs, 2001, McGrew et al., 1995, McGrew et al., 1997, Sive et al., 1990, Takada et al., 1994).

Dorso-ventral (DV) patterning

Fgf signaling has also been shown to be required for DV axis specification. In Xenopus, Fgfs were shown to be involved in the specification of the DV axis of the embryo (Kumano and Smith, 2000, Kumano et al., 2001, Kumano and Smith, 2002). Fgf signaling was also shown to regulate MAPK activity resulting in the expression of MAPK in an animal vegetal pattern (Curran and Grainger, 2000, Christen and Slack, 1999, Kumano et al., 2001). Injection of DN-Fgfr in contraorganizer marginal zone resulted in the loss of the caudal somites. Fgf signaling was shown to direct cells towards dorsal fates in the animal region of the marginal zone (Kumano and Smith, 2002). This would explain the reason why Fgf4, Fgf8 and Fgf20 were found to express in the animal region of the marginal zone and was absent in the vegetal region of the marginal zone (Christen and Slack, 1999, Isaacs et al., 1992, Lea et al., 2009). However, this DV patterning of the embryo is not performed by Fgf signaling alone. Wnt-β catenin signaling pathway and BMP signaling pathway were shown to be primarily required for the formation of the axis (De Robertis, 2009, Little and Mullins, 2006, Schier and Talbot, 2005, Weaver and Kimelman, 2004). In zebrafish, dorso-ventral (DV) patterning was observed to be altered during ectopic Fgf8 expression, suggesting the role of Fgf8 in the formation of dorsal ventral patterns (Furthauer et al., 1997). Figure 3, shows an overview of the diffferent roles of Fgf during embryonic development.

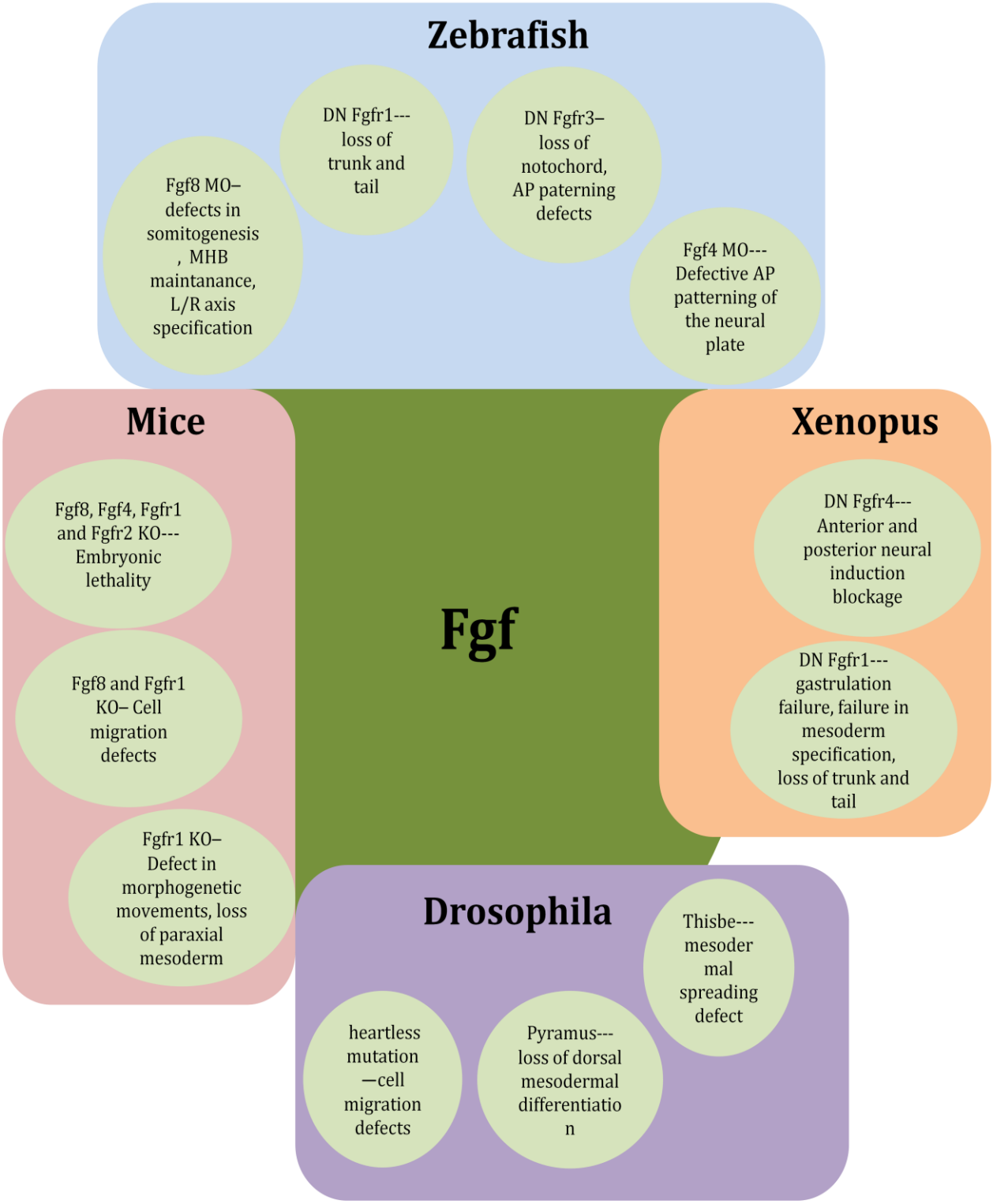

Figure 3: **An overview of the roles of Fgf during embryonic development**

Human pathologies related to Fgf signaling

Studies analyzing the importance of Fgf signaling showed that alteration of the signaling resulted in a numerous number of diseases both pathological as well as congenital in humans. Increase in the expression of Fgf2/Fgf6, Fgf19, Fgf23 lead to prostate cancer, Liver, colon and lung carcinomas as well as osteomalacia respectively. Loss of function of Fgf3,8,9,10,14,23 lead to deafness, Kallman syndrome, colorectal, endometrial and ovarian carcinomas, aplasia of lacrymal and salivary glands, non-syndromic cleft lip and palate, hearing loss, spinocerebellar ataxia, and Familial tumoural calcinosis (FTC) respectively. Increase in Fgfr1 can lead to breast, ovarian and bladder cancers whereas increase in Fgfr2 can lead to gastric and breast cancers (Beenken and Mohammadi, 2009, Krejci et al., 2009, Turner and Grose, 2010, Wilkie, 2005).

Fgf8

Fgf8 is one member of the Fgf family with key inductive functions during development of neural ectoderm, mesoderm and limb formation (Meyers et al., 1998, Reifers et al., 1998, Draper et al., 2003, Martin, 2001, Scholpp et al., 2003, Esain et al., 2010). In mice, loss of Fgf8 function, lead to lethality in embryos as well as cell migration defects during gastrulation (Meyers et al., 1998, Sun et al., 1999). In Xenopus, knock-down of Fgf8 showed reduced paraxial mesoderm, hindbrain and spinal cord, whereas knock-down of Fgf8a lead to lesser formation of posterior neuronal tissue (Fletcher et al., 2006). In zebrafish, Fgf8 mutants showed L/R axis specification defects, defects in the maintenance of MHB and somitogenesis as well as defects in formations of posterior mesoderm (Fletcher et al., 2006, Draper et al., 2003, Reifers et al., 1998, Albertson and Yelick, 2005). Fgf8 performs its functions mainly through the activation of Fgfr1 and Fgfr3 (Scholpp and Brand, 2004, Kataoka and Shimogori, 2008, Mott et al., 2010). Fgf8 was shown to be responsible for the autoregulation of the gene expression its two cognate receptors Fgfr1 and Fgfr3 although this was a cell type specific occurance (Mott et al., 2010).

Fgf8 expression in zebrafish

In the dorsal margin of the zebrafish embryo, cells displayed an accumulation of Fgf8 transcripts at the sphere stage immediately after the midblastula transition. This marginal expression was seen to quickly expand to additional ventral cells at the start of epiboly, and the presence Fgf8 RNA was observed all around the margin. At the start of the gastrulation stage, Fgf8 transcripts were observed to be restricted at the dorsal part of the marginal region and *fgf8* expression was observed at the margin of zebrafish embryos in a typical dorsal ventral gradient. Cells expressing Fgf8 were not oberved in the hypoblastic deep cells which would later become the prechordal plate. However, the outward epiblast layer cells of the embryonic shield contained cells expressing Fgf8. Towards the course of gastrulation, the marginal domain of *fgf8* expression was restricted to the epiblastic cells that were in direct contact with the inward hypoblast. Apart from this, in the dorsal part of the embryo, Fgf8 was also observed in the paraxial hypoblast region. At the beginning of 70% epiboly towards somitogenesis stages, Fgf8 transcripts were also observed in the epiblast layer. During somitogenesis, *fgf8* expression was then observed in the anterior forebrain, rhombomeres 1, 2 and 4 as well as the epiphysis and in the anterior somatic border. *fgf8* expression was closely associated with signaling centres such as the facial ectoderm, tail bud, the apical ectodermal ridge of the fin bud and the mesencephalon-telencephalon junction which is similar to chick embryos and mice (Furthauer et al., 1997, Reifers et al., 1998)**.**

Fgfs as morphogens

Fgfs, as they are secreted growth factors, have the ability to function as morphogens. Therefore they form concentration gradients through the taget tissue hence providing spatial information which is relative to the source, to individual cells (Wolpert, 1969). The main evidence for the role of Fgfs as morphogens in zebrafish development arises from its ability in the patterning of the brain as well as the dorso ventral axis. During gastrulation in zebrafish, two sources, the anterior hindbrain anlage and the blastoderm margin secrete Fgf ligands (Furthauer et al., 1997, Reifers et al., 1998). The target genes are expressed around these sources upon activation of Fgf signaling (Furthauer et al., 2004, Roehl and Nusslein-Volhard, 2001, Raible and Brand, 2001). Altered Fgf levels result in a differential target gene response thereby suggesting that the expression of the target genes is dose dependent (Furthauer et al., 2004, Scholpp and Brand, 2004). Activation of Erk by Fgf over several cell

diameters away from its source suggested that Fgfs can diffuse over a certain distance from its source (Christen and Slack, 1999). Quantification of the protein concentration of Fgf8-EGFP from a restricted source showed that the protein concentration decreased with increasing distance from the source. This confirmed the theory of the establishement of a gradient in the tissue by Fgf8. Fluorescent correlation spectroscopy (FCS) studies also showed that this along with the ability of Fgf8 to diffuse freely through the tissue and the internalization of Fgf8 through receptor mediated endoctyosis were responsible for the maintanence of a Fgf8 gradient (Yu et al., 2009). FCS studies also showed that an increase in the endocytic activity, lead to a steepening of the Fgf8 gradient and a decrease in the endocytic activity lead to a flattening of the gradient slope. Endocytic sorting through regulation of ubiquitin ligase Cbl, was also shown to be responsible for the modulation of Fgf8 morphogen gradient interpretation (Nowak et al., 2011).

Regulation of Fgf morphogen gradient by endocytosis

Analysis of uptake of Fgfs revealed that the Fgfrs internalization took place via Clathrin Mediated Endocytosis (CME). This process of receptor internalization via CME was ligand dependent. Further analysis showed that increase in the rate of Fgfrs endocytosis may result in a decrease in the availablilty of receptor bound ligand at the cell surface (Bokel and Brand, 2013, Auciello et al., 2013, Lin et al., 2012). Alteration in the internalization and spreading of chemically labelled Fgf8 through manipulation of the endocytic rates, and the subsequent effects of this on the marker gene expression confirms the theory of Fgf8 function as a restrictive clearance model (Scholpp and Brand, 2004). Analysis of Fgf8 gradient in live zebrafish embryos using FCS showed the requirement of a degradation term corresponding to the increased Fgf8 internalization (Yu et al., 2009). Blockage of endocytosis by overexpressing DN-dynamin2 mutant resulted in an increased lifetime of extracellular Fgf8, a shallower Fgf8 gradient, as well as an expansion in the target gene expression domains. However, early endosomal protein Rab5c overexpression reduced the extracellular ligand lifetime and formed steeper transcriptional response as well as the Fgf8 gradient (Lin et al., 2012).

Clathrin Mediated Endocytosis (CME)

CME is initiated by the process of coat nucleation mediated by phosphatidylinositol(4,5)-bisphosphate, PI(4,5)P2 and the recruitment of assembly protein (AP-2) which is cargo dependent. AP-2, a heterotetrameric adaptor complex functions by linking various cargo to the accessory proteins, the clathrin coat as well as other adaptors. Clustering of the cargo molecules takes place in the emerging pit and membrane invagination occurs with the help of BAR (Bin–Amphiphysin–Rvs) domain containing proteins. After the membrane invagination and coat assembly, GTPase dynamin is recruited to the neck of the growing vesicle and catalyzes vesicle fission. At this time, membrane scission occurs with dynamin acting together with SH3 domain containing proteins. During the process of vesicle uncoating, RAB5, a small GTPase that plays a role in early endosome docking, fusion, as well as the transport to early endosomes, maybe recruited by the primary endocytic vesicles. Then, in a process that requires early endosomal SN**A**P (Soluble NSF Attachment Protein) Receptor (SNAREs) and RAB5 effector proteins, primary endocytic vesicles fuse with early endosomes that express phosphatidylinositol(3)-phosphate, PI(3)P. At the level of clathrin coated pits, the beginning of cargo sorting for late endosomal-lysosomal degradation, (requires RAB7), or recycling (requires RAB11 and possibly RAB4) occurs and this process is then completed at the early endosomal subdomains (Wieffer et al., 2009).

Vesicle formation is followed by the dissociation of clathrin coats from clathrin coated vesicles (CCVs), which can then be reutilized for the further endocytic processes (Schlossman et al., 1984, Chappell et al., 1986, Chang et al., 2002). In 1984, 70kDa polypeptide was found to be involved in the dissociation of clathrin coats in an ATP dependent manner and hence named the uncoating ATPase. This uncoating activity was detected in yeast, Drosophila Kc cells, Chinese hamster ovary cells, primary chick embryo fibroblasts and the cytoplasmic matrix from rat and bovine liver. The 70 kDa uncoating ATPase was later found to be a member of the heat shock family of proteins and was named Hsc70. Members of the heat shock family of proteins, apart from clathrin diassembly, are also involved in many ATP hydrolysis dependent cellular processes such as translocation of proteins acrosss membranes, folding of polypeptides and together with other chaperones, glucocorticoid receptor activation. *In vitro,* Hsc70 binds to clathrin, and disrupts the clathrin

cage through ATP hydrolysis thereby promoting the release of the clathrin triskelions from CCVs (Schlossman et al., 1984, Hannan et al., 1998).

Hsc70 has intrinsically low ATPase activity which is similar to the other members of its family. This ATPase activity is stimulated by cofactors (Ungewickell et al., 1995, Bukau and Horwich, 1998). One such cofactor involved in the uncoating process is Auxilin. Auxilin is a nerve specific protein that belongs to the Dnaj protein family and contains a conserved J-domain motif. Auxilin also contains a clathrin binding domain, indicating that the ATP-bound Hsc70 is recruited by Auxilin via its J domain after it binds to the CCVs (Ungewickell et al., 1995, Holstein et al., 1996). Auxilin binds to Hsc70 with the help of this HPD motif (Ahle and Ungewickell, 1990, Ungewickell et al., 1995). After the discovery of Auxilin as a co-chaperone, another member belonging to the auxilin family was also shown to be involved in the uncoating process. Cyclin G associated kinase, referred to as GAK or Auxilin-2 was found to be ubiquitously expressed (Kanaoka et al., 1997, Umeda et al., 2000). The research that followed through the years supported the importance of Hsc70 in CME. DN-mutants of Hsc70, even when present at higher concentrations, failed to efficiently remove clathrin from CCVs suggesting the necessity of ATPase cycling for CCV uncoating by Hsc70. Increased co-localization of internalized ligand and clathrin in addition to accumulation of coated pits at the cell surface were observed after microinjection of anti-Hsc70 antibody. To further validate the role of Hsc70 in the uncoating of CCVs, Transferrin uptake and recycling was analyzed as the result of defects in uncoating of the CCVs would be alteration in cellular uptake and sorting. The mutant expressing cells showed defects in endocytosis and recycling of Transferrin. These studies provided additional evidence for the effect of Hsc70 on CCV disassembly and the subsequet effects on endocytosis and cellular sorting (Newmyer and Schmid, 2001).

Aim of this study

Gradients of signaling molecules or morphogens have been shown to be responsible for tissue patterning and morphogenesis during embryonic development (Stumpf, 1966, Wolpert, 1969, Crick, 1970). This study focusses on one such morphogen Fibroblast Growth Factor (Fgf), which plays an important role in the control of morphogenetic movements, somitogenesis, anteroposterior patterning, induction, maintenance of mesoderm and neuroectoderm, and the development of various organs (Bottcher and Niehrs, 2005, Itoh, 2007, McIntosh et al., 2000) during embryonic development and maintenance and the effect of endocytosis on the signal transduction as well as its diffusion through the tissues. I start by introducing the morphogens and the importance of a morphogen gradient formation during embryonic development. I then introduce the model system used during this study. I evaluate the role of CME in the development and regulation of these morphogen gradients via diffusion. I analyze the role of Heat shock cognate protein (Hsc70), a critical CME regulator in this development and maintenance of morphogen gradients. The Fgf signaling range was analyzed during changes in the rates of CME through loss and gain of Hsc70 function. For this, the expression of Fgf target genes was studied. The localization and spreading of the Fgf8 was also investigated during Hsc70 functional studies. Apart from this, the activity of Fgf signaling during CME was also evaluated.

Materials and Methods

Materials

Equipment and Tools

PCR machine	9700, 96 well-plate (Applied Biosystems)
Photometer	NanoDrop (Thermo Scientific Inc.)
Microscopes	Olympus SZX10 / SZX16 ZEISS Axiophot Trinocular LEICA SP5 X confocal microscope
Microinjector	FemtoJet, with integrated pressure supply (Eppendorf)
Needle holder	Microelectrode holder (WPI Inc.)
Needle puller	P-97 Flaming/Brown Micropipette Puller (Sutter Instrument)
Glass needle .	1.0mm outer diameter, 0.58mm inner diameter, with filament (TW100,WPI Inc.)
Micro- manipulator	Manual, M3301R (WPI Inc.)
Microloader Pipette Tips	930001007 (Eppendorf)
Dissection forceps	Fine tip No.5 (Dumont)
Tungsten needle	TGW1510, Ø 0.38 mm (WPI Inc.) 30

Agar plates and culture media

LB (Luria Broth)-plates:	15g Agar (Gibco) to 1000ml with LB-media, autoclaved, cool down to 40°C, add 100mg/ml Ampicillin, pour 50ml into petri dishes and store at 4°C
LB (Luria Broth)-media:	Growth medium 0.5% Yeast extract (Gibco BRL) 200mM NaCl 1 % Trypton (Difco) upto 1000ml with H2O autoclaved, stored at 4°C

Bacterial strains

E.coli One Shot TOP10 chemical competent cells (Invitrogen)

Genotype: DH10B™ strain 31

E.coli NovaBlue chemical competent cells (Invitrogen)

Genotype K-12 strain

Molecular biology kits

Rapid DNA Ligation (Roche)

Plasmid Midi Kit (Qiagen)

Plasmid Mini Kit (Qiagen)

QIAquick Gel Extraction Kit (Qiagen)

DIG/FITC RNA Labelling (Roche)

TOPO™ TA Cloning™ (Invitrogen)

SuperScript® III RT synthesis (Invitrogen)

Reagents for molecular biology

DNA markers

25 bp DNA ladder (25 bp - 450 bp)

1 kb DNA ladder (100 bp - 12 kb)

Plasmids and vectors

pCR™4-TOPO® cloning vector (Invitrogen)

pCS2+Fgf8 GFP plasmid (Yu et al., 2009)

pGEM-erm (Michael Brand)

pGEM-pea3 (Michael Brand)

pcDNA3.1DynK44A (S. Schmid),

mRFP-Clathrin (Ernst Ungewickell)

RFP-Rab5a (human) from Ari Helenius

pCS2+mCherry-dmRab7 (Jim Smith)

dsRed-LAMP1 (Erez Raz)

Enzyme

All enzymes were purchased from New England Biolabs and Fermentas Thermo Scientific.

Antibodies

Digoxigenin (DIG) (Roche)	Anti-Digoxigenin-AP, Fab fragments from sheep Used in 1:2000 dilution
Fluorescein (FITC) (Roche)	Anti-Fluorescein-AP, Fab fragments from sheep Used in 1:1000 dilution

Chemicals

All chemical supplies, unless otherwise stated, were bought from ROTH, SIGMA, MERCK, FISHER SCIENTIFIC or ROCHE. The agarose was ordered.

Media for zebrafish breeding and manipulation

1x Embryo rearing medium (E3)	0.1% NaCl 33 0.003% KCl 0.004% CaCl2 x 2H2O 0.016% MgSO4 x 7H2O 0.0001% methylene blue
1x Ringer's	116 mM NaCl 2.9 mM KCl 1.8 mM CaCl 5 mM
PTU	0.003% 1-phenyl- 2-thiourea in 1x PBS

Media for imaging

1.5 % LMP-agarose (GIBCO) in 1 x Ringer's solution

Fish strains

Danio rerio, zebrafish

Wild-type strain: AB2O2 (Institute of Toxicology and Genetics)

Transgeic line: Dusp6 eGFP (Michael Tsang)

Solutions for *in situ* hybridization

1) 4% PFA: 500ml of water was heated up to 50-60°C. 40 gram of paraformaldehyde was added and stirred into the warm water. Sodium Hydroxide (NaOH) was added to the solution till dissolved. The solution was the filled upto 1 litre with H2O.

2) 20% Tween20: (for 50ml): 10 ml of Tween 20 was added to 40ml of water and dissolved.

3) PBST: (for 1l): 100ml of 10x PBS, 5ml of Tween 20 were dissolved in 895ml of waterand stored at room temperature.

4) Glycine: 2 mg/ml of Glycine was dissolved in PBST and stored in -20°C.

5) Proteinase K: 5 mg/ml of proteinase K was dissolved in PBST and stored in -20°C.

6) 20x SSC : In 800 ml of water, 175.3 grams of sodium chloride (NaCl) and 88,2 g Na_3citrate-$2H_2O$ was added. The pH was then regulated to 6.0 with 1M Citric acid. The solution was then filled upto 1 litre with water and stored at room temperature.

7) Hyb+: 500ml Formamide, 250ml 20xSSC and 5ml 20% Tween20 were mixed together. Then, 0,5g Torula (yeast) RNA and 0,05g Heparin were added to the solution, and filled upto 1 L with water. The solution was then stored in -20°C.

8) Hyb-: 500ml Formamide, 250ml 20xSSC, 5ml 20% Tween20 were mixed together and water was added and filled upto to 1 litre.The solution was stored in -20°C.

9) 25% Hyb-: 125ml Formamide, 100ml 20xSSC, 5ml 20% Tween20 were mixed together and the solution was filled uptil 1 litre with water and stored in -20°C.
10) 2x SSCT: 100ml of 20x SSC, 5ml 20% Tween 20 were mixed together and filled upto 1 litre with water and stored in -20°C.
11) 0.2x SSCT: 10ml of 20xSSC, 5ml of 20% Tween 20 were mixed together and filled 1 litre with water and stored in -20°C.
12) 5x MAB: 58,04g Maleic acid, 43,83g NaCl, 38g Sodium Hydroxide (NaOH) pellets were dissolved in 800 ml of water. The pH was regulated to 7.5 with NaOH and the solution was filled upto to 1litre with water. The solution was the filtrated with a 0,22µm filter and stored at room temperature.
13) MABT: 200ml of 5x MAB, 5ml of 20% Tween 20 were mioxed together and filled upto to 1 litre with water. The solution was then stored at room temperature.
14) Dig-block: 2% blocking reagent was dissolved in MABT and heated upto 60 °C till dissolved. The solution was then stored at 20°C.
15) 70% Glycerol: 70ml of 100% Glycerol was dissolved in 30 ml of PBST and stored at room temperature.

16) NTMT was prepared by the following method

	Stock	5ml sol.	10ml sol.	20ml sol.	35ml sol.	50ml sol.
100mM NaCl	5M	0.1ml	0.2ml	0.4ml	0.7ml	1.0ml
100mM Tris	2M	0.25ml	0.5ml	1.0ml	1.75ml	2.5ml
1% Tween	20%	0.25ml	0.5ml	1.0ml	1.75ml	2.5ml
H2O (autoclaved)		4.6ml	8.8ml	17.6ml	30.8ml	44ml

Immunoblot blot (Gels and buffers)

Gels

Separating gel

Ingredients	**2 gels on 1.0 mm**
1.5 M Tris-HCl pH	2.5 ml

8.8	
dH_2O	4.9 ml
10% SDS	100 µl
Acrylamide	2.6 ml
10% APS	50 µl
TEMED	15 µl

Stacking gel

Ingredients	**2 gels**	**4 gels**
0.5 M Tris-HCl pH 6.8	1.25 ml	2.50 ml
dH_2O	3.125 ml	6.25 ml
10% SDS	50 µl	100 µl
Acrylamide	0.65 ml	1.3 ml
10% APS	25 µl	50 µl
TEMED	10 µl	20 µl

Buffers

10X TBS

Ingredients	**Concentrations and amts. In 1.0 L solution**
Tris base	200 mM (24.2 g in 1 L)
NaCl	3.0 M (175.3 g in 1 L)
pH 7.5	adjusted with HCl
dH_2O	Volume upto 1 L

1 X TTBS (membrane washing)

Ingredients	**Concentrations and amts. In 1.0 L solution**
10x TBS	100 ml in 1.0 L
Tween 20	0.1% (1 ml in 1.0 L)

10X TGS buffer

Ingredients	Concentrations and amts. In 1.0 L solution
Tris base	250 mM (30.285 g in 1.0 L)
Glycine	1.92 M (144.13 g in 1.0 L)
Sodium dodecylsulphate	1% (10 g in 1.0 L)
dH_2O	Volume upto 1.0 L

Ingredients	Concentrations and amts. In 1.0 L solution
10X TGS	100 ml
dH_2O	900 ml

20% Transfer buffer with methanol

Ingredients	Concentrations and amts. In 1.0 L solution
Tris base, pH ~8.3	25 mM (3.03 g in 1.0 L)
Glycine	192 mM (14.4 g in 1.0 L)
Methanol	20% (200 ml in 1.0L)
dH_2O	Volume up to 1.0 L

Ponceau stain (50 ml)

Ingredients	Concentrations and amts. In 1.0 L solution
Ponceau S	0.1% (0.05 g in 50 ml)
Glacial acetic acid	5% (2.5 ml in 50 ml)
dH_2O	Volume upto 50 ml

1° Blocking solution with sodium azide

Ingredients	Concentrations and amts. In 1.0 L solution
Skim milk powder	5% (5 g in 100 ml)
Sodium azide	0.05% (0.05 g in 100 ml)
TTBS	Volume up to 100 ml

2° Blocking solution (NO sodium azide)

Ingredients	Concentrations and amts. In 1.0 L solution
Skim milk powder	5% (5 g in 100 ml)
TTBS	100 ml

Stripping buffer

Ingredients	Concentrations and amts. In 1.0 L solution
2-mercaptoethanol >=98%	200 mM (14.4 ml in 1.0 L)
Sodium dodecylsulphate	2% (20 g in 1.0 L)
Tris HCl, 1 M, pH 6.8	62.5 mM (62.5 ml)
dH_2O	Volume up to 1.0 L

Method

Plasmid making and transformation

RNA extraction

To obtain a sufficient amount of RNA around 50 Zebrafish embryos were added in a 1.5 ml microfuge tube and excess water removed. 250 ul of TRIzol reagent was then added and the embryos were lysed and homegenized using a pellet pestle (Eppendorf). To facilitate the dissociation of the nucleoprotein complexes, the homogenised sample was then incubated for a period of 5 minutes at room temperature. 40 µl of chloroform was then added to the sample and centrifuged at 4 °C for a period of 15 minutes at 13,000 rpm. The mixture then gets seperated into 3 layers with the uppermost phase containing the RNA. The upper phase containing the RNA was then tranferred to a new microfuge and the RNA was preceipitated using 100 µl isopropanol. This was then incubated at room temperature for 10 minutes and centrifuged at 4 °C, 13,000 rpm for 10 minutes. The pellet was then washed with ethanol and resuspended in 50 µl of nuclease free water.

cDNA synthesis

cDNA was synthesized using the Invitrogen SuperScript First-Strand Synthesis System using 50 -500ng of RNA primed with oligo (dT), and primer (Roche Biochemicals).

Primer Design

Primers for *hsc70* mRNA (forward/reverse); 5'-TGG TGG CAC TTT TGA TGT GT-3'/5'-TCC CTC TCT GCA GTC TGG TT-3', were designed with the help of the *Primer3* program (Rozen et al.,2000) according to the protocol in Wu et al., 1991.

Polymerase Chain (PCR) reaction

10xDream Taq buffer 5 µl
10mM dNTPs 1 µl
DNA 2 µl
primer forward 1 µl
primer reverse 1 µl
Taq-DNA polymerase 0.25µl
H2O 14.75 µl
Total 25 µl

Parameters for amplification

Denature 94 °C	10 min
3 cycles Denature 94 °C	1 min
Annealing 58 °C	1 min
Extension 72 °C	45 s
Denature 94 °C	30 s
32 cycles Annealing 72 °C	30
Extension 72°C	45 s
Last cycle Extension 72 °C	10 min

After the PCR, the samples were loaded onto the 1% agarose gel and subjected to Gel Electrophoresis.

DNA Extraction

The band of the desired size from the gel was removed using a razor blade. The gel containing the band was then added to a microfuge and QIAamp DNA Mini Kit was used to purify and extract the DNA.

DNA cloning

General cloning procedures were performed as described in Maniatis et al., 1989.

Cloning of PCR products

TOPO TA Cloning Kit from Invitrogen was used for cloning of PCR products.

Transforming Competent Cells

For transformation, TOP10 competent cells from Invitrogen or Novablue competent cells were used and plated overnight at 37°C in LB plates with Ampicillin or Kanamycin as in the protocol from the Cloning Kit.

Plasmid mini-preparation (Qiagen Mini-Prep)

A single colony was picked, transfected with 5 ml LB-medium and incubated overnight at 37°C. On the next day 4 ml of the culture was transferred into an eppendorf tube and centrifuged for 5 min at 8,000 rpm speed. The gained bacterial pellet was dissolved in 200µl P1 and 400µl P2 solution. After an incubation time of 5 min at room temperature, 300µl of P3 solution was added and incubated for 5 min at ice. The bacteria solution was centrifuged for 5 min at 14,000rpm speed and the supernatant was transferred in a new 2.0ml eppendorf tube, adding 1m isopropanol. Incubated for 20min at room temperature, the supernatant was centrifuged for 10min at 14,000rpm speed, washed with 70% ethanol.

Preparation of plasmid (Qiagen Maxi-Prep)

The plasmid was isolated according to the manufacturer's protocol form Qiagen Maxi Prep Kit.

Synthesis of sense mRNA for injection

5 µg of the desired plasmid containing the gene of interest was linearised at the 3'end of the gene. The restriction digest was phenol-purified, precipitated and resuspended in 10 µl H2O. 1µg of the linearised plasmid was then used for mRNA transcription using Message Machine KIT (Ambion).

The mRNA was then resuspended in 15µl H2O and the concentration was determined via measurement of the OD. The mRNAwas then stored in aliquots of 1 µl at –80 °C.

Morpholino antisense oligomers

Morpholino-antisense oligomers (Morpholinos, MOs, GeneTools LLC) were designed for the transient knockdown of hsc70. *hsc70* MOs prime in the 5'-UTR, spanning over the start codon thereby blocking the translation. Two *hsc70* MOs targeting two different regions within the 5' cap to start region were designed.

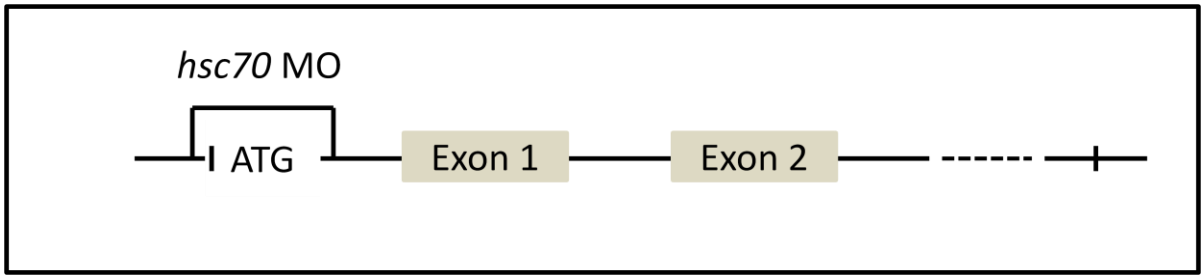

Figure 1: Generation of ATG morpholinos. ATG morpholinos (*hsc70)* bind to the endogenous mRNA and block the translation complex.

Morpholino sequences:

hsc70 MO 1 (5'ATAAAACAGAGATGGATGAAGATGC 3')

hsc70 MO 2 (5' AGCTGGTCCCTTGGACATTGTGTCA 3')

Injection of Morpholino-antisense oligomeres

I injected MOs into the yolk cell close to the blastomeres at one to two-cell stages at a concentration of 0.5mM. A randomly mispriming MO was used as a Control MO at a concentration of 15 ng/nl. Injected embryos were then incubated at 28.5 °C till the desired

stage and then either subjected to confocal microscopy or fixed O/N for in 4% paraformaldehyde (PFA)/ PBS overnight at 4 degrees for *in situ* hybridization.

Zebrafish maintenance

Breeding zebrafish (*Danio rerio*) was maintained at 28 °C on a 14-h light/10-h dark cycle (Brand *et al*, 2002). The data I present in this study were acquired from analysis of wild-type zebrafish of ITG (AB_2O_2) and the transgenic zebrafish line TG (Dusp6: EGFP) ^{pt6}, which was received from Michael Tsang.

Injection

Preparation

The pneumatic pico pump PV820 with foot trigger (World Precision instruments) along with the microcapillary holder MPH6S (World Precision instruments) were used. The capillary holder was mounted on the micromanipulator MN-151 (Narishige) with a magnetic arrest mechanism M1 near the stereomicroscope. For injection, the embryos were dechorionated either with DuMont forceps or by treatment in a proteinase solution, 1 mg/ml; Sigma P-6911, after which the embryos were washed twice in E3 medium and transferred to 2 % agarose coated dishes and then placed in a row of 50 embryos in a special agarose embryo carrier (Westerfield, 1994). This carried was then placed under the stereomicroscope for injection of the embryos. The injection of solutions to Zebrafish at 1 to 2 cell stage was performed using thin walled borosilicate capillaries (World Precision Instruments). The solution is always injected into the cell, making sure that it is not injected into the yolk. Prior to injections, the tips of the capillaries were pulled using the Flaming/Brown microcapillary puller P-97, with the following parameters: Heat (H): 270, Force (P): 120, Velocity (V): 80, and Duration (T): 150. Using a stereomicroscope, the capillary tips were then cut to diameters of 3 μm. The solution was then loaded on to the capillaries using microloader tips from Eppendorf.

Injection of mRNA

pCS2+Fgf8 GFP plasmid (Yu et al., 2009) and pcDNA3.1DynK44A (S. Schmid), pCS2+Rab5 plasmid were linearized using NOT1 and transcribed with Sp6 Message Machine Kit (Ambion). *Hsc70* full length coding sequence was amplified with primer pairs (forward/reverse); 5'-TGG TGG CAC TTT TGA TGT GT-3'/5'-TCC CTC TCT GCA GTC TGG TT-3' from a zebrafish cDNA library at stage 24h. The Hsc70 full length cDNA was cloned in the expression vector pCS2+. The plasmid was then linearized with NOT1 and transcribed using SP6 Message Machine Kit (Ambion). To detect the injection, 0.2 % phenol red was added to the solution and approximately 1 - 2 NL was injected in each embryo. The embryos were washed 3 times in E3 and fixed at the desired stage for *in situ* hybridization or mounted at the desired stage for confocal analysis. For confocal analysis, embryos were embedded for live imaging in 1.5% low melting point agarose (Sigma-Aldrich) dissolved in 1x E3 solution.

RNA probe preparation

For linearizing the plasmid, 10 μg of the plasmid was digested. Using phenol or chloroform, the digest was then purified and precipitated. After this, the digest was resuspended in 10 μl of water. A transcription reaction was then assembled with 1 μg of the restricted digest and the DIG-RNA Labelling Kit (Roche Biochemicals) using the manufacturer's protocol. For the preparation of Digoxigenin labelled probes, the corresponding labelled UTPs- mix was used.

***In situ* hybridization**

Whole-mount mRNA *in situ* hybridisations (ISH) were performed as described in Scholpp and Brand, 2003. Embryos were fixed in 4% paraformaldehyde/PBS for 24 h at 4°C, followed by dehydration and storage in 100% methanol at -20°C. For ISH, embryos were re-hydrated, treated with proteinase K, refixed in 4% paraformaldehyde/PBS, and then prepared for ISH Fluorescein- and digoxygenin-labelled probes were stained in blue using 1mg/ml NBT/BCIP (Roche) in NTMT (pH 9.5), or stained in Fast Red Tablets (Roche) dissolved in 0.1mM Tris-Hcl (pH 8.2).

SYTOX staining

To visualize the cell nuclei, embryos were fixed in 4% paraformaldehyde/PBS at room temperature for 2 hours and transferred in 1x PBS. Fixed brains were hemisected with a tungsten needle and incubated overnight in a 24 well plate with 25µM SYTOX® nucleic acid staining solution (Invitrogen). After washing in 1x PBS, the stained brain was mounted laterally in a 1.5% low melting agarose drop for confocal imaging analysis.

Image acquisition

Prior to imaging, embryos were mounted on 70% glycerol. Images were taken with the help of an Olympus SZX16 microscope equipped with a DP71 digital camera using the imaging software Cell A.

Cell Culture

Zebrafish PAC2 cells were used to study the intracellular localization of Fgf8. Seeded cells were first washed with 10ml of 1xPBS. PBS was then removed and 2ml Trypsin/EDTA was added onto the cells. The cells were incubated until their detachment was observed. 8ml of medium was then added and mixed to resuspend the cells. 10-20 µl of the cell suspension was added to the neubaur-chamber and the cells were counted. The resuspended cells were then transferred to petridishes (Sigma-Aldrich) according to the number of transfections performed. After 24 hours, the cells were transfected. The following endosomal markers were used: RFP-Rab5a (human) from Ari Helenius, pCS2+mCherry-dmRab7 from Jim Smith, mRFP-Clathrin from Ernst Ungewickell, dsRed-LAMP1 from Erez Raz. Cells were transfected separately with Fgf8-GFP at a concentration of 1µg and Hsc70 transfected along with the desired marker: mRFP-Clathrin, RFP-Rab5a, mCherry-Rab7 at a concentration of 600ng in DMEM solution (Sigma Aldrich). 24 hours post transfection, Fgf8-GFP transfected cells were co-cultured with cells transfected with Hsc70 and the respective endosomal markers.

Chemical Treatments

Inhibition of Fgf8 signaling

Fgf receptor-mediated signaling was inhibited bby icubation of live embryos in 16 μM of SU5402 (Calbiochem) in 1% DMSO at 30% epiboly stage. 1% DMSO without SU5402 was used as control. The embryos were incubated for 3 hours and fixed at 75% epiboly *for in situ* hybridization analysis.

Inhibition of intracellular transport of Fgf8

Molecular transportation from early to late endosomes was inhibited by treatment with 100nM bafilomycin A1 (Sigma-Aldrich) in 1% DMSO. 1% DMS0 alone was used as control. These embryos were incubated with the chemical for a period of 1 hour at 30% epiboly stage subjected to live imaging or fixed at 75% epiboly stage for *in situ* hybridization experiments. Texas red Transferrin was purchased from Invitrogen.

Confocal image analysis

The embryos were then maintained in Ringer medium till the desired stage and analyzed using confocal microscopy. Prior to imaging, embryos were mounted on 70% glycerol. For confocal analysis, embryos were embedded for live imaging in 0.7-1% low melting point agarose (Sigma-Aldrich) dissolved in 1x E3 solution at 50% epiboly stage. Live embryos as well as cells were imaged using 20x and 63x water immersion objective. Confocal image stacks were then obtained using the Leica TCS SP5 X confocal laser-scanning microscope. To reconstruct the imaged area, I composed a series of optical planes (z stacks). The step size for the z-stack was usually 1-2 μm and was chosen upon calculation of the theoretical z-resolution of the objective. Images were further processed using Imaris 6 (Bitplane AG).

Immunoblot experiment

HEK 293 cells were cultivated to 70–80% confluency before transfection. For transfection of Fgf8 and Hsc70 cells were seeded at 2 x 10^6 cells in a 10cm plate. After 24 hours cells were

transfected according to the manufacturer's protocol using Promofectin (Promocell). Briefly two mixtures containing DNA/serum free DMEM and Promofectin/serum-free DMEM were combined, incubated for 20 min at RT and added to the cells. 24 hrs after transfection the culture medium was replaced and Bafilomycin A1 was added. 24 hrs later the cells were lysed in sodium dodecyl sulfate (SDS)–sample buffer containing 100mM dithiothreitol (DTT) and subjected to Western blot analysis. Activated Erk was monitored using an antibody against phosphorylated Erk (phospho-p44/42, Cell Signaling). For the loading control the membrane was stripped (62.5mM Tris, pH 6.8, 2% SDS, 0.8% DTT) and reprobed with an Erk antibody (Erk 1 (K-23) Santa Cruz). Blots were stained using the enhanced chemiluminescence system (Thermo Fisher Scientific). The quantification of Bands in Western blot analysis was performed using the program ImageJ (National Institutes of Health).

Immunoblot experiment with cell lysates

HEK 293 cells were cultivated to 70–80% confluency before transfection. For transfection of Fgf8 and Hsc70 cells were seeded at 2 x 10^6 cells in a 10cm plate. After 24 hours cells were transfected according to the manufacturer's protocol using Promofectin (Promocell). Briefly two mixtures containing DNA/serum free DMEM and Promofectin/serum-free DMEM were combined, incubated for 20 min at RT and added to the cells. 24 hrs after transfection the culture medium was replaced and Bafilomycin A1 was added. 24 hrs later the cells were lysed in sodium dodecyl sulfate (SDS)–sample buffer containing 100mM dithiothreitol (DTT) and subjected to Western blot analysis. Activated Erk was monitored using an antibody against phosphorylated Erk (phospho-p44/42, Cell Signaling). For the loading control the membrane was stripped (62.5mM Tris, pH 6.8, 2% SDS, 0.8% DTT) and reprobed with an Erk antibody (Erk 1 (K-23) Santa Cruz). Blots were stained using the enhanced chemiluminescence system (Thermo Fisher Scientific). The quantification of Bands in Western blot analysis was performed using the program ImageJ (National Institutes of Health).

Quantification and statistical analysis

For quantification of the *in situ* data, the area of the Fgf target gene expression *erm* and *pea3*,

were measured using Olympus Cell A and D softwares. The area of expression was calculated with respect to the area of the entire embryo. For immunoblot experiments, statistical analysis was performed on three independent experiments using ImageJ software. All quantifications were given as mean plus SD. For data acquired through confocal imaging quantification was performed using Imaris 6 (Bitplane AG).

RESULTS

To determine the role of CME in the regulation of Fgf signaling during embryonic development, I first analyzed the effect of Hsc70 loss or gain of functions in Fgf target gene expression. Then I analyzed the effect of altered CME rates through Hsc70, on Fgf8 localization and spreading. After this, I studied the alterations in the Fgf signaling activity during altered rates of CME and endocytic trafficking.

Optimization of experimental conditions

To determine the function of Hsc70 its expression was knocked down using a Morpholino (MO)-oligomer based antisense approach. Two different ATG Morpholino oligomeres (1 and 2) targeting different regions around the start codon for knock-down, were analyzed for their efficiency in knocking down the expression of protein Hsc70. Western blot analysis showed a significant reduction in the expression of Hsc70 when in the Hsc70 morphant samples when compared with the control. Overexpression of Hsc70 showed a significant increase in Hsc70 expression when compared with control. Samples with 50nM (1:20) of *hsc70* MO concentration exhibited optimal knockdown of expression as shown in figure 1. 50nM was used as the standard concentration throughout this work to determine the role of Hsc70 on Fgf8 signaling as Fgf8 is the main ligand of Fgf during zebrafish gastrulation (Reifers et al., 1998).

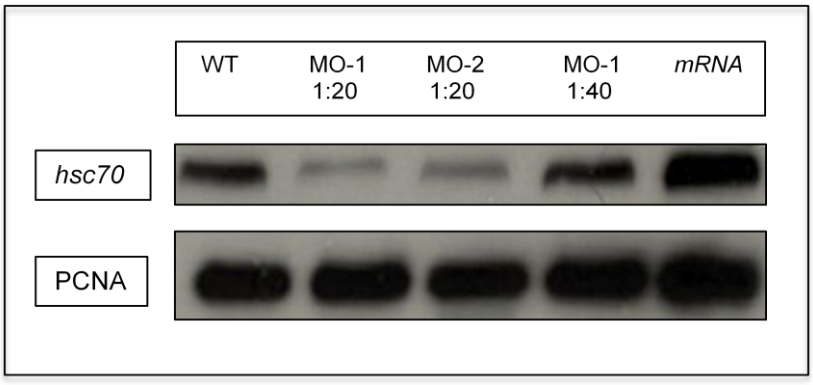

Figure 1: Optimization/Calibration of experimental conditions**.**Immunoblot analysis of the expression of Hsc70 protein duringknockdown and overexpression of Hsc70. Embryos were injected with *hsc70* MOs as well as *hsc70* mRNA and samples at 28hpf were subjected to immunoblot analysis. Embryos injected with *hsc70* MOs showed a reduction in the expression of Hsc70 when compared to the expression in wild type samples. Embryos overexpressed with Hsc70 showed an increase in the expression of Hsc70 when compared to the expression in the wild type.

Hsc70 regulates Fgf signaling range

Towards the goal of analyzing the effect of Hsc70 on Fgf8 signaling, the expression of known sensitive target genes of Fgf8 signaling *erm* and *pea3*, were studied by altering the level of Hsc70 in zebrafish. For loss and gain of Hsc70 function, Injection of *hsc70* MO as well as *hsc70* mRNA were performed at one to two cell stage. Fgf8 expresison is detected at 30 % epiboly stage at the blastoderm margin. At shield stage, Fgf8 is expressed at the germ ring in the form of a gradient that is dorsoventral in manner. The gradient expression of Fgf8 remains till as late as 90% epiboly stage (Reifers et al., 1998). The expressions of the general targets of Fgf8, *erm* and *pea3*, are nested close to the Fgf8 source, more specifically at the Fgf8 source and its surrounding tissue (Roehl and Nusslein-Volhard, 2001). To study the alterations in such a gradient formation due to Hsc70 function, experiments were conducted in zebrafish withing this stage (50%, 75% epiboly stage). The expression of Fgf target genes was analyzed by *in situ* hybridization (ISH) (Raible and Brand, 2001).

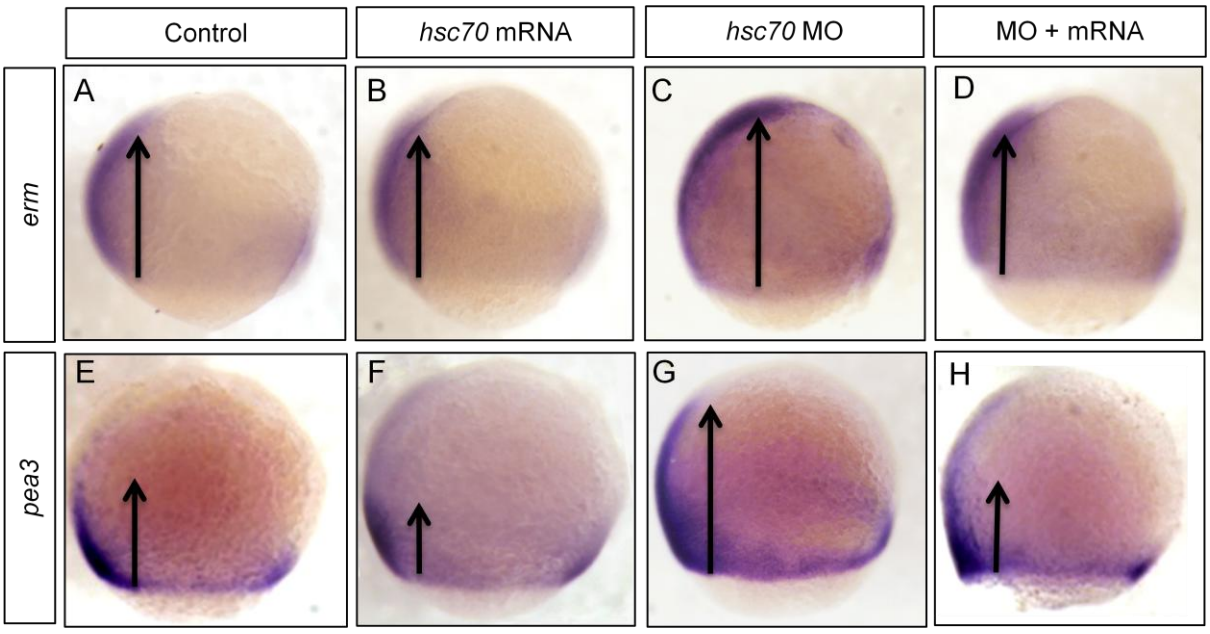

Figure 2: Hsc70 regulates Fgf8 signaling range. *In situ* hybridization for Fgf target genes *erm* and *pea3* at 75% epiboly stage. Embryos were mounted laterally with the animal pole to the top and dorsal region towards the left. Expression of Fgf target genes *erm* and *pea3* in control embryos (A, E). The target gene expression of *erm* and *pea3* were not altered due to overexpression of Hsc70 (B, F). In contrast, knockdown of Hsc70 showed an expansion of target gene expressions to the animal pole (C, G). The expansion of the target gene expression during Hsc70 knockdown could be rescued by simultaneous overexpression of ectopic *hsc70* mRNA (D, H).

From the *in situ* hybridization analysis, the gain of function of Hsc70 by ectopic expression of *hsc70* mRNA (Figure 2B) did not alter the expression area of *erm* in comparison with control embryos (Figure 2A). Interestingly, the down-regulation of Hsc70 expression using *hsc70* MO (Figure 2C) led to an expansion of *erm* expression in comparison with control embryos (Figure 2A). To confirm if the expansion of *erm* expression in the Hsc70 knockdown was specifically due to the effect of Hsc70, coexpression of *hsc70* MO and *hsc70* mRNA (Figure 2D) was performed. In these embryos, the Fgf signaling range was rescued.

Similarly, analysis of expression of Fgf target gene *pea3* revealed that the gain of function of Hsc70 (Figure 2F) did not alter the expression of *pea3* whe compared with control embryos (Figure 2E). However, the knockdown of Hsc70 function (Figure 2G), displayed an expansion of *pea3* expression in comparison with control (Figure 2E). Once again, to determine the specificity of the role of Hsc70 in the alteration of Fgf target expression, *hsc70* MO and *hsc70* mRNA were co expressed and the expansion of *pea3* expression due to loss of Hsc70 function was observed to be rescued (Figure 2H). From these results we can reasonably infer that Hsc70 plays a specific role in the regulation of Fgf signaling range.

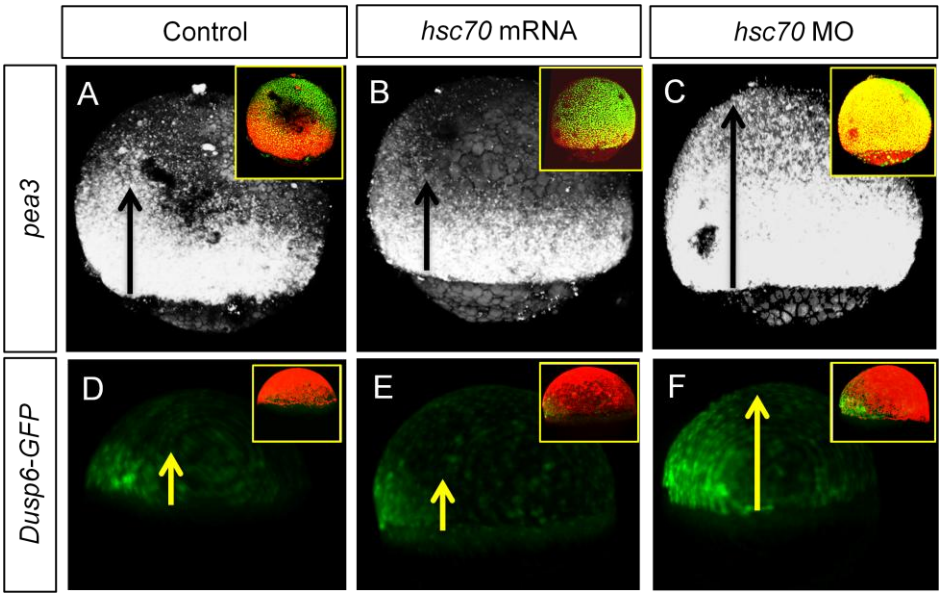

Figure 3: Fluorescent ISH for target gene expression *pea3* showed that the expression of *pea3* remained unaltered during overexpression of Hsc70 (B), in comparison with control embryos (A). However, knockdown of Hsc70 led to an expansion of *pea3* expression (C) when compared to the control embryos (A). Expression of

Dusp6-EGFP in live zebrafish embryos at 50% epiboly stage showed a similar unaltered expression during overexpression of Hsc70 (E) and an expansion of expression during knockdown of Hsc70 (F) when compared to the control embryos (D).

In addition, the range of Fgf signaling with respect to Hsc70 was analyzed using a high-sensitive fluorescent ISH approach. A similar expansion of *pea3* expression, in *hsc70* morphant embryos (Figure 3C) was observed in comparison with control embryos (Figure 3A). *Pea3* expression in embryos overexpressed with Hsc70 (Figure 3B) remained unchanged.

DUSP6 has been shown to regulate *in vivo* as well as *in vit*ro levels of dpErk expression thereby suggestion that it plays a role of a negative regulator of Fgf signaling during vertebrate development (Echevarria et al., 2005, Gomez et al., 2005, Smith et al., 2005, Eblaghie et al., 2003, Kawakami et al., 2003). Studies suggest that Dusp6 maybe a conserved transcriptional target of Fgf signaling as it is commonly expressed in patterns that correspond to areas of active Fgf signaling in many vertebrate species during embryonic development (Dickinson et al., 2002, Klock and Herrmann, 2002, Eblaghie et al., 2003, Kawakami et al., 2003, Tsang and Dawid, 2004, Gomez et al., 2005). In order to analyze if Hsc70 affected other Fgf target genes, a stable transgenic Dusp6-GFP (Dual specificity phosphatase 6) expressing Zebrafish line was used as an *in-vivo* Fgf signaling reporter (Molina et al., 2007) as shown in Figure 3D, E, F. As shown in Figure 3, loss of function of Hsc70 (Figure 3F), in Zebrafish embryos displayed an increase in the expression of Dusp6-GFP in comparison with control embryos (Figure 3D). The DUSP6 expression in embryos overexpressing Hsc70 was however unaltered when compared with control embryos (Figure 3D, 3E).

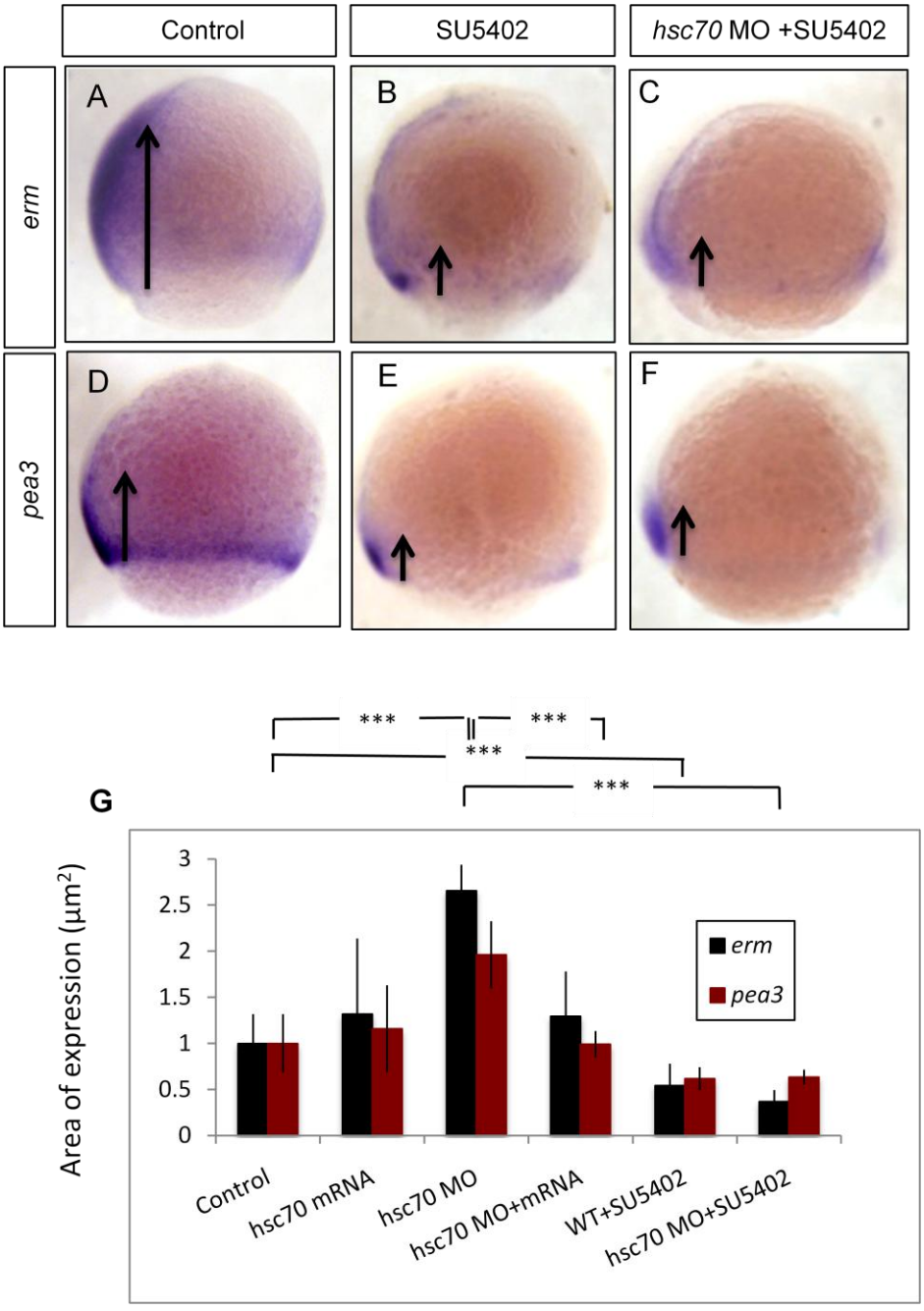

Figure 4: Hsc70 regulates Fgfr mediated signaling.Treatment of embryos with 16µM SU5402 showed an inhibition of *erm* and *pea3* expression (B, E). Embryos knocked down for Hsc70 function treated with SU5402 also showed an inhibition of *erm* and *pea3* expression (C, F).Quantification of the area of expression of target genes *erm* and *pea3*, show a siginificant increase in the area of *erm* and *pea3* expression in *hsc70* morphant embryos and a significant decrease in the area of expression in SU5402 treated embryos compared to the control embryos (G).

Hsc70 regulates Fgfr mediated signaling

To verify whether the effect of Hsc70 on Fgf target genes was dependant on Fgf receptor mediated signaling, the embryos were treated with an Fgf receptor inhibitor. SU5402 specifically inhibits Fgfr phosphorylation with affecting other growth factor receptors (Mohammadi et al., 1997). As shown in Figure 4, SU5402 treatment reduced *erm* expression (Figure 4B) in comparison with control embryos (Figure 4A). A similar downregulation of *erm* was also observed in Hsc70 knocked-down embryos (Figure 4C), and this it can be inferred that Hsc70 influences specifically Fgfr mediated signaling. Similarly treatment of embryos with SU5402, showed a significant reduction in the expression of pea3 (Figure 4E) when compared with control embryos (Figure 4D). Loss of Hsc70 function also displayed a similar reduction in pea3 expression (Figure 4F) in comparison with control embryos (Figure 4D).

Hsc70 does not alter the Fgf ligand expression

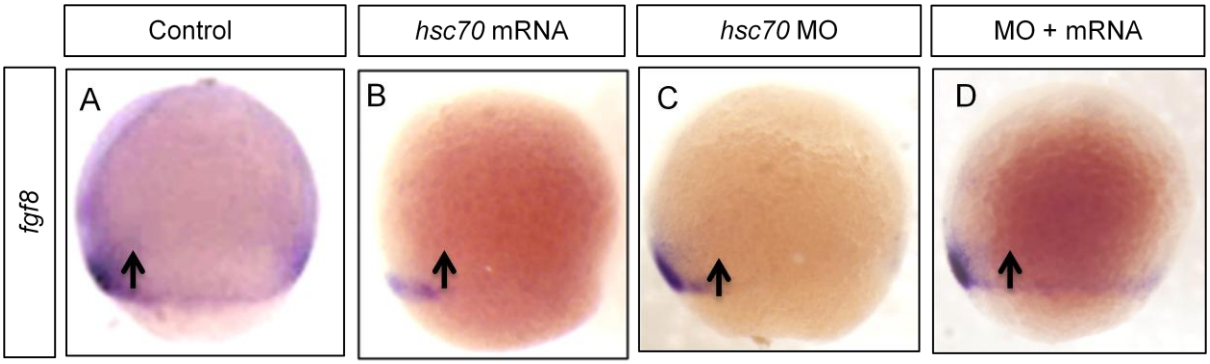

Figure 5: Shows the expression of Fgf8 at 75% epiboly stage. Fgf8 expression remains unaltered during overexpression (B), knock-down of Hsc70 (C), as well as during co- injection of *hsc70* MO and *hsc70* mRNA (D).

To determine if Hsc70 affects the expression of the ligand Fgf8, *in situ* hybridization experiment was performed to analyze the expression of Fgf8 during loss and gain of function of Hsc70 as shown in Figure 5. Overexpression of Hsc70 did not alter the expression of the ligand Fgf8 in comparison with the control embryos (Figure 5A, 5B). Similarly, knockdown of Hsc70 function as well as rescued embryos (Figure 5C, 5D), did not display a change in

the expression of Fgf8 in comprison with the control embryos (Figure 5C, 5A). Therefore, although the loss of Hsc70 expression altered the expression of Fgf target genes *erm* and *pea3*, the expression of the ligand Fgf8 per se remains unaltered during loss or gain of function of Hsc70.

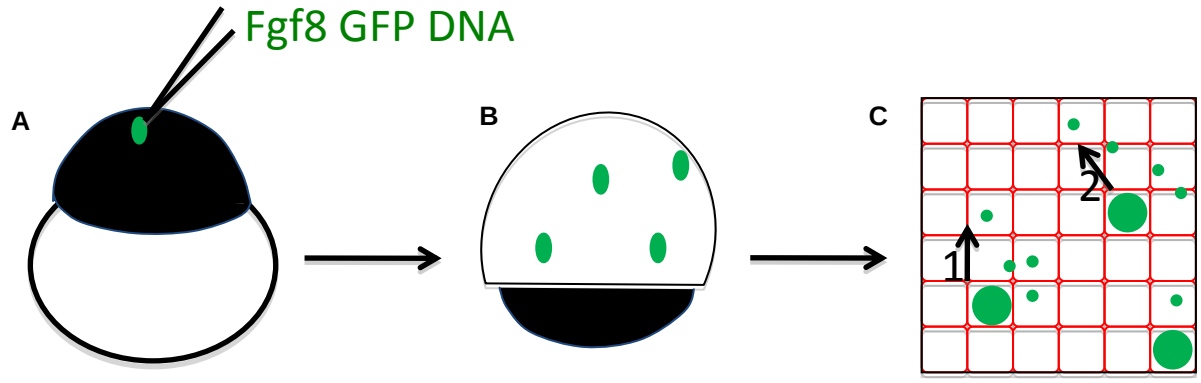

Figure 6:Shows the injection of Fgf8 GFP DNA at one cell stage, live zebrafish embryos. Fgf8 DNA is produced in certain cells and the secretion and travel can be analyzed from the focal sources generated.

Expression of Fgf8 DNA *in vivo*

To determine the role of Hsc70 in the localization and spreading of Fgf8 *in vivo*, live imaging of zebrafish embryos was performed to analyze the distribution of Fgf8 from its source and its subsequent uptake into cells. A GFP-tagged form of Fgf8 mRNA (Yu et al., 2009), was injected into the cells and visualized at blastula stage.

To address the question of how Hsc70 function interferes with Fgf8 internalization and subsequent signaling, we visualized the uptake of Fgf8 into cells in blastula-stage embryos by analyzing the distribution of a GFP-tagged form of Fgf8 (Yu et al., 2009) in the living embryo. Injection of DNA causes a mosaic expression (Figure 6B), therefore creating Fgf8 “sources” from which the signaling molecules travel to the neighbouring cells and get internalized as shown in Figure 6C. The creation of such an expression makes it possible to determine the distance travelled by Fgf8 from the source during loss and gain of Hsc70 function. Since Hsc70 showed to play a role in altering the range of Fgf signaling, it was interesting to determine its role in the localization of Fgf8.

Hsc70 loss of function regulates Fgf8 internalization

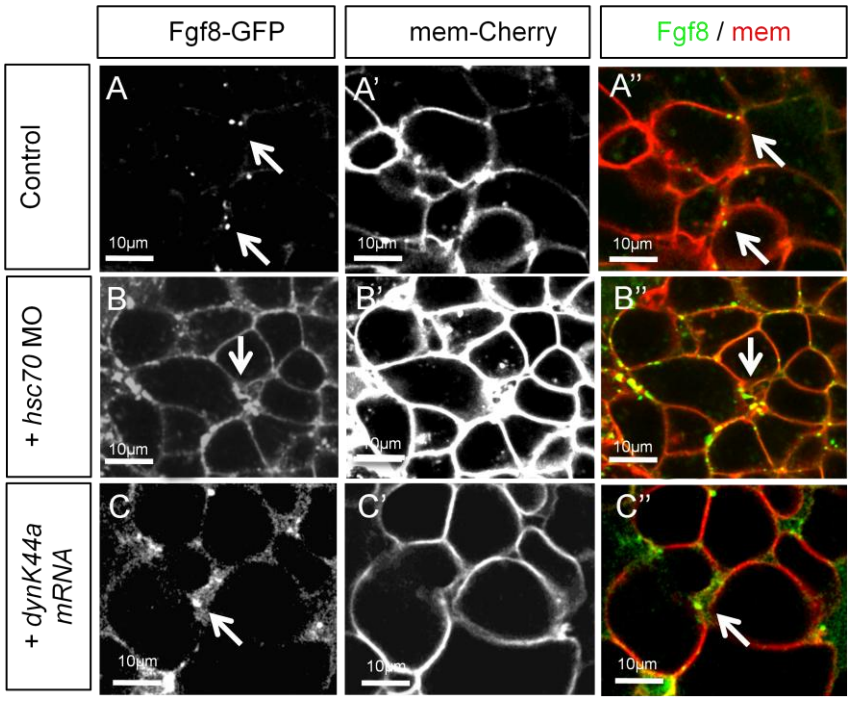

Figure 7: **Hsc70 regulates Fgf8 internalization**. Confocal analysis of live embryos, at 50% epiboly stage imaged at the animal pole. Fgf8-GFP DNA was injected along with the red membrane marker mCherry at one cell stage and the localization and spreading of Fgf8 from the source cell to the neighboring cells was analyzed using confocal microscopy. In control embryos, Fgf8 was localized both at the membrane and inside the cell (A-A"). Knockdown of Hsc70 resulted in an inhibition of Fgf8 internalization resulting in the accumulation of Fgf8 in the extracellular space (B-B"). Injection of dominant-negative dynamin2 (K44A) variant showed a similar extracellular accumulation of Fgf8 (C-C").

To determine the localization of Fgf8 during loss and gain of Hsc70 function, embryos were injected with Fgf8 GFP DNA+ Control MO/ *hsc70* MO/ *hsc70* mRNA, along with membrane marker mCherry at one to two cell stages. Embryos were subjected to live imaging at 30% epiboly stage.

In control embryos, localization of Fgf8 was observed at the membrane as well as intracellular clusters as shown in Figure 7A-A''. In Hsc70 knock-down, Fgf8 accumulation was observed in the extracellular space (ECS) and intracellular clusters were significantly reduced (Figure 7B-B"). A similar accumulation of Fgf8 in the ECS was also observed in embryos were endocytosis was inhibited by blockage of Dynamin 2 function (Figure 7C-C''). Although Dynamin2 and Hsc70 play crucial roles in the process of CME, they work at

different levels to carry out their functions. Dynamin is required for the very first step of endocytosis, where it assembles itself to the coated pits formed as a result of the invagination of the membrane; whereas, Hsc70 function in diassembly of the Clathrin Coated Vesicles formed after they are pinched off by Dynamin2 (Hinshaw and Schmid, 1995, Schlossman et al., 1984). This might be the reason why even though the loss of both these proteins results in the accumulation of Fgf8 in the ECS, the diffusion of Fgf8 appears to be different (Figure 7B-B'',7C-C''). The increase in the extracellular localization of Fgf8 resulting from loss of Hsc70 function shows that Hsc70 plays a critical role in clathrin mediated endocytosis of Fgf8.

Hsc70 expression leads to intracellular clustering of Fgf8

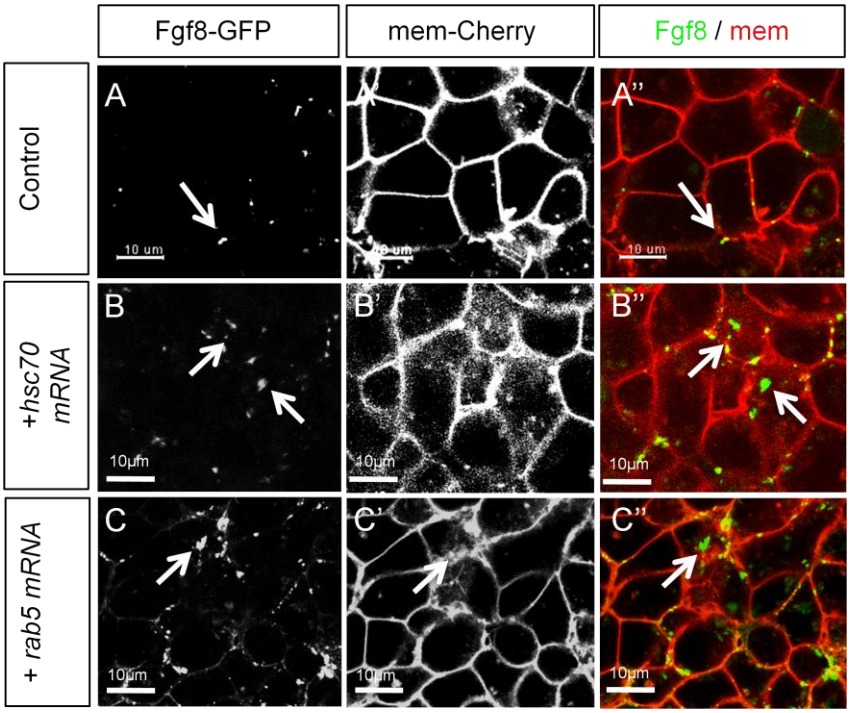

Figure 8: Overexpression of Hsc70 showed the formation of enhanced intracellular clusters of Fgf8 and reduced accumulation of Fgf8 at the membrane or extracellularly (B-B") in comparison with control embryos (A-A''). Overexpression of rab5 also shows a similar formation of intracellular clusters (C-C'') when compared to the control embryos (A-A'').

To determine the effect of Hsc70 expression on Fgf8 internalization, embryos were overexpressed with Hsc70 along with the cellular marker mCherry and subjected to live confocal imaging. Converse to the previous experiment (Figure 7), overexpression of Hsc70 led to enhanced intracellular clustering of (Figure 8B-B'') and loss of extracellular accumulation of Fgf8 (Figure 8B-B''), in comparison with the control embryos (Figure 8A-A'). The loss of extracellular Fgf8 accumulation observed during Hsc70 expression might be due to an increase in the rate of endocytosis. In cytoplasm, Rab5 occurs as part of complex where Rab5 GDP is bound to Rab GDI (Gdp dissociation inhibitor). This complex is dissociated upon membrane association which leads to the release of Rab GDI into the cytoplasm and the conversion of Rab5GDP into the active Rab5 GTP form by GDP/GTP exchange factors (Soldati et al., 1994, Ullrich et al., 1994). Activated Rab5 controls the transport between the cell membrane and the early endosomes. It also regulates homotypic fusion of early endocomes (Gorvel et al., 1991, Bucci et al., 1992). Similar to Hsc70 overexpression, an increase in the rate of endocytosis due to GTPase Rab5 overexpression led to intracellular clusters as shown in Figure 8C-C''. Apart from intracellular Fgf8 cluster formation, increase in the rate of endocytosis due to Rab5 overexpression also decreased the amount of Fgf8 present extracellularly. This reduction in the extracellular Fgf8 is similar to Hsc70 overexpression (Figure 8B-B'')

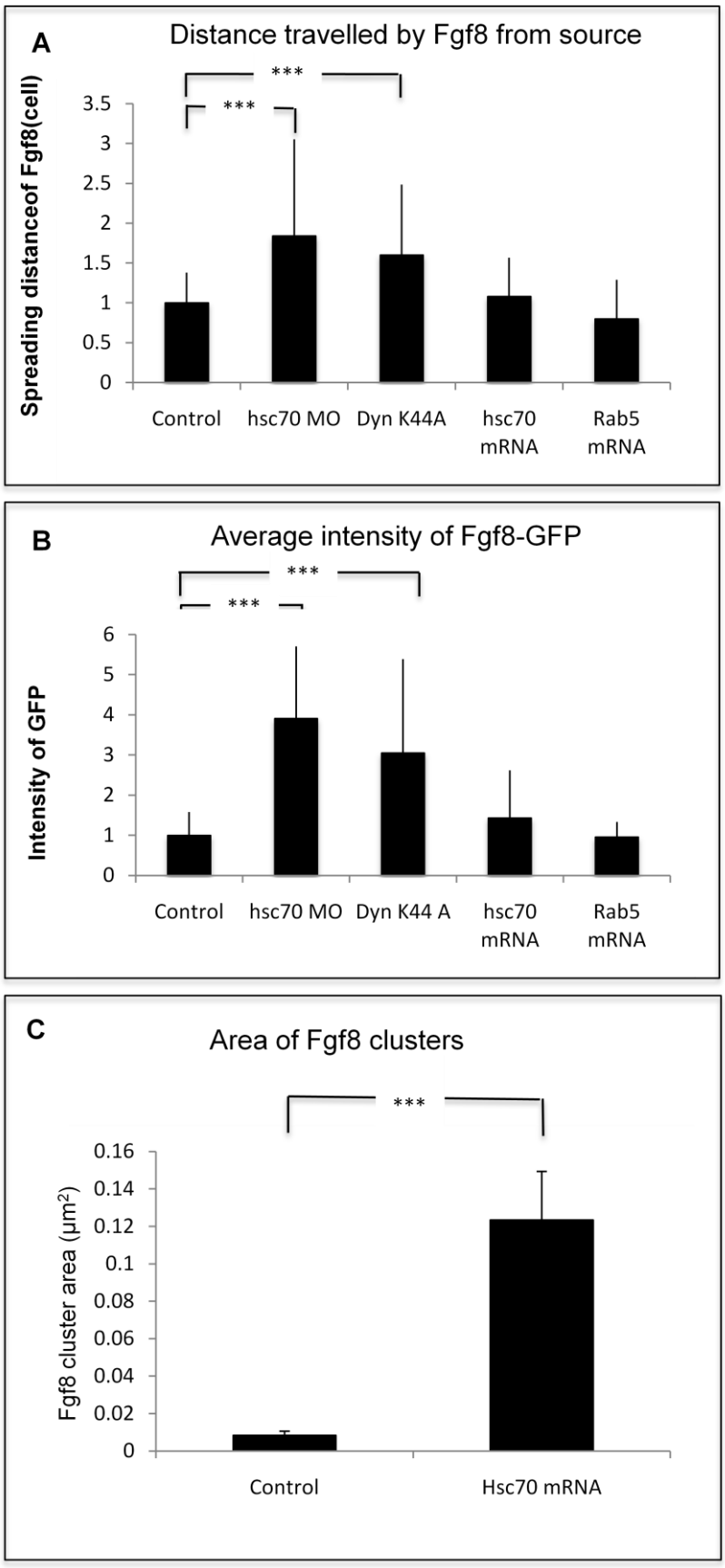

Figure 9: **Quantification of the distance of diffusion and intensity of GFP**. Quantification of the distance travelled by Fgf8 confirmed that there was a significant increase in Fgf8 spreading away from its source during

knockdown of Hsc70 and injection of *dyn2-K44A* mRNA when compared to control. However, the distance travelled by Fgf8 from its source during overexpression of Hsc70 and Rab5 was similar to the control situation (A). Quantification of the average intensity of Fgf8-GFP showed a significant increase in the intensity levels of Fgf8-GFP during Hsc70 knockdown and injection of *dyn2-K44A* mRNA when compared to the control embryos. Overexpression of Hsc70 and Rab5 showed the intensity levels similar to control embryos (B). Quantification of area of Fgf8 clusters in Hsc70 overexpressed embryos when compared to control embryos. (C). ($p<0.05$)

Quantification of the distance of diffusion and intensity of GFP

Using software-based, automated quantificatin method (Olympus Cell D software) the area of *erm* and *pea3* expression was analyzed and this further confirmed the significant increase in target gene expression in Hsc70 knock-down embryos. The length and the width of *erm* and *pea3* expression were measured and the corresponding area for each was calculated for the control, Hsc70 knock-down as well as Hsc70 overexpressed embryos. The area of expression was then compared during control, Hsc70 knockdown and Hsc70 overexpression to anlyze if the area of Fgf target gene expression altered during Hsc70 loss or gain of function. The quantification analysis displayed that the area of expression of *erm* in Hsc70 overexpressed embryos did not show a significant change when compared to the control embryos. However, a significant increase in the area of expression of *erm* and *pea3* in the Hsc70 knock-down embryos was seen in comparison with the area of expression in control embryos. Ectopic injection of Hsc70 mRNA in Hsc70 morphant embryos rescued the area of expression of *erm* and *pea3* down to a level similar to the control embryos as shown in Figure 4G. The same procedure was followed for analysis of change in the area of expression in SU5402 treated embryos. The quantification analysis showed that area of target gene expression in SU5402 treated embryos as shown in Figure 4G was significantly reduced when compared with control embryos. Hsc70 knock-down embryos treated with SU5402 also showed a significant reduction in the Fgf target gene expressions when compared with the control embryos (Figure 4G; Statistically significant, $p<0.05$).

To determine if Fgf8 spreading from its source was altered during loss or gain of Hsc70 function, the distance travelled by Fgf8 from its source *in vivo* was measured by confocal data analysis using IMARIS. Blockage of Hsc70 function led to an increase in the range of spreading of Fgf8 to upto 7 cells when compared to control embryos where Fgf8 spread to a distance of about 4 cells away from the source tissue as shown in Figure 9A.

Expression of dominant negative mutant of Dynamin2, Dyn2 K44A, also led to an increase in the range of spreading of Fgf8 of about 6 cells away from the source tissue l. Gain of Hsc70 function showed a range of Fgf8 spreading of about 4 cells away from its source similar to that of control embryos. Expression of Rab5 also showed no change in the range of Fgf8 spreading from the source tissue.

These results are consistent with our ISH based analysis of the endogenous Fgf8 signaling range (Figure 2), wherein the range of Fgf8 signaling was significantly increased during Hsc70 loss of function but did not alter during Hsc70 gain of function.

Next the fluorescence intensity of Fgf8-GFP was measured using IMARIS software and it was quantified to measure of the stability of Fgf8 in embryos (Figure 9B). In Control, Hsc70 knockdown, Hsc70 overexpressed, Dyn2 K44A and Rab5 mRNA injected embryos, the average pixel intensity was measured. The analysis of flourescence intensity showed that Fgf8 protein expression was significantly higher when internalization was blocked in Hsc70 knockdown and Dyn2 K44A injected embryos in comparison with control embryos. However, intensity analysis showed that Fgf8 protein expression during Hsc70 and Rab5 function was similar to control embryos. This data suggests that the increased internalization and the subsequent accumulation in endosomes are associated with Fgf8 degradation. Flourescence intensity measurement has been used as a valid method for protein expression analysis in the past (Wang et al., 2006, Toyoda et al., 2010, Nowak et al., 2011).

To determine if clustering of Fgf8indeed occurs during Hsc70 expression, the area of Fgf8 clusters was measured in comparison with control. Anlysis of Fgf8 cluster area was performed using ImageJ data analysis software as shown in Figure 9C. The area of Fgf8 clusters was significantly increased in Hsc70 expressing embryos in comparison with the control (Statistically significant, $p<0.05$). This confirms the theory that Fgf8 does indeed get intracellularly accumulated during Hsc70 expression.

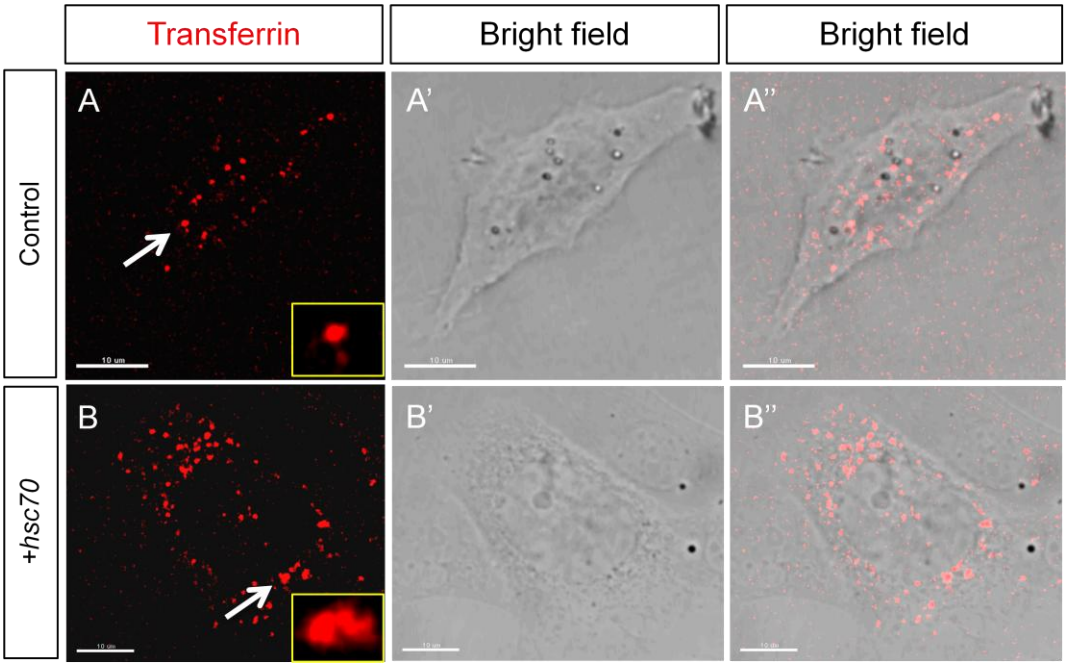

Figure 10: **Intracellular clustering of molecules due to Hsc70 function a general mechanism.**Confocal analysis of Texas Red Transferrin localization in zebrafish PAC2 cells. Overexpression of Hsc70 (B-B") showed intracellular clustering of Texas Red Transferrin when compared to the control (A-A").

Intracellular clustering of molecules due to Hsc70 function a general mechanism

Endocytosis of transferrin was seen through EM autoradiography (Morgan et al., 1967). The process involves the binding of transferrin to its receptor at the plasma membrane and the internalization of the ligand receptor complex through the process of endocytosis into intracellular vesicles. This process has been well studies in several cell types (Octave et al., 1981, Nunez et al., 1977, Ward et al., 1982, Sullivan et al., 1976).

To test whether the effect of Hsc70 on endocytosis is a general mechanism, we used a well-described cargo to visualize CME, the activated transferrin receptor complex. Transferrin was observed to be in the form of clusters in Hsc70 stimulated cells (Figure 10B-B'') in comparison to control (Figure 10A-A''). This phenotype is similar to the clustering Fgf8 in zebrafish embryos during Hsc70 expression (Figure 8B-B"). Previous studies have shown that an increase in the rate of endocytosis due to Rab5 overexpression led to enlarged endosomes (Bucci et al., 1992).

To better understand which intracellular compartment is associated with Fgf8 localization that is increased by Hsc70 overexpression, a cell culture assay was performed.

Three sets of samples Zebrafish PAC2 cells were transfected with Fgf8 GFP, a tagged endocytic marker (Clathrin, Rab 5-mCherry, Rab7 or LAMP1) alone serving as a control and Hsc70 along with the respective intracellular marker. The Fgf8 transfected cells were then co transfected with the control cells as well as cells expressing Hsc70.

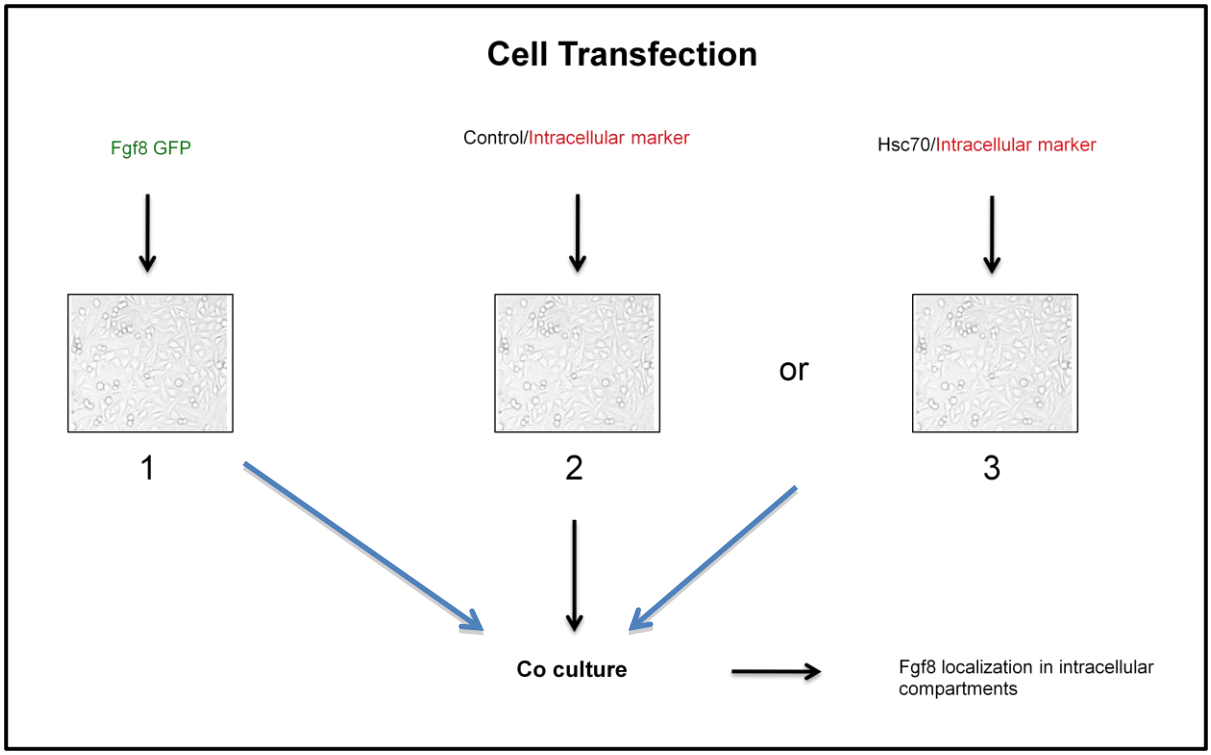

Figure 11: Cell transfection: Co-transfection of Fgf8 GFP in control as well as Hsc70 expressing cells along with an endocytic marker used as an assay to determine localization of Fgf8.

Determination of the role of clathrin in Hsc70 mediated Fgf8 uptake

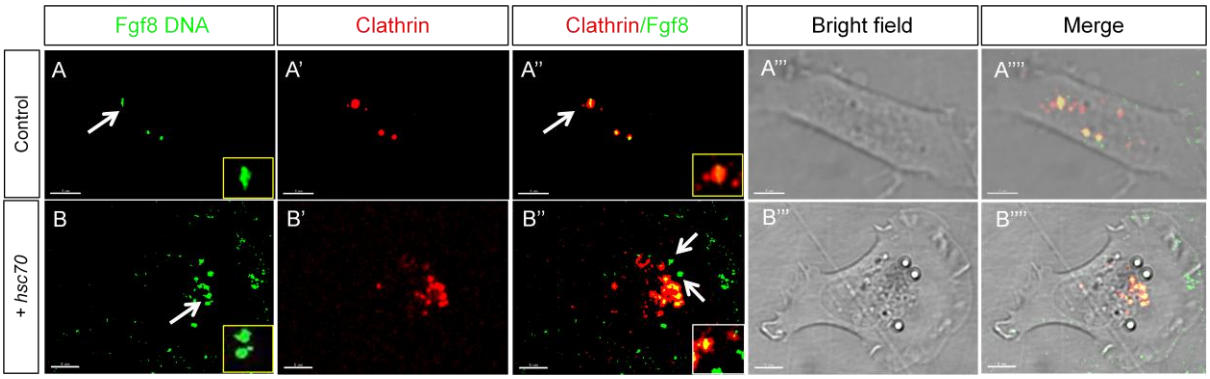

Figure 12: Determination of the role of clathrin in Hsc70 mediated Fgf8 uptake. (A, B). Showed intracellular localization of Fgf8-GFP in zebrafish PAC2 cells. Over expression of Hsc70 (B-B") showed a decrease in the localization of Fgf8 in clathrin positive vesicles in comparison with control (A-A").

When clathrin coated vesicles were marked with m-RFP clathrin light chain A in transfected cells, a strong colocalization of clathrin was found with Fgf8 as shown in Figure 12A-A''''. Co-transfection of Hsc70 and clathrin displayed Fgf8 clusters that were negative for clathrin (Figure 12B-B''''), suggesting that Hsc70 may aid in the removal of clathrin coat from the vesicles (Holstein et al., 1996, Ungewickell et al., 1995, Newmyer and Schmid, 2001).

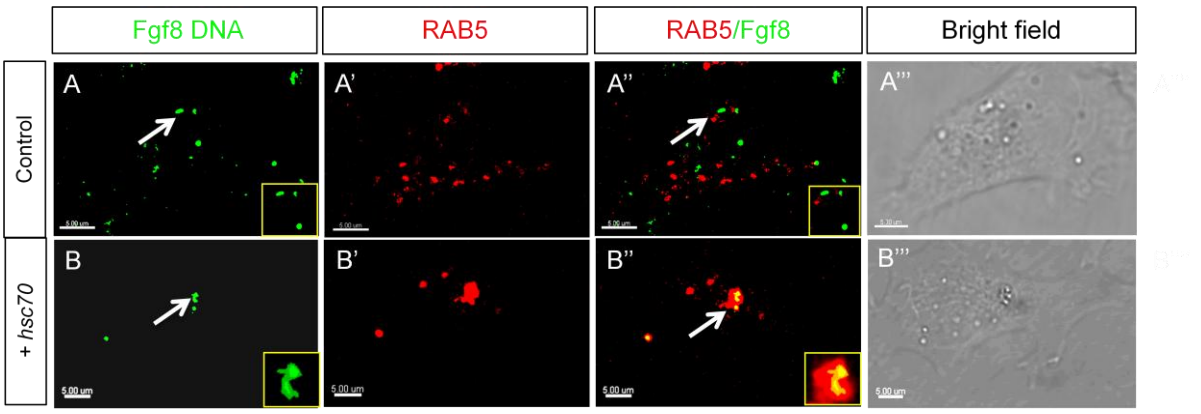

Figure 13: Hsc70 facilitates Fgf8 uptake in early endosomes. (A, B) shows localization of Fgf8 in Rab5 positive vesicles during presence and absence of Hsc70. Overexpression of Hsc70 showed an increase in the localization of Fgf8 in Rab5 positive vesicles (B-B'''') when compared to the control (A-A").

Hsc70 facilitates Fgf8 uptake in early endosomes

To further analyze the localization of Fgf8 clusters formed during Hsc70 overexpression, the cells were transfected with Rab 5-mCherry, a tagged early endosomal marker, as shown in Figure 13. These cells were then co-transfected with Hsc70 expressing cells. Fgf8 colocalized with Rab5-mCherry positive vesicles in control cells (Figure 13A-A''''), thereby indicating that Fgf8 uptake in early endosomes occurs in a fast and transient manner. Conversely, when the cells were transfected with Hsc70, Fgf8 clusters colocalized with Rab5 positive early endosomes (Figure 13B-B''''). These results suggest that the expression of Hsc70 triggered the formation of Fgf8 clusters/accumulation of Fgf8, at Rab5 positive early endosomes.

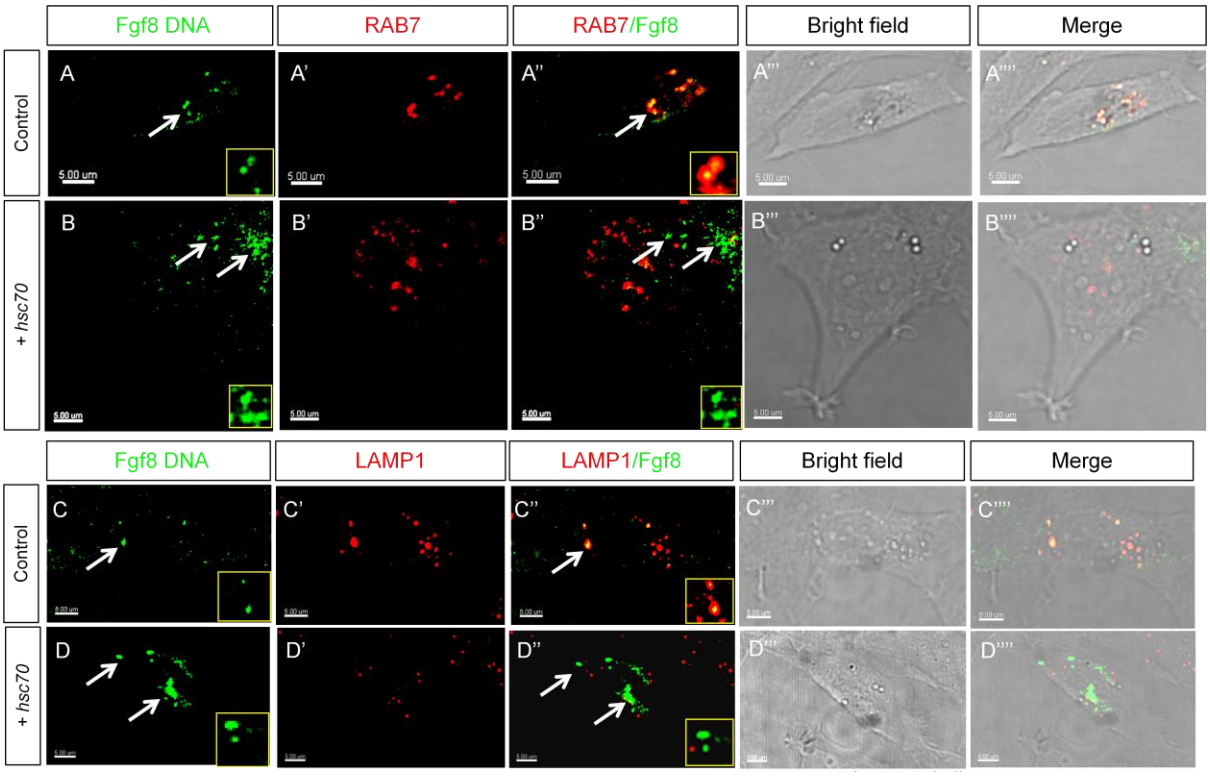

Figure 14: Showed localization of Fgf8 in Rab7and LAMP1 positive vesicles during presence and absence of Hsc70. Overexpression of Hsc70 (B-B") showed a decrease in the localization of Fgf8 in Rab7 and LAMP 1 (D-D'') positive vesicles when compared to the control (A-A", C-C'''').

To further study the role of Hsc70 in Fgf8 uptake, cells were transfected with a tagged version of late endosomal marker, Rab7-mCherry. Colocalization of Fgf8 and Rab7 was then analyzed in control as well as Hsc70 expressing cells, as shown in Figure 14. In control cells, Fgf8 was observed to colocalize with Rab7 (Figure 14A-A’’’’). Again, Hsc70 activated cells showed clustering of Fgf8. However, these Fgf8 clusters were not found to colocalize with Rab7 positive vesicles (Figure14B-B’’’’).

To analyze the localization of Fgf8 at lysosomes, cells were transfected with lysosomal marker LAMP1. Fgf8 localization was analyzed during Hsc70 function. Results from these studies, as shown in Figure 14D-D’’’’, displayed minor colocalization of Fgf8 and LAMP1 in control cells. Cells activated with Hsc70 also showed minimal colocalization of Fgf8 and LAMP1. Weak colocalization of Fgf8 with Lamp1 positive lysosomes (Figure 14D-D’’’’), may be explained by fast degradation of fluorescent signal of Fgf8-GFP. Also, reduced colocalization of Fgf8 at the lysosomal compartment may be due to change in the intracellular trafficking leading to accumulation of Fgf8 in the early endosome.

Quantification of Fgf8 localization

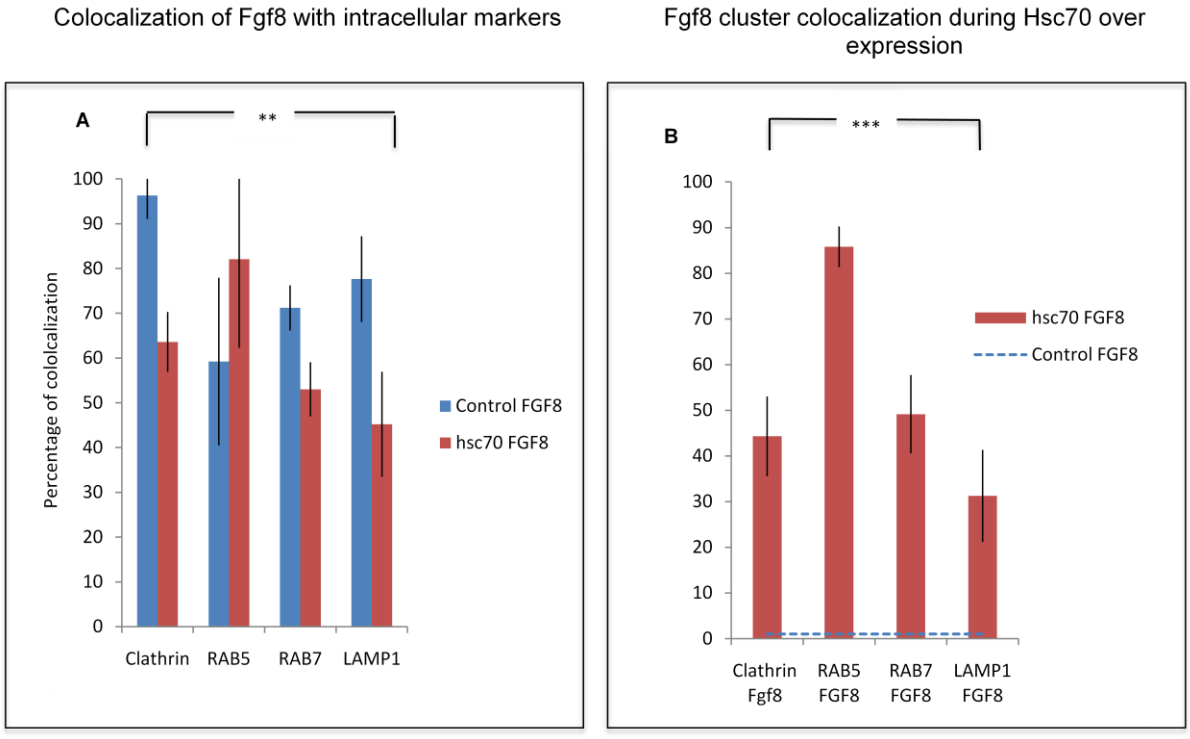

Figure 15. Quantitative analysis of localization of Fgf8 during overexpression of Hsc70. Quantification of colocalization of Fgf8 with different endosomal markers showed an increase in the colocalization of Fgf8 and Rab5 during Hsc70 overexpression in comparison with control (A). Quantification of the localization of Fgf8 clusters found during overexpression of Hsc70 showed an increase in the localization of Fgf8 clusters in Rab5 positive vesicles when compared to Clathrin, Rab7 and LAMP1 positive vesicles (B).

The localization of Fgf8 in Clathrin, Rab5, Rab7, and LAMP1 vesicles was analyzed by confocal microscopy and measured using IMARIS software as shown in Figure 15. In control as well as Hsc70 stimulated cells, the number of Fgf8 molecules as well as the vesicle marked were counted using IMARIS confocal and data analysis software. Twenty cells each in control and Hsc70 expressing cells marked for Clathrin, Rab5 and Rab7 as well as LAMP1 were analyzed for the localization of Fgf8 in the various endosomes. In control cells marked for clathrin, about 97% colocalization of Fgf8 and Clathrin was observed. Cells expressing Hsc70 however, showed a reduction in colocalization of Fgf8 and Clathrin to about 65%. Control cells marked for the early endosomal marker Rab5 showed a 60% colocalization of Rab5 and Fgf8. However, cells expressing Hsc70 showed an increase in the colocalization of Fgf8 and Rab5 to about 85%. Control cells marked for the late endosomal marker showed a 70% colocalization of Fgf8 and Rab7. However, upon Hsc70 stimulation, the localization of Fgf8 at the late endosomes was reduced to 55%.

Cells marked for lysosomes with LAMP1 showed a percentage of localization of Fgf8 and LAMP1 at about 80%. However, Hsc70 stimulated cells showed a decrease in the localization of Fgf8 in LAMP1 to about 50%. The analysis of the localization of Fgf8 in the endosomes during Hsc70 expression displayed an increase in the uptake of Fgf8 by CME. Upon Hsc70 function, Fgf8 is then routed through Rab5, and accumulated at the early endosomes (Figure 15A, B). The accumulation of Fgf8 during Hsc70 expression might in turn lead to a delay in its transport to the late endosomes as well as lysosomes (Statistically significant, $p<0.05$).

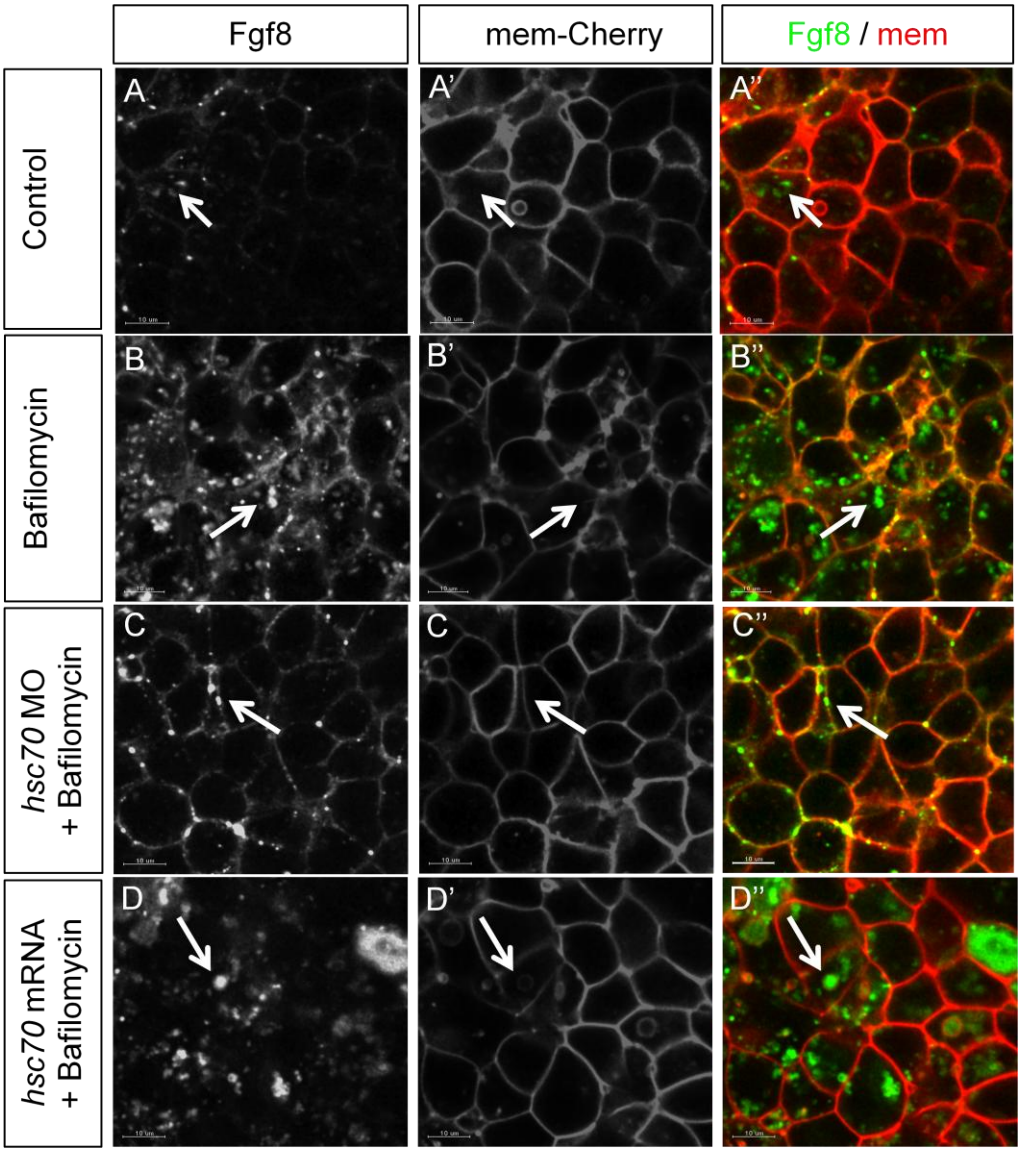

Figure 16: Inhibition of Fgf8 transport from early to late endosome results in cluster formation. Analysis of localization of Fgf8-GFP during inhibition of endocytic transport from early to late endosomes by treatment with Bafilomycin A1. Embryos were injected with Fgf8-GFP along with the membrane marker mCherry at one cell stage, treated with 100 nM Bafilomycin at 30% epiboly stage for a period of 1 hr and subjected to live imaging using confocal microscopy at 50% epiboly stage. Treatment of embryos with Bafilomycin resulted in an increased formation of intracellular clusters of Fgf8 (B-B") compared to control untreated embryos which showed localization of Fgf8 at the membrane and intracellularly (A-A"). Knockdown of Hsc70 showed an inhibition of internalization of Fgf8 and an accumulation of Fgf8 in the extracellular space (C-C") Overexpression of Hsc70 showed an increase in the intracellular clustering of Fgf8 (D-D'').

Inhibition of Fgf8 transport from early to late endosome results in cluster formation

To analyze the localization of Fgf8 during blockage of transport from early to late endsomes, embryos were treated with Bafilomycin A1, an inhibitor of cargo transport from early to late endosomes (Hurtado-Lorenzo et al., 2006), and analyzed at blastula stage, as shown in Figure 16. Wildtype embryos, treated with Bafilomycin displayed the formation of intracellular clusters (Figure 16B-B''), in comparison with control embryos (Figure 15A-A'').Embryos knockdown for Hsc70 Figure 16C-C'' and treated with Bafilomycin did not display any intracellular clusters, but showed extracellular accumulation of Fgf8 similar to the Hsc70 knockdown phenotype. Embryos overexpressed with Hsc70 (Figure 16D-D'') displayed enhanced intracellular clustering of Hsc70 in comparison with the control embryos (Figure 16A-A'').

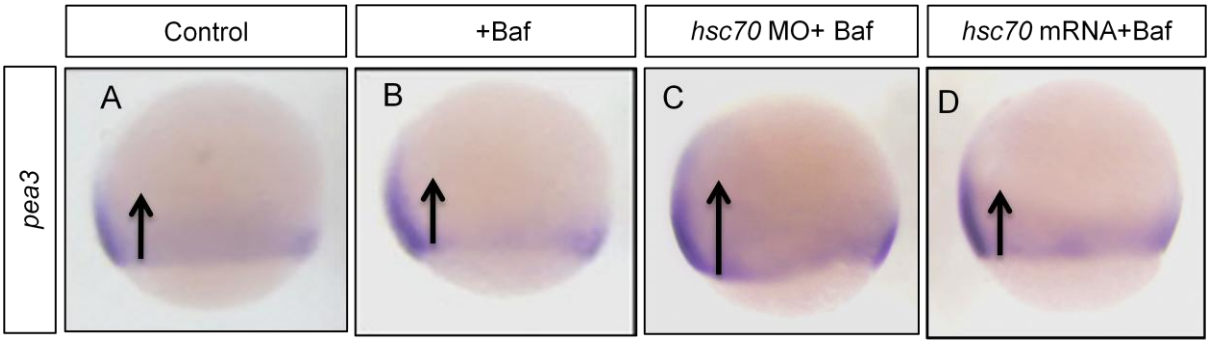

Figure 17: Inhibition of Fgf8 transport from early to late endosome does not alter signaling range. Bafilomycin A1, treatment does not alter induction of *pea3* induction (A, D). Knockdown of Hsc70 lead to an increased activation of *pea3* expression (C), however, overexpression of Hsc70 does not alter the signaling range of Fgf8 (D) in comparison with the control embryos (A).

Blockage of transport from early to late endosomes does not alter the range of Fgf signaling

To determine if blockage of transport from early to late endosome affects the Fgf signaling range, *In situ* hybridzation of Control, *hsc70* morphant as well as *hsc70* over expressed embryos treated with Bafilomycin was performed as shown in Figure 17. Embryos treated with Bafilomycin did not show an enhancement of the expression of *pea3* in comparison with the control embryos (Figure 17A, B). *hsc70* morphant embryos treated with Bafilomycin however showed an enhancement of pea3 expression compared with the control embryos (Figure 17C, A). *hsc70* overexpressed embryos did not show a difference in the

expression pattern in comparison with the control embryos (Figure 17D, A).The above results suggest that blockage of transport of Fgf8 from early to late endosomes performed with Bafilomycin, does not alter the range of Fgf signaling. This is similar to the results showing that even though Fgf8 is accumulatedat the early endosomes (Figure 13), the range of Fgf signaling remains unaltered during Hsc70 function (Figure 2).

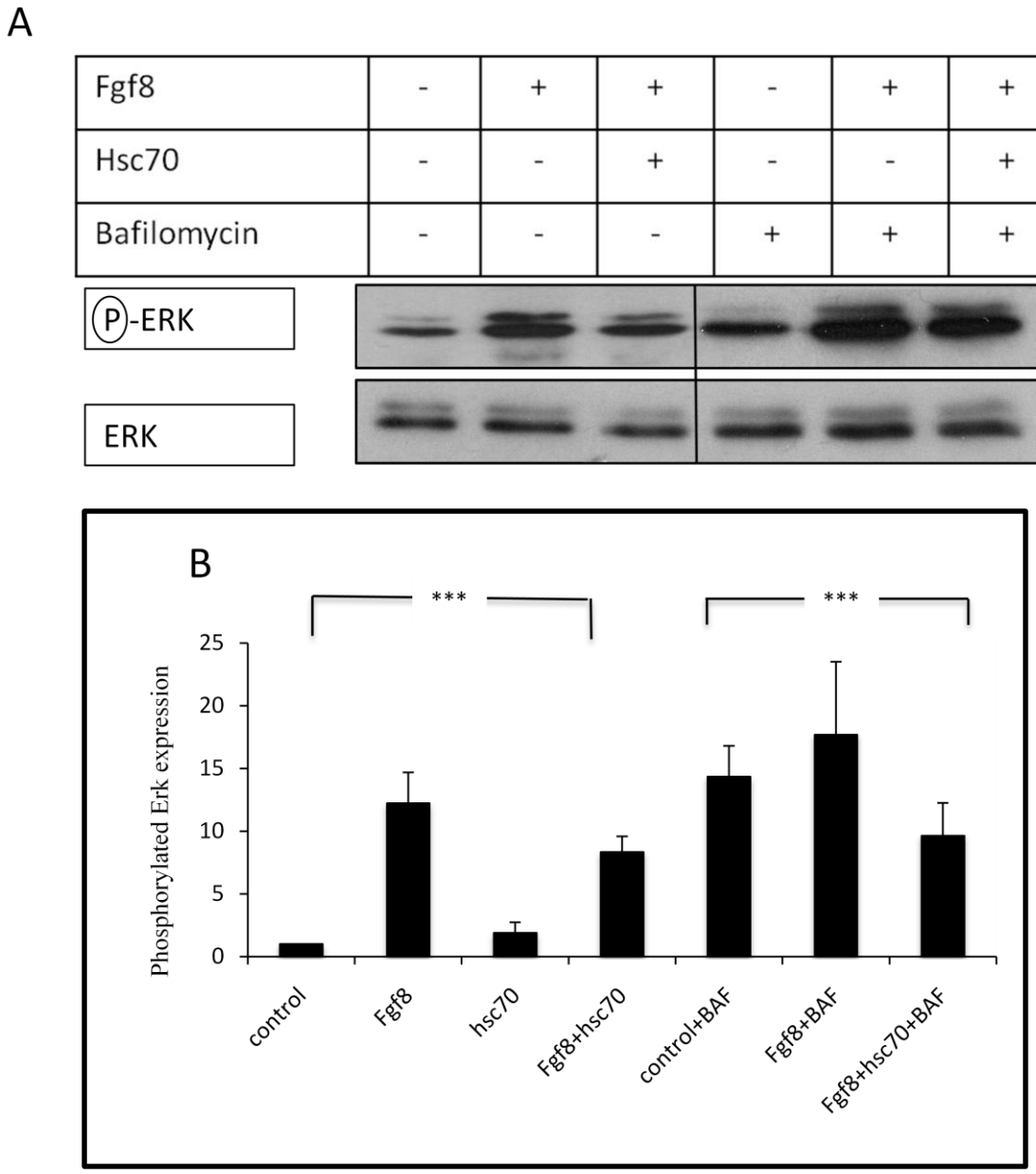

Figure 18: Transport of Fgf8 from early to late endosomes controls signal activity**. A.**Cultivation of HEK293 cells after transfection with Fgf8, and Hsc70 with and without treatment of Bafilomycin A1. Three independent experiments were analyzed and the ratio between activated Erk1/2 and Erk total was calculated. Cells transfected with Fgf8 show a significant 3.3-fold increase in Erk1/2 phosphorylation compared to the untransfected control.

Co-transfection of Hsc70 and Fgf8 leads to a decrease of phosphorylation of Erk. Treatment with Bafilomycin A1 leads to a significant increase of phosphorylated Erk1/2 levels. Activation by co-transfection of Fgf8 also leads to a significant increase, whereas co-transfection of Hsc70 and Fgf8 reduced the activation of double phosphorylated Erk. B. Quantification.

Hsc70 reduces the signaling activity of Fgf8

To determine the effect of Fgf8 endocytosis on its signaling activity, a cell cultivation assay was performed in which effective activity of Fgf8 signaling was analyzed by quantification of levels of Erk1 and Erk2 phosphorylation as shown in Figure 18 A, B. Transfection of Fgf8 led to a significant increase in the level of Erk½ phosphorylation compared to the unstimulated control cell. However, co transfection of Fgf8 and Hsc70 showed a significant decrease in the level of Erk½ phosphorylation when compared to the cells transfected only with Fgf8. Previous experiments showed that during Hsc70 expression, the presence of Fgf8 in the extracellular space was significantly reduced compared to normal conditions (Figure 8). Furthermore, accumulation of Fgf8 at the early endosomes might suggest that Hsc70 increases the rate of internalization and transport of Fgf8 to early endosomes. However, quantification of the fluorescence of Fgf8-GFP indicated that degradation of Fgf8 is not altered by Hsc70 overexpression. With regard to this, an increase in the Erk1/2 phosphorylation levels during Fgf8 tranfection shows that the increase in the activity of Fgf8 signaling might be due to the increase in the amount of Fgf8 at the plasma membrane, suggesting that Fgf8 signaling predominantly takes place at the plasma membrane. However, transfection of Hsc70 along with Fgf8 decreased the level of Erk1/2 phosphorylation suggesting that the signaling activity of Fgf8 is reduced upon internalization into early endosomes.

Fgf8 signaling activity increased during blockage of transport from early to late endosomes

To determine if the activity of Fgf8 signaling is altered during its accumulation at the early endosomes, Bafilomycin was used for blockage of early to late endosomal transport and the expression levels of phosphorylated Erk1/2 was measured by western blot analysis. Treatment with Bafilomycin A1 led to an increase in the level of Erk½ phosphorylation in comparison with the control experiment, suggesting that Pac2 Fibroblasts express endogenous Fgf ligands (Figure 18 A, B). Co-transfection of Fgf8 further increased the Erk1/2 phosphorylation levels. An increase in the activity of Fgf8 signaling during Bafilomycin treatment might be due to the loss of Fgf8 degradation as its transport to the late endosomes and lysosomes was inhibited. Therefore the transport from early to late endosomes might be a required step for the regulation of the signaling activity of Fgf8. However, co-transfection of Hsc70 and Fgf8 showed a significant decrease in the level of Erk1/2 phosphorylation. This observation supports the idea that Fgf8 has an increased signaling activity at the plasma membrane compared to the early endosomes. The increase in Fgf8 signaling activity in the presence of Bafilomycin A1 only might also be due to loss of degradation as the transport to late endosomes was inhibitied. The increase in Fgf signaling during Bafilomycin A1 treatment may also be due to increased accumulation of Fgf8 at the plasma membrane because of the intracellular trafficking caused by the function of Bafilomycin. An increase in the extracellular accumulation of Fgf8 during Bafilomycin treatment as shown in Figure 16, is consistent with this.

Discussion

AIM 1	To determine the role of Hsc70 on the range of Fgf signaling during • early Zebrafish development. *In situ* Hybridization
AIM 2	To analyze the effect of Hsc70 on Fgf8 localization and spreading Confocal Microscopy Analysis
AIM 3	To evaluate the change in the activity of Fgf signaling upon endocytosis Western Blot
AIM 4	To analyze the activity of Fgf signaling during inhibition of transport to the late endosomes Western Blot
AIM 5	To validate the efficacy of Hsc70 function in CME *in vivo* using Zebrafish model

Outcomes

- Hsc70 regulates Fgf signaling in early Zebrafish development
- Loss of Hsc70 function leads to an increase in the Fgf signaling range
- Gain of Hsc70 function does not alter the Fgf signaling range
- Loss of Hsc70 function leads to an inhibiton of Fgf8 endocytosis and an increase in its accumulation at the plasma membrane
- Gain of Hsc70 function leads to a decrease in the extracellular accumulation of Fgf8 and an increase in the formation of intracellular Fgf8 clusters
- The intracellular clusters of Fgf8 formed during Hsc70 expression were localized at the early endosome.
- Inhibiton of Fgf8 transport from early to late endosome showed a similar intracellular Fgf8 clustering as well as an increase in the amount of Fgf8 at the plasma membrane
- Hsc70 reduces Fgf signaling activity
- Inibition of Fgf8 transport from the early to late endosomes increases the Fgf signaling activity
- Fgf signaling activity takes place predominantly at the plasma membrane and is reduced upon internalization

Figure 18: The schematic diagram shows the overview of the study.

Morphogens

The concept that "positional information" is received by cells that directs them to develop specifically based on their position within a tissue, was brought about over a century ago (Wolpert, 1969). In the years that followed, signaling gradients were shown to be responsible for providing this information (Nahmad and Stathopoulos, 2010, Green, 2002) and these signals were termed as morphogens (Ashe and Briscoe, 2006). A morphogen may be defined as a signaling molecule that regulates cellular behavior in a concentration dependent manner by eliciting specific cellular responses (Tabat and Takei, 2004).

Morphogen Gradient

Through the formation of morphogen gradients, morphogens have been shown to be responsible for formation of tissue patterns during embryonic development (Lewis et al., 1977, Green and Smith, 1991, Gurdon and Bourillot, 2001, Tabata and Takei, 2004). As the signaling molecule spreads from a localized source to the surrounding region, a concentration gradient is formed. The graded signal then directs the cells to identify changes in gene expression as well as to specify cell fate, in a concentration dependent fashion. In this manner, the ligand concentration provides information to the cells of their position in relation to the signal source thereby, organizing the patterning of cell differentiation (Ashe and Briscoe 2006). The fate of the cell therefore, is dependent on its distance from the source of the morphogen. This along with the presence of other morphogen gradients together results in the formation of intricate patterns during the organism development (Bollenbach et al., 2005). The morphogen gradient induces the expression of distinct set of genes leading to patterning of the tissue during development (Morgan, 1901, Stumpf, 1966, Wolpert, 1969, Crick, 1970). The formation of such a gradient and the subsequent signaling range greatly depends on the mechanism by which these morphogens are transported even though the exact mechanism of transport have not been conveyed by them (Müller et al 2013). Also, in order to maintain a morphogen gradient in a stable steady state, morphogens need to be degraded at a constant rate (Wartlick et al., 2009).

In this study I analyzed the regulation of Fgf8 signaling by a mechanism that controls morphogen transport and degradation, CME**.** For this I discuss my results with respect to two seperate processes in Fgf signaling: The range of Fgf signaling and the activity of Fgf signaling during altered rates of CME. I then summarize my results and conclude with possible future experiments with respect to this study.

Role of CME in Fgf signaling range

The most common receptors for Fgf8, Fgfr1, Fgfr3 and Fgfr2, have been known to localize to clathrin coated pits (Jean et al., 2010)(Jean et al., 2010)(Jean et al., 2010)(Jean et al., 2010)(Jean et al., 2010)(Jean et al., 2010)(Jean et al., 2010)(Jean et al., 2010)(Jean et al., 2010)(Jean et al., 2010)(Jean et al., 2010)(Jean et al., 2010)(Jean et al., 2010)(Jean et al., 2010). This was confirmed by inhibition of Fgfr2 endocytosis in models where clathrin was depleted (Belleudi F, 2005). Although the role of Fgf8 in the embryonic development of zebrafish has been well studied (Tabata, T. & Takei, Y., 2004, Reifers et al., 1998, Scholp and Brand, 2004), the concept of how Fgf8 diffuses through the tissue seems to be one that is controversial. Analysis of Fgf8 diffusion showed that Fgf8 travelled from a conserved source forming a concentration gradient as it spreads through the tissue (Yu et al., 2009). The transport of Fgf8 was shown to be regulated by receptor-mediated endocytosis in the target tissue (Scholpp and Brand, 2004), which in turn altered the formation of a morphogen gradient. Furthermore, it was suggested that apart from the internalization of Fgf8, the endocytic trafficking of Fgf8 is also responsible for the regulation of a morphogen gradient (Nowak et al., 2011). Fgf8 was also shown to be internalized through caveolin mediated endocytosis (Nowak et al., 2011). In my study I show that Fgf8 is internalized via CME and its spreading through the tissue is also influenced by the same process. Indeed, previous studies have shown the crucial role of Hsc70 in CME (Eisenberg E, Greene LE., 2007, Holstein SE et al, 1996, Ungewickell E et al 1997, Schlossman et al., 1984, Chappell et al., 1986). The ATPase activity of Hsc70 is naturally low and this ATPase activity is stimulated by cofactors such as Auxilin and Cyclin G associated Kinase (GAK) (Ungewickell et al., 1995, Bukau and Horwich, 1998, Kanaoka et al., 1997, Umeda et al., 2000). Auxilin contains a conserved J-domain motif and a clathrin binding domain, and the ATP- bound Hsc70 is recruited by Auxilin via this J domain after it binds to the CCVs (Ungewickell et al., 1995, Holstein et al., 1996). At the start of CME, Hsc70 and its co-chaperone auxilin or GAK, assist clathrin as well as the adaptors to bind to

the cell membrane. During invagination of the Clathrin Coated Pits (CCP), Hsc70 and its co-chaperone Auxilin, initiate clathrin exchange thereby altering the pit curvature. After budding, Hsc70 and Auxilin initiate the uncoating of the CCVs. Hsc70 then removes Clathrin and primes it for its binding to the plasma membrane pits (Jiang et al, 2000). In this way, it has been shown through *in vitro* studies that CCVs are uncoated through the attachment of Hsc70 and its co chaperone Auxilin. Clathrin is subsequently removed through ATP hydrolysis (Eisenberg and Greene, 2007, Holstein et al., 1996, Schlossman et al., 1984, Chappell et al., 1986, Ungewickell et al., 1995). Hsc70 is therefore required for endocytosis and loss of Hsc70 function shows defects in endocytosis.

The schematic diagram as shown in Figure 19, displays the role of Hsc70 in CME.

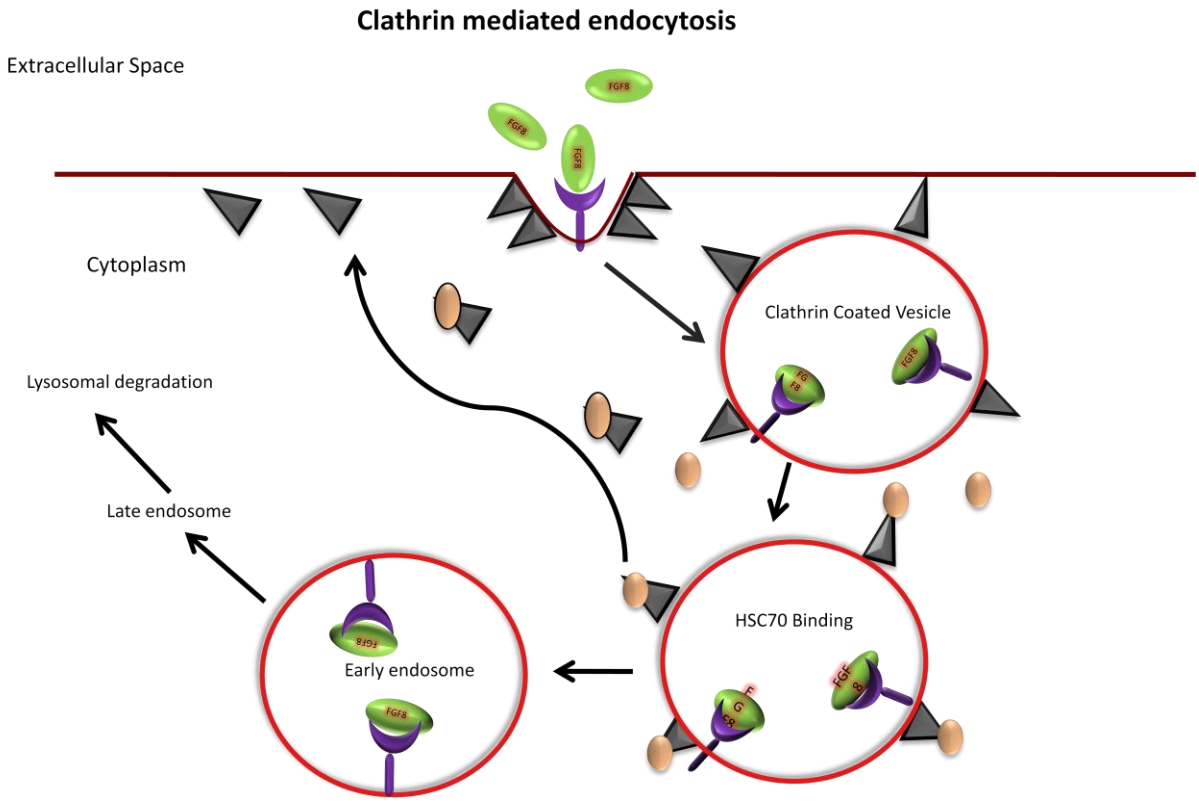

Figure 19: Clathrin mediated endocytosis (CME) of Fgf8. Fgf8 binds to the receptor and is internalized into CCVs. Hsc70 uncoats the CCVs and the ligand receptor comples is sorted to late endosomes and towards lysosomal degradation.The rate of CME is accelerated by Hsc70.

Does Hsc70 play a similar role *in vivo* in zebrafish is an interesting question that has not been addressed so far. My study shows that Hsc70 does indeed regulate endocytosis more specifically CME of Fgf8 as well as endocytic trafficking of Fgf8 during zebrafish development.

Inhibition of endocytosis by Hsc70 knockdown leads to increase in Fgf signaling range

Previous studies have shown that loss of endocytosis leads to an increase in the signaling range of Fgf (Scholpp and Brand, 2004, Nowak et al., 2011). In my study I show that loss of Hsc70 function also leads to an expansion of the Fgf target gene expressions as shown in Figure 1 and 2. Knockdown of Hsc70 function lead to a significant expansion of the Fgf target genes *erm* and *pea3* in comparison with the control embryos. As previously described, Hsc70 is a critical regulator of CME, these results may suggest that the Fgf signaling range is regulated by the process of CME through Hsc70 (as shown in the schematic diagram Figure 19). This has also been shown in previous studies, where an increase in Fgf signaling range was also observed when CME was inhibited by blockage of Rab5 function through RN-Tre (Scholpp et al., 2004b). These results were further supported by (Nowak et al., 2011), who blocked the ubiquitination of receptors and lysosomal transport by Cbl. This lead to a pronounced spreading of the signaling molecule from its source thereby increasing Fgf signaling range. Therefore we can infer that Fgf signaling range is increased during loss of CME as shown in Figure 1 and 2.

Increased rate of endocytosis does not alter Fgf signaling range

To analyze if the rate of CME by Hsc70 has an effect on the signaling range of Fgfs, expression of Fgf target genes *erm*, *pea3* were studied in Hsc70 overexpressed embryos (Figure 1 and 2). The expression domain of *erm* and *pea3* did not change during Hsc70 overexpression in comparison with the control conditions. This could be due to enhanced cell migration (epiboly) during the developmental stage investigated and hence a reduction in the expression domains of *erm* and *pea3* could not be observed. In support of our results, it has been shown that an increased rate of endocytosis uncoupled from cell migration leads to a decrease of the spreading range (Scholpp et al., 2004b).

Hsc70 regulates Fgfr mediated signaling

The results shown in Figure 1 and 2 suggest that Fgf signaling is regulated by CME through Hsc70. To further clarify the specific role of Hsc70 in Fgf signaling, its effect on Fgfr mediated signaling was analysed using Fgfr inhibitor SU5402. SU5402 is a commonly used inhibitor of Fgfr and has been previously used to study the role of Fgfr mediated signaling during embryonic development (Widberg et al., 2009, Shinya et al., 2001, Londin et al., 2007). In my studies, I show that treatment of embryos with SU5402 (Figure 4), showed a significant reduction in the Fgf target gene expressions in control as well as Hsc70 knockdown embryos. The reduction in the Fgf target expressions due to SU5402 treatment and the maintenance of such a reduced expression in Hsc70 knockdown embryos suggest that Hsc70 does indeed inhibit Fgfr mediated signaling. This is consistent with a previous study where SU5402 treatment lead to a significant reduction in Fgf target gene expression in comparison with the control embryos (Scholpp and Brand, 2004). This suggests that Fgfr mediated signaling is regulated by CME through Hsc70. My studies however show that while the Fgf target gene expressions were altered during inhibition of endocytosis, the expression domain of the protein Fgf8 remained unaltered (Figure 5). This is consistent with previous study where even though inhibition of endocytosis displayed alterations in Fgf target gene expressions, the expression of the ligand Fgf8 remained unchanged (Nowak et al., 2011).

Fgf morphogen gradient achieved through CME

In order for a diffusive morphogen gradient to attain a steady state, there needs to be a ligand "sink" (Muller and Schier, 2011, Wartlick et al., 2009, Muller et al., 2013). This could be achieved through endocytic removal of the ligand-receptor complexes from the surface of the cell, otherwise refered to as the restrictive clearance model. Previous studies have shown that internalization of Fgfrs occur through CME in a ligand dependent manner (Nowak et al., 2011, Yu et al., 2009, Auciello et al., 2013, Jean et al., 2010). Alterations in internalization and spreading of Fgf8 due to changes in the rate of endocytosis and the subsequent alterations in gene expression supports the theory of restrictive clearance of Fgf8 (Scholpp and Brand, 2004). Movement of Fgfs via the model of hindered diffusion for morphogen transport has also been suggested by recent studies in zebrafish embryos, as well as in mammalian cells *in vitro.* These have shed further light on Fgf movement, especially Fgf2 and Fgf8 over nano

and microscales (Duchesne et al., 2012, Yu et al., 2009, Nowak et al., 2011, Muller et al., 2013). The dorsoventral and animal vegetal axes of the zebrafish are patterned by Fgf8 during embryogenesis. Fgf8 signaling is characterized by the ligand production at a localized source, gradient formation through the process of diffusion, and the subsequent restrictive clearance through endocytosis (Scholpp and Brand, 2004, Yu et al., 2009). The pattern of Fgf8 gradient formation occurs at a slow rate and reaches equilibrium after 3 to 4 hours. The formation of such a gradient pattern over time is supported by the hindered diffusion model (Yu et al., 2009). In my studies, I show that alterations in the rate of CME by Hsc70 loss or gain of function results in changes in Fgf8 internalization and spreading. Embryos knocked down for Hsc70 function showed an accumulation of Fgf8 at the plasma membrane and ECS. During increase in the rate of endocytosis by Hsc70 overexpression, Fgf8 was not observed to be accumulated at the plasma membrane but was observed in the form of intracellular clusters. My results showing the alterations in uptake and spreading of Fgf8 during changes in the rates of CME by Hsc70 are in line with the theory of 'restrictive clearance' of Fgf8.

Role of CME in Fgf8 localization and trafficking

In my study I show that, inhibition of CME through loss of Hsc70 function leads to alterations in Fgf8 localization and spreading. The loss of Hsc70 function showed an increase in the accumulation of Fgf8 at the plasma membrane and in the ECS. Loss of Hsc70 function also showed a reduction in the presence of intracellular Fgf8 molecules (Figure 7). Since this loss of Hsc70 is associated with the inhibition of CME, the increase in the extracellular level of Fgf8 suggests that the uptake of Fgf8 by CME was inhibited. This is consistent with previous studies wherein Hsc70 mutant expressing cells showed a significant 10 fold reduction in Transferrin uptake in comparison to the wild type expression (Newmyer and Schmid, 2001). Studies have also shown the requirement of Hsc70 for the rebinding of the Clathrin to the CCPs (Eisenberg and Greene, 2007, Yim et al., 2010) suggesting that Hsc70 is required the maintenance of endocytosis.

In my studies I show that, blockage of CME by loss of Dynamin 2 function also leads to a similar extracellular Fgf8 accumulation when compared to the control embryos (Figure 7), suggesting that the loss of Hsc70 function does indeed inhibit endocytosis, and this therefore results in an increased amount of extracellular Fgf8. Consistent to this, it has been

previously shown that the inhibition of endocytosis through dynamin mutant Dyn2 k44a, does indeed result in a shallower concentration gradient of Fgf8 (Yu et al., 2009).

My studies show that gain of function of Hsc70 (Figure 8), on the other hand did not display an extracellular accumulation of Fgf8. Instead they showed an increase in the formation of intracellular Fgf8 clusters, as shown in Figure 8. As mentioned before, Hsc70 plays a key role in the uncoating of Clathrin Coated Vesicles (CCVs) during CME (Braell et al., 1984, Schlossman et al., 1984, Chappell et al., 1986, Prasad et al., 1993, Ungewickell et al., 1995, Greene and Eisenberg, 1990, Barouch et al., 1994). Hsc70 mutant cells showed inefficient CCV unocating activity in comparison with wildtype cells highlighting the requirement of Hsc70 in CCV uncoating (Newmyer and Schmid 2001). It has also been shown that the rate of the CCV uncoating activity is directly proportional to Hsc70 concentration (Flaherty et al., 1990, Morgan et al., 2001). Therefore expression of Hsc70 would result in endocytic trafficking of molecules in a concentration dependent manner. In my studies, the formation of intracellular clusters during Hsc70 overexpression (Figure 8), therefore suggests the development of endocytic trafficking due to Hsc70 function. At this stage, Hsc70 is also required for the recruitment of clathrin to the plasma membrane (Eisenberg and Greene, 2007). Therefore, an increase in the Hsc70 expression would then lead to an increase in the recruitment of clathrin to novel invagination sites for further endocytosis of Fgf8. This could possibly explain the lesser availability of Fgf8 at the plasma membrane during Hsc70 overexpression. In my studies, I show that an increase in the endocytic rate via Rab5 mRNA (Figure 8), also exhibit a similar loss of extracellular Fgf8 accumulation and an increase in the intracellular clustering of Fgf8. This suggests that intracellular clustering of Fgf8 maybe due to increased rates of CME by Hsc70 and Rab5. The analysis of the localization of these clusters of Fgf8 during Hsc70 expression was highly interesting. Measurement of the size of Fgf8 clusters in wildtype as well as embryos with Hsc70 overexpression, displayed a significant increase in the size of the Fgf8 clusters in test embryos in comparison with control embryos. This suggests that Hsc70 may indeed play a role in the formation of intracellular clusters of Fgf8 (Figure 9C).

The effect of Hsc70 on Fgf8 spreading

I analyzed the distance travelled by Fgf8 during Hsc70 loss or gain of function by measuring the distance of Fgf8-GFP molecules from the source cell. Quantification analysis as shown in Figure 9, suggests that the distance travelled by Fgf8 during loss of Hsc70 was significantly increased in comparison to wildtype. This shows that inhibition of CME through results in an increase in the distance travelled by Fgf8 from its. Indeed it has been shown that blockage of endocytosis by dynamin mutant leads to a shallowed Fgf8 gradient (Scholpp and Brand, 2004, Lin, 2004). Quantitative analysis of my data also shows that during increased rate of CME (by Hsc70 overexpression), the distance travelled by Fgf8 is comparable to the control conditions. The presence of Fgf8 molecules at a similar distance from the source as the control conditions maybe due to the recycling of Fgf8 back to the surface. Indeed it has been shown previously that recycling of endocytosed Fgf8 in embryonic tissue maybe be responsible for the gradient shape and maintenance (Nowak et al., 2011, Scholpp and Brand, 2004).

Upon analysis of the intensity of GFP in Fgf8-GFP, my results show that the GFP intensity seemed to increase during inhibition of CME through loss of Hsc70. Similarly my studies show that GFP intensity in Fgf8-GFP was also increased via Dynamin2 function. However, the intensity was decreased during increased rates of CME through gain of Hsc70 as well as Rab5 function. The increase in GFP intensity during CME inhibition might possibly be due to the inhibition of the rate of uptake and the subsequent degradation of Fgf8-GFP. A reduction in the GFP intensity during increased rates of CME maybe because increased rates of CME would result in the faster uptake and degradation of Fgf-GFP. Studies have shown that failure of transportation of the proteins by the chaperones results in the chaperones facilitating the degradation of the proteins (Sherman and Goldberg, 1992, Berkovich et al., 1997). Immunodepletion of Hsc70 from reticulocyte lysate showed that Hsc70 is required for the conjugation and degradation of substrates such as lysozyme, oxidized RNase A and BSA (Berkovich et al 1997). Therefore, apart from increasing the rates of CME, Hsc70 overexpression may result in endocytic trafficking leading to a faster degradation of Fgf8-GFP.

Intracellular movement of Fgf8

Previous studies have shown that upon internalization, the Fgf-Fgfr complexes enter the early endosomes and mainly proceed towards lysosomal degradation. While the Fgfr4 is sorted to the recycling endosomes, Fgfr1-3, the cognate receptors of Fgf8 (Mott et al., 2010), mostly proceeds towards lysosomal degradation (Haugsten et al., 2005, Citores et al., 1999). Fgf8 has also been shown to be mainly endocytosed by CME and its localization at the early, late, lysosomal and recycling compartments have previously been analyzed (Nowak et al 2011).

In an attempt to study the location of the intracellular clusters formed during increased rates of CME, colocalization of Fgf8 with endosomal markers was analyzed in Zebrafish PAC2 cells. My studies show that during Hsc70 gain of function, a decrease in the colocalization of Fgf8 with clathrin was observed in comparison with the control cells (Figure 12). This suggests that an increase in the endocytic rate by Hsc70 may result in the faster transport of Fgf8 from CCVs to other endosomal compartments. Indeed it has been shown previously that the process of uncoating of clathrin was a rapid one occurring soon after the membrane fission at approximately 5 seconds and this process was further catalysed by Hsc70 (Schmid and Rothman, 1985, Chappell et al., 1986, Greene and Eisenberg, 1990).

Upon further analysis of the intracellular localization of Fgf8, my studies show an increase in the colocalization of Fgf8 with the early endosomal marker Rab5, during Hsc70 expression in comparison with the control cells (Figure 13). Since Hsc70 has been shown to stimulate the rate of CCV uncoating (Morgan et al., 2001, Flaherty et al., 1990), Hsc70 expression might therefore increase the rate of Fgf8 transport from the plasma membrane to the early endosomes through its role in CCV uncoating. This could explain the accumulation of Fgf8 at the early endosomes during Hsc70 function. However, colocalization analysis of Fgf8 with the late endosomal marker Rab7 (Figure 14), showed no change during Hsc70 expression. Experiments using the lysosomal marker LAMP1 (Figure 14) also showed no change in the colocalization of Fgf8 with the lysosomal marker in comparison with the control cells. This suggests that during Hsc70 expression, although increased rate of uptake results in the accumulation of Fgf8 at the early endosomes, the subsequent rate of Fgf8 transport from early to late endosomal and the lysosomal compartment maybe unaltered. My quantitative data also show Fgf8 clusters localize at the early endosomes during Hsc70 expression (Figure 15).

These results together show that Hsc70 expression may lead to increased uptake of Fgf8 leading and its subsequent clustering at the early endosome.

Inhibition of Fgf8 transport from early to late endosomes results in Fgf8 accumulation

After CME, Fgf8 localizes to early and late endosomes. My results show that Hsc70 expression leads to the accumulation Fgf8 at the early endosomes (Figure 16) but does not affect Fgf8 transport to late endosomes and lysosomes. To analyze the effect of endocytic trafficking on Fgf8 localization, the transport of Fgf8 from early to late endosome was pharmocologically blocked with the help of that Bafilomycin A1 which blocks the acidification of early endosomes by inhibitin V-ATPase activity and thereby inhibiting cargo transport from early endosomes to late endosomes assisted by Arf6/ARNO (Hurtado-Lorenzo et al., 2006). As shown in Figure 16, blockage of Fgf8 transport to late endosomes with the help of Bafilomycin A1, resulted in intracellular clustering of Fgf8 similar to the clustering observed during Hsc70 overexpression. Therefore, increase in the rate of CCV uncoating as well as blockage of transport from the early to late endosomes both resulted in Fgf8 clustering at early endosomes. To study the role of endosomal localization of Fgf8 in the range of Fgf signaling, embryos treated with Bafilomycin A1 were analyzed for Fgf target gene expression (Figure 17). Inhibition of Fgf8 transport from early to late endosomes by Bafilomycin A1, however, did not alter the range of Fgf signaling as shown in Figure 17. This shows that endocytic trafficking by Bafilomycin A1 may not correlate with Fgf signaling range.

CME of Fgf8 decreases the activity of Fgf signaling

The activity of a signal depends on the rate at which the morphogen bound to the plasma membrane is degraded. The process of degradation of the membrane bound morphogen occurs through endocytosis and this consists of several steps. It begins with the invagination of sections of the membrane containing the protein and vesiculation and fusion with the early endosome. Fusion of the early endosome to the lysosome enables the degradation of the proten/morphogen by the several non specific proteases and lipases present in the lysosomes (Hochstrasser, 2009). The mechanism of endocytosis of the ligand Fgf8 and the effect on signaling range has been shown before (Nowak et al, 2011; Scholpp and Brand 2004). In this study I have evaluated the effect of endocytosis of Fgf8 on the Fgf signal activity. As show in Figure 18, expression of phosphorylated Erk12 levels was significantly reduced upon Hsc70 activation. This shows that the activity of Fgf signaling is reduced upon internalization. This suggests that Fgf signaling activity predominantly takes place at the plasma membrane.

To determine if the signaling activity of Fgf8 was altered during CME, levels of phosphorylated Erk1/2 expression was analyzed. Upon Fgf8 stimulation, expression of phosphorylated Erk1/2 significantly increased in comparison with the control cells (Figure 17). However, in cells stimulated with Fgf8 as well as Hsc70, the expression of phosphorylated Erk1/2 significantly decreased when compared to the expression in control cells. Previously my results showed that Hsc70 expression lead to a decrease in the extracellular accumulation of Fgf8 (Figure 17). With that in mind, a decrease in phosphorylated Erk1/2 expression during Hsc70 function would suggest that Fgf signaling takes place mainly at the plasma membrane and an increase in the endocytic rate may therefore lead to a decrease in Fgf signaling due to a faster uptake of the ligand receptor complexes. Consistent to this, previous studies have shown that after endocytosis, activated sorting of Fgfrs towards degradation results in the termination of Erk signaling (Persaud et al., 2011). Studies have also shown that expression of Hsc70 results in an increase in the rate of its association with proteins resulting in the promotion of their degradation (Berkovich et al., 1997; (Vila-Carriles et al., 2007). This might also explain the reduction in the Fgf signaling activity due to Hsc70 expression. Previous studies have shown the significance of endocytosis in signal transduction. It has been previously shown that Egfr signaling is regulated by CME. The extended duration of Egfr signaling was shown to be dependant on

CME and that this was due to the recycling of the receptors rather than its degradation (Sigismund et al., 2008). In Nodal/TGF-β signaling, CME stimulates signal transduction and degradation through raft pathway (Di Guglielmo et al., 2003). Internalization of Wnt has been shown to be essential for signaling *in vivo* (Seto and Bellen, 2006) and *in vitro* (Blitzer and Nusse, 2006). Wnt3a signaling has been shown to occur through the receptor LRP6 in the caveolin/raft dependant endocytosis and that endocytosis and phosphrylation were both required for the signal trasnduction suggesting the signaling to take place at the endosomes (Yamamoto et al., 2011). In my studies, I show that Hsc70 expression causes a decrease in Fgf signaling activity due to increased rate of CME. Therefore my studies show that internalization of Fgfs may reduce the lifetime of Fgf signaling due to its degradation. The decrease in Fgf signaling activity during Hsc70 expression also shows that CME may mainly target the Fgfr towards degradation and not in the direction of recycling because recycling of the Fgfrs would facilitate several cycles of signaling at the plasma membrane as well as the endosomes.

Translocation of Fgf8 from the EE to the LE terminates signaling

I show that cells treated with Bafilomycin A1 display an increase in the expression of phosphorylated Erk1/2 in comparison with the control cells (Figure). This shows that inhibition of transport from early to late endosomes results in an increase in Fgf signaling activity. Using Fluorescence correlation spectroscopy (FCS), and automated imaging, (Nowak et al., 2011), showed that a delay in intracellular sorting towards the degradation pathway can extend the active signalling lifetime of occupied Fgfrs within signaling competent endosomes. FCS is an analytical tool which studies miniscule fluctuations in the fluorescent intensity of molecules and this is then further evaluated by statistical correlation analysis for measuring the interactions of molecules, their concentration as well as their propagation in living cells (Kim et al., 2007). It has been suggested previously that Fgf signaling may occur through the entire endocytic route (Stoscheck and Carpenter, 1984, Beguinot et al., 1984). In consistent to this my study also shows that Fgf signaling takes place throughout the CME route. The increase in Fgf signaling acitivity during Bafilomycin A1 treatment maybe due to the loss of degradation as transport from the early to late endosomes is terminated. My results show that stimulation of Hsc70 in Bafilomycin A1 treated cells however displayed a decrease in the Fgf signaling activity. Since Hsc70 increases the rate of

CME, a decrease in the Fgf signaling activity in Bafilomycin A1 treated cells upon Hsc70 stimulation suggests that signaling might mainly occur at the plasma membrane and endocytosis would facilitate the reduction in the lifetime of Fgf signaling.

Hsc70 mediated clustering a general mechanism

The fact that Hsc70 expression leads to intracellular clustering of Fgf8 suggests that the role of Hsc70 in the process of CCV uncoating during CME may trigger the uptake of Fgf8 and its intracellular clustering. In my studies I show that co-expression of Hsc70 and transferrin in zebrafish PAC2 cells, also displayed intracellular clusters of Transferrin (Figure 10), similar to the intracellular Fgf8 clusters observed during Hsc70 overexpression. This suggests that the role of Hsc70 in endocytic trafficking of molecules maybe a general mechanism

Summary

In summary, this study reveals the interaction between Fgf signaling and CME during early Zebrafish development. My study shows the requirement of Hsc70 for the regulation of Fgf signaling through the process of CME. Inhibition of endocytosis through Hsc70 loss of function leads to an increase in the Fgf signaling range in comparison with the control conditions. However, Fgf signalling range remains unaltered during Hsc70 overexpression. Analysis of Fgf8 localization revealed that loss of Hsc70 function leads to an inhibition of Fgf8 endocytosis and an increase in the Fgf8 accumulation at the plasma membrane and the EC space. Hsc70 overexpression showed a decrease in the accumulation of Fgf8 at the plasma membrane and the presence of intracellular Fgf8 clusters. Evaluation of the intracellular localization of Fgf8 showed that Hsc70 overexpression lead to intracellular clustering of Fgf8 at the early endosome. Blockage of Fgf8 transport from early to late endosomes by Bafilomycin A1 revealed a similar intracellular clustering of Fgf8 and an increase in the accumulation of Fgf8 at the plasma membrane. Determination of the effect of endocytosis on Fgf8 showed that the internalization of Fgf8 by Hsc70 decreased the expression of phosphrylated Erk1/2 levels in comparison with the normal conditions. Blockage of Fgf8 transport from early to late endosomes displayed an increase in the phosphrylated Erk1/2 expresison levels. However, co transfection of Hsc70, decreased the expression of phosphrylated Erk1/2 levels stating that Fgf signaling takes places mainly at the plasma membrane and the activity of the signal is reduced upon internalization.

Conclusion

This study has addressed the effect of Hsc70 on Fgf signaling. CME was manipulated with the help of Hsc70, a protein required for the uncoating of the CCVs as well as the recruitment of Clathrin to the plasma membrane during CME and is crucial for the endocytic process (Eisenberg and Greene, 2007), (Holstein et al., 1996), Ungewickell E et al., 1997, (Schlossman et al., 1984, Chappell et al., 1986, Ungewickell et al., 1995) This study has revealed the importance of Hsc70 on two different aspects of Fgf signaling. The first one is if Hsc70 affects the range to which the Fgf signal spreads referred to as the signaling range. The signaling range was determined by analyzing the expression of Fgf target genes *erm*, *pea3* and *dusp6.* The second part was the determination of the Fgf signaling activity and if this was altered during changes in CME by Hsc70 function. For this, the expression of phosphorylated Erk1/2 was analyzed during normal and increased rate of endocytosis by Hsc70. The flourescence intensity of Fgf8-GFP was measured as an indirect analysis of Fgf8 stability.

Role of Hsc70 in Fgf signaling

This study addresses the role of Hsc70 on Fgf signaling. Hsc70 is required for the uncoating of CCVs during CME. The experiments performed in this study show that loss of Hsc70 results in the inhibition of endocytosis and an accumulation of Fgf8 at the plasma membrane. We hypothesize that the inhibition of endocytosis is due to the role of Hsc70 in CCV uncoating and recruitment of clathrin to the plasma membrane. Therefore loss of Hsc70 function results in a failure in CCV uncoating as well as the recruitment of Clathrin back to the plasma membrane for further endocytosis. Due to this, Fgf8 is not take up by the cells and is therefore accumulated at the plasma membrane (Figure 21). As a result the range of Fgf signaling is increased.

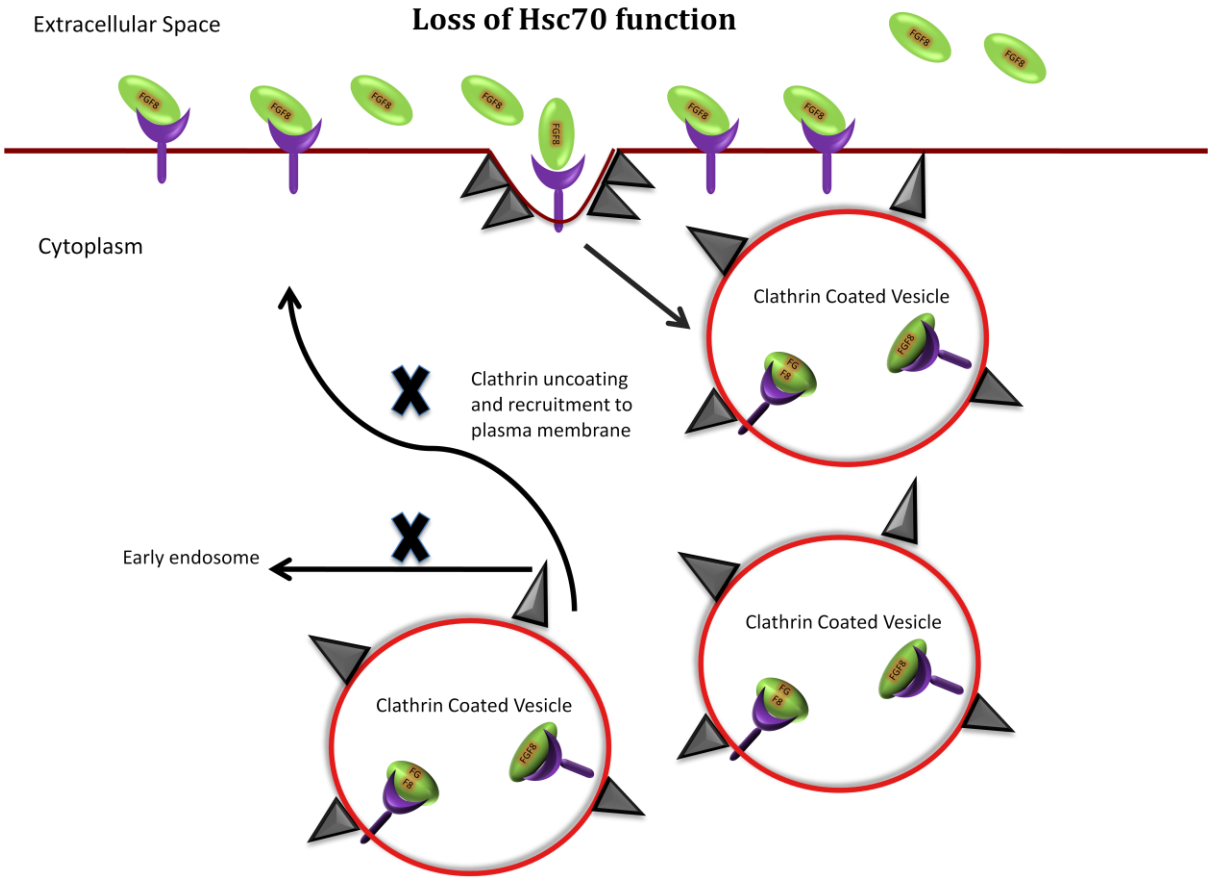

Figure 21: Loss of Hsc70 function. Hsc70 loss of function leads to failure in CCV uncoating and the recruitment of clathrin back to the plasma membrane, which results in the inhibition of endocytosis. Therefore an accumulation of Fgf8 at the plasma membrane is observed.

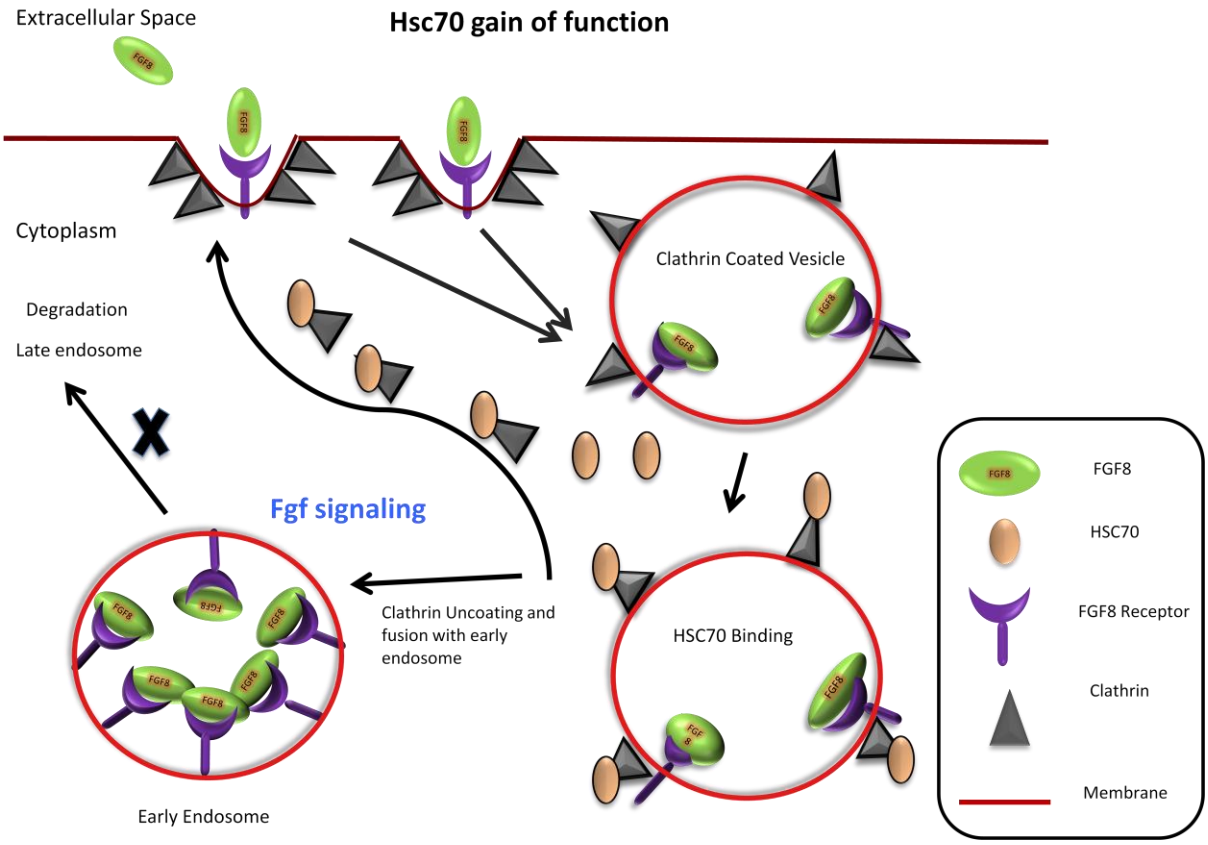

Figure 22: Hsc70 gain of function. Hsc70 overexpression leads to rapid uncoating of CCVs leading to an accumulation of Fgf8 in the early endosomes. Due to rapid uncoating, more clathrin gets recruited to the plasma membrane and therefore rate of internalization is increased leading to lesser availability of extracellular Fgf8.

As shown in Figure 22, gain of Hsc70 function results in an increase in an increase in the rate of CCV uncoating and the recruitment of Clathrin to the plasma membrane. Therefore rate of internalization is increased this results in a decrease in the accumulation of Fgf8 at the plasma membrane. Since the rate of CCV uncoating is elevated, Fgf8 is accumulated at the early endosome and but the transportation towards degradation remains unaltered. The increase in the Fgf8 uptake, its degradation and the resultant decrease in the amount of Fgf8 at the plasma membrane leads to a decrease in the activity of Fgf signaling.

Fgf Signaling range

This study revealed that inhibition of CME by loss of Hsc70 function resulted in an increase in the range of Fgf signaling, in comparison with the control embryos. However, an increase in the rate of CME by Hsc70 overexpression did not alter the range of Fgf signaling as shown Figure 1, 2 and 3.

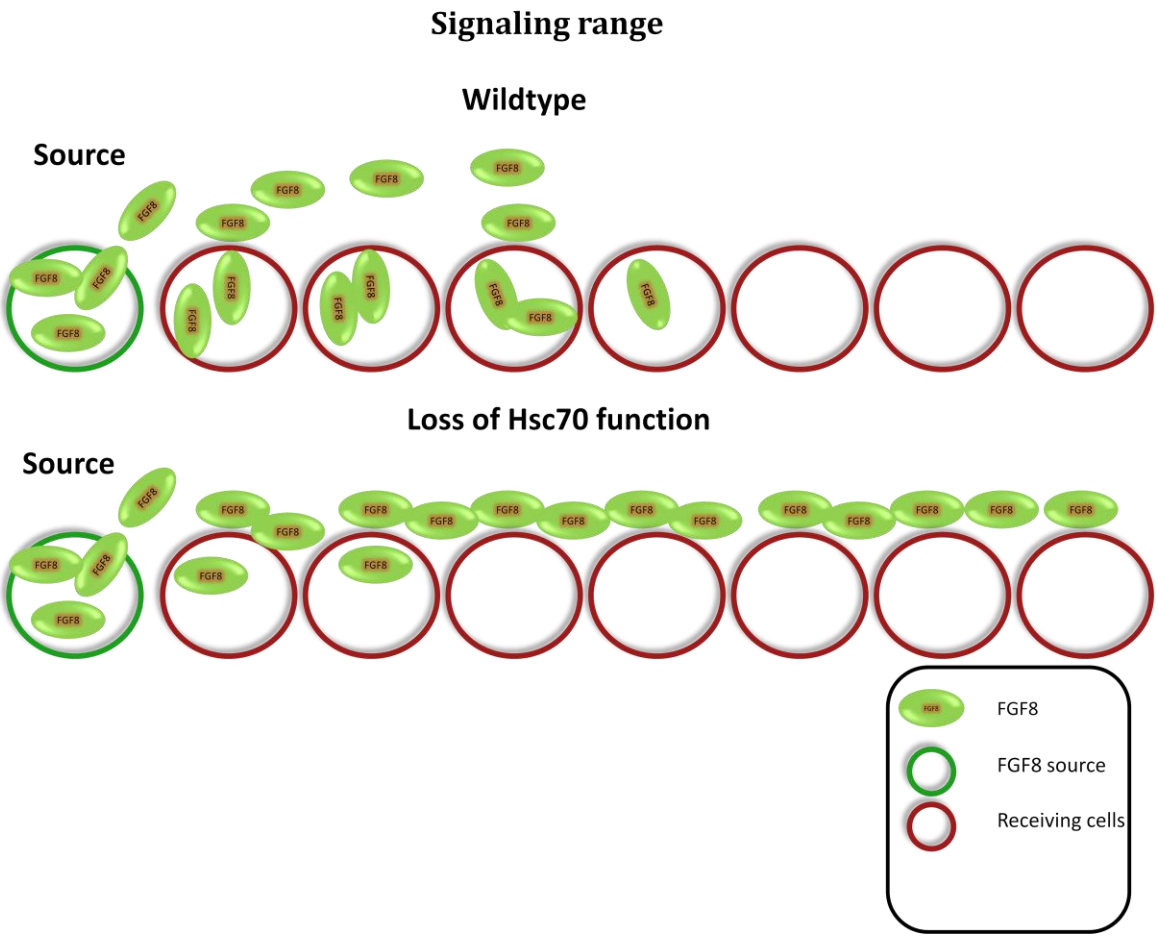

Figure 20: Signaling range. Fgf8 spreading is altered during loss of Hsc70 function when compared with wildtype. This alteration leads to an increase in the range of Fgf signaling when compared to control.

Figure 20 shows a schematic representation of the Fgf signaling range. In wildtype embryos, Fgf8 is released from a source cell and is endocytosed by the neighbouring cells. Fgf8 spreads to a distance of 4 cells away from the source. However, during loss of Hsc70 function, endocytosis is inhibited and therefore Fgf8 spreads further away from the source to a distance of about 7 cells.

Localization of Fgf8

In this study, I show that Fgf8 localization is altered during changes in the rates of CME. My results show that inhibition of CME leads to an extracellular accumulation of Fgf8 and an increased rate in CME leads to intracellular clustering of Fgf8 at the early endosome. The alteration in the localization of Fgf8 during changes in CME confirms that formation of the Fgf8 gradient and its maintanence is through the process of 'restrictive clearance'. My results also show that inhibition of transport from early to late endosomes by Bafilomycin A1 also results in Fgf8 accumulation at the early endosomes. This suggests that endocytic trafficking by Hsc70 or Bafilomycin A1 may alter the localization of Fgf8.

Fgf Signaling activity

This study addresses the effect on increased CME rates on the activity of Fgf signaling. Phosphorylated Erk1/2 expression showed that increased rates of CME rates resulted in a decrease in the expression levels of Phosphorylated Erk1/2. This suggests that increase in the uptake of the Fgf ligand receptor complexes results in a decrease in the Fgf signaling activity. With this experiment as well as the experiments revealing the localization of Fgf8 during Hsc70 expression, this study shows that Fgf signaling predominantly occurs at the plasma membrane and the signal is reduced significantly once internalized. The reduction in the signal after internalization might be due to the rapid degradation of the signaling molecule. Experiments with Bafilomycin A1 showed that inhibition of transport form the early to late endosomes alos results in an increase in the Phosphorylated Erk1/2 expression levels. This might be due to the loss of degradation of the signaling molecule as well as the resulting accumulation of Fgf8 at the plasma membrane due to endocytic trafficking. With these results I conclude that the receiving cells may regulat Fgf8 signaling at two independent levels: firstly the dynamics of CME may regulate the activity range of Fgf8 and secondly the rate of transport of Fgf8 from the plasma membrane to early endosomes may decrease signaling and further routing to late endosomes terminates Fgf8 signaling entirely.

Previous work on Hsc70, has implied that apart from internalization, Hsc70 may also responsible for several steps involved in the endocytic pathway (Newmyer and Schmid 2001). Therefore, although the role of Hsc70 in CME is specific, there might be other factors apart from Auxilin and GAK, assisting its functioning. Apart from CME, Fgf8 has also been shown to be internalized through caveolin (Nowak et al., 2011). Therefore its regulation may also be dependant on the caveloin pathway. It has been shown that signaling in the endosomal compartment could also be assisted by several other proteins apart from Hsc70. Ubiquitin ligase Cbl has been shown to be responsible for the regulation of Fgf signaling through endocytic trafficking (Nowak et al., 2011). It has also been shown that the endocytic Ap2 complex that links the clathrin coat to the internalized cargo is shed off prior to fusion of the vesicle with the early endosome (Kirchhausen, 2012), which opens up the possibility of interactions with other adaptor proteins such as Eps8 and Src (Auciello et al., 2013). Fgf signaling has also been shown to be regulated through several other factors. It has been suggested that Fgf signaling maybe regulated by extracellular inhibitors (Trueb and Steinberg, 2011). For example, high-temperature requirement A1 (HtrA1) was shown to regulate Fgf signaling by regulating the levels of Fgf8 (Kim et al., 2012). Synaptotagmin-like protein E-Syt2, a membrane protein involved in receptor mediated endocytosis was also shown to be required for the activation of Fgf signaling (Jean et al., 2010).

Although the localization of Fgf8 in the early endosomes, late endosomes and lysosomes have been analyzed in this study, Fgf8 localization in the recycling endosomes and the subsequent alteration during changes in the rate of CME have not been adddressed and therefore would be a highly interesting work to be considered in the future. Previous studies have indeed shown that Hsc70 mutants displayed defects in transferrin recycling (Newmyer and Schmid, 2001), suggesting that inhibition of CME due to loss of Hsc70 function may alter the rate of recycling. It would also be interesting to analyze the rate of recycling during increased rate of CME by Hsc70 expression. Since it has been shown that CME regulates other signaling pathways, it would therefore also be interesting to determine the effect of CME in the establishment of other morphogen gradients.

REFERENCES

AHLE, S. & UNGEWICKELL, E. 1990. Auxilin, a newly identified clathrin-associated protein in coated vesicles from bovine brain. *J Cell Biol,* 111**,** 19-29.

AKIN, Z. N. & NAZARALI, A. J. 2005. Hox genes and their candidate downstream targets in the developing central nervous system. *Cell Mol Neurobiol,* 25**,** 697-741.

ALBERTSON, R. C. & YELICK, P. C. 2005. Roles for fgf8 signaling in left-right patterning of the visceral organs and craniofacial skeleton. *Dev Biol,* 283**,** 310-21.

AMAYA, E., MUSCI, T. J. & KIRSCHNER, M. W. 1991. Expression of a dominant negative mutant of the FGF receptor disrupts mesoderm formation in Xenopus embryos. *Cell,* 66**,** 257-70.

AMAYA, E., STEIN, P. A., MUSCI, T. J. & KIRSCHNER, M. W. 1993. FGF signalling in the early specification of mesoderm in Xenopus. *Development,* 118**,** 477-87.

ARMAN, E., HAFFNER-KRAUSZ, R., CHEN, Y., HEATH, J. K. & LONAI, P. 1998. Targeted disruption of fibroblast growth factor (FGF) receptor 2 suggests a role for FGF signaling in pregastrulation mammalian development. *Proc Natl Acad Sci U S A,* 95**,** 5082-7.

ASHE, H. L. & BRISCOE, J. 2006. The interpretation of morphogen gradients. *Development,* 133**,** 385-94.

AUCIELLO, G., CUNNINGHAM, D. L., TATAR, T., HEATH, J. K. & RAPPOPORT, J. Z. 2013. Regulation of fibroblast growth factor receptor signalling and trafficking by Src and Eps8. *J Cell Sci,* 126**,** 613-24.

BAEG, G. H., SELVA, E. M., GOODMAN, R. M., DASGUPTA, R. & PERRIMON, N. 2004. The Wingless morphogen gradient is established by the cooperative action of Frizzled and Heparan Sulfate Proteoglycan receptors. *Dev Biol,* 276**,** 89-100.

BAROUCH, W., PRASAD, K., GREENE, L. E. & EISENBERG, E. 1994. ATPase activity associated with the uncoating of clathrin baskets by Hsp70. *J Biol Chem,* 269**,** 28563-8.

BAYHA, E., JORGENSEN, M. C., SERUP, P. & GRAPIN-BOTTON, A. 2009. Retinoic acid signaling organizes endodermal organ specification along the entire antero-posterior axis. *PLoS One,* 4**,** e5845.

BEENKEN, A. & MOHAMMADI, M. 2009. The FGF family: biology, pathophysiology and therapy. *Nat Rev Drug Discov,* 8**,** 235-53.

BEGUINOT, L., LYALL, R. M., WILLINGHAM, M. C. & PASTAN, I. 1984. Down-regulation of the epidermal growth factor receptor in KB cells is due to receptor internalization and subsequent degradation in lysosomes. *Proc Natl Acad Sci U S A,* 81**,** 2384-8.

BEIMAN, M., SHILO, B. Z. & VOLK, T. 1996. Heartless, a Drosophila FGF receptor homolog, is essential for cell migration and establishment of several mesodermal lineages. *Genes Dev,* 10**,** 2993-3002.

BELENKAYA, T. Y., HAN, C., YAN, D., OPOKA, R. J., KHODOUN, M., LIU, H. & LIN, X. 2004. Drosophila Dpp morphogen movement is independent of dynamin-mediated endocytosis but regulated by the glypican members of heparan sulfate proteoglycans. *Cell,* 119**,** 231-44.

BEN-ZVI, D., PYROWOLAKIS, G., BARKAI, N. & SHILO, B. Z. 2011. Expansion-repression mechanism for scaling the Dpp activation gradient in Drosophila wing imaginal discs. *Curr Biol,* 21**,** 1391-6.

BENTLEY, D. & TOROIAN-RAYMOND, A. 1986. Disoriented pathfinding by pioneer neurone growth cones deprived of filopodia by cytochalasin treatment. *Nature,* 323**,** 712-5.

BLITZER, J. T. & NUSSE, R. 2006. A critical role for endocytosis in Wnt signaling. *BMC Cell Biol,* 7**,** 28.

BLUMBERG, B., BOLADO, J., JR., MORENO, T. A., KINTNER, C., EVANS, R. M. & PAPALOPULU, N. 1997. An essential role for retinoid signaling in anteroposterior neural patterning. *Development,* 124**,** 373-9.

BOKEL, C. & BRAND, M. 2013. Generation and interpretation of FGF morphogen gradients in vertebrates. *Curr Opin Genet Dev*.

BOLLENBACH, T., KRUSE, K., PANTAZIS, P., GONZALEZ-GAITAN, M. & JULICHER, F. 2005. Robust formation of morphogen gradients. *Phys Rev Lett,* 94**,** 018103.

BOTTCHER, R. T. & NIEHRS, C. 2005. Fibroblast growth factor signaling during early vertebrate development. *Endocr Rev,* 26**,** 63-77.

BRAELL, W. A., SCHLOSSMAN, D. M., SCHMID, S. L. & ROTHMAN, J. E. 1984. Dissociation of clathrin coats coupled to the hydrolysis of ATP: role of an uncoating ATPase. *J Cell Biol,* 99**,** 734-41.

BUCCI, C., PARTON, R. G., MATHER, I. H., STUNNENBERG, H., SIMONS, K., HOFLACK, B. & ZERIAL, M. 1992. The small GTPase rab5 functions as a regulatory factor in the early endocytic pathway. *Cell,* 70**,** 715-28.

BUKAU, B. & HORWICH, A. L. 1998. The Hsp70 and Hsp60 chaperone machines. *Cell,* 92**,** 351-66.

CALLEJO, A., BILIONI, A., MOLLICA, E., GORFINKIEL, N., ANDRES, G., IBANEZ, C., TORROJA, C., DOGLIO, L., SIERRA, J. & GUERRERO, I. 2011. Dispatched mediates Hedgehog basolateral release to form the long-range morphogenetic gradient in the Drosophila wing disk epithelium. *Proc Natl Acad Sci U S A,* 108**,** 12591-8.

CALLEJO, A., TORROJA, C., QUIJADA, L. & GUERRERO, I. 2006. Hedgehog lipid modifications are required for Hedgehog stabilization in the extracellular matrix. *Development,* 133**,** 471-83.
CHANG, H. C., NEWMYER, S. L., HULL, M. J., EBERSOLD, M., SCHMID, S. L. & MELLMAN, I. 2002. Hsc70 is required for endocytosis and clathrin function in Drosophila. *J Cell Biol,* 159**,** 477-87.
CHAPPELL, T. G., WELCH, W. J., SCHLOSSMAN, D. M., PALTER, K. B., SCHLESINGER, M. J. & ROTHMAN, J. E. 1986. Uncoating ATPase is a member of the 70 kilodalton family of stress proteins. *Cell,* 45**,** 3-13.
CHRISTEN, B. & SLACK, J. M. 1999. Spatial response to fibroblast growth factor signalling in Xenopus embryos. *Development,* 126**,** 119-25.
CIRUNA, B. G., SCHWARTZ, L., HARPAL, K., YAMAGUCHI, T. P. & ROSSANT, J. 1997. Chimeric analysis of fibroblast growth factor receptor-1 (Fgfr1) function: a role for FGFR1 in morphogenetic movement through the primitive streak. *Development,* 124**,** 2829-41.
COHEN, M., BAUM, B. & MIODOWNIK, M. 2011. The importance of structured noise in the generation of self-organizing tissue patterns through contact-mediated cell-cell signalling. *J R Soc Interface,* 8**,** 787-98.
COHEN, M., GEORGIOU, M., STEVENSON, N. L., MIODOWNIK, M. & BAUM, B. 2010. Dynamic filopodia transmit intermittent Delta-Notch signaling to drive pattern refinement during lateral inhibition. *Dev Cell,* 19**,** 78-89.
COTTON, L. M., O'BRYAN, M. K. & HINTON, B. T. 2008. Cellular signaling by fibroblast growth factors (FGFs) and their receptors (FGFRs) in male reproduction. *Endocr Rev,* 29**,** 193-216.
COX, W. G. & HEMMATI-BRIVANLOU, A. 1995. Caudalization of neural fate by tissue recombination and bFGF. *Development,* 121**,** 4349-58.
CRICK, F. 1970. Diffusion in embryogenesis. *Nature,* 225**,** 420-2.
CURRAN, K. L. & GRAINGER, R. M. 2000. Expression of activated MAP kinase in Xenopus laevis embryos: evaluating the roles of FGF and other signaling pathways in early induction and patterning. *Dev Biol,* 228**,** 41-56.
D'MELLO, N. P. & JAZWINSKI, S. M. 1991. Telomere length constancy during aging of Saccharomyces cerevisiae. *J Bacteriol,* 173**,** 6709-13.
DAVIDSON, B. P., CHENG, L., KINDER, S. J. & TAM, P. P. 2000. Exogenous FGF-4 can suppress anterior development in the mouse embryo during neurulation and early organogenesis. *Dev Biol,* 221**,** 41-52.
DE JOUSSINEAU, C., SOULE, J., MARTIN, M., ANGUILLE, C., MONTCOURRIER, P. & ALEXANDRE, D. 2003. Delta-promoted filopodia mediate long-range lateral inhibition in Drosophila. *Nature,* 426**,** 555-9.
DE ROBERTIS, E. M. 2009. Spemann's organizer and the self-regulation of embryonic fields. *Mech Dev,* 126**,** 925-41.
DEMONTIS, F. & DAHMANN, C. 2007. Apical and lateral cell protrusions interconnect epithelial cells in live Drosophila wing imaginal discs. *Dev Dyn,* 236**,** 3408-18.
DENG, C. X., WYNSHAW-BORIS, A., SHEN, M. M., DAUGHERTY, C., ORNITZ, D. M. & LEDER, P. 1994. Murine FGFR-1 is required for early postimplantation growth and axial organization. *Genes Dev,* 8**,** 3045-57.
DESSAUD, E., RIBES, V., BALASKAS, N., YANG, L. L., PIERANI, A., KICHEVA, A., NOVITCH, B. G., BRISCOE, J. & SASAI, N. 2010. Dynamic assignment and maintenance of positional identity in the ventral neural tube by the morphogen sonic hedgehog. *PLoS Biol,* 8**,** e1000382.
DESSIMOZ, J., OPOKA, R., KORDICH, J. J., GRAPIN-BOTTON, A. & WELLS, J. M. 2006. FGF signaling is necessary for establishing gut tube domains along the anterior-posterior axis in vivo. *Mech Dev,* 123**,** 42-55.
DEUCHAR, E. M. 1970. Diffusion in embryogenesis. *Nature,* 225**,** 671.
DI GUGLIELMO, G. M., LE ROY, C., GOODFELLOW, A. F. & WRANA, J. L. 2003. Distinct endocytic pathways regulate TGF-beta receptor signalling and turnover. *Nat Cell Biol,* 5**,** 410-21.
DICKINSON, R. J., WILLIAMS, D. J., SLACK, D. N., WILLIAMSON, J., SETERNES, O. M. & KEYSE, S. M. 2002. Characterization of a murine gene encoding a developmentally regulated cytoplasmic dual-specificity mitogen-activated protein kinase phosphatase. *Biochem J,* 364**,** 145-55.
DOHERTY, P. & WALSH, F. S. 1996. CAM-FGF Receptor Interactions: A Model for Axonal Growth. *Mol Cell Neurosci,* 8**,** 99-111.
DRAPER, B. W., STOCK, D. W. & KIMMEL, C. B. 2003. Zebrafish fgf24 functions with fgf8 to promote posterior mesodermal development. *Development,* 130**,** 4639-54.
DUCHESNE, L., OCTEAU, V., BEARON, R. N., BECKETT, A., PRIOR, I. A., LOUNIS, B. & FERNIG, D. G. 2012. Transport of fibroblast growth factor 2 in the pericellular matrix is controlled by the spatial distribution of its binding sites in heparan sulfate. *PLoS Biol,* 10**,** e1001361.

DURSTON, A. J., TIMMERMANS, J. P., HAGE, W. J., HENDRIKS, H. F., DE VRIES, N. J., HEIDEVELD, M. & NIEUWKOOP, P. D. 1989. Retinoic acid causes an anteroposterior transformation in the developing central nervous system. *Nature,* 340**,** 140-4.

EBLAGHIE, M. C., LUNN, J. S., DICKINSON, R. J., MUNSTERBERG, A. E., SANZ-EZQUERRO, J. J., FARRELL, E. R., MATHERS, J., KEYSE, S. M., STOREY, K. & TICKLE, C. 2003. Negative feedback regulation of FGF signaling levels by Pyst1/MKP3 in chick embryos. *Curr Biol,* 13**,** 1009-18.

ECHEVARRIA, D., MARTINEZ, S., MARQUES, S., LUCAS-TEIXEIRA, V. & BELO, J. A. 2005. Mkp3 is a negative feedback modulator of Fgf8 signaling in the mammalian isthmic organizer. *Dev Biol,* 277**,** 114-28.

EISENBERG, E. & GREENE, L. E. 2007. Multiple roles of auxilin and hsc70 in clathrin-mediated endocytosis. *Traffic,* 8**,** 640-6.

ELDAR, A., DORFMAN, R., WEISS, D., ASHE, H., SHILO, B. Z. & BARKAI, N. 2002. Robustness of the BMP morphogen gradient in Drosophila embryonic patterning. *Nature,* 419**,** 304-8.

ELDAR, A., ROSIN, D., SHILO, B. Z. & BARKAI, N. 2003. Self-enhanced ligand degradation underlies robustness of morphogen gradients. *Dev Cell,* 5**,** 635-46.

ERIKSSON, A. E., COUSENS, L. S., WEAVER, L. H. & MATTHEWS, B. W. 1991. Three-dimensional structure of human basic fibroblast growth factor. *Proc Natl Acad Sci U S A,* 88**,** 3441-5.

ESAIN, V., POSTLETHWAIT, J. H., CHARNAY, P. & GHISLAIN, J. 2010. FGF-receptor signalling controls neural cell diversity in the zebrafish hindbrain by regulating olig2 and sox9. *Development,* 137**,** 33-42.

FELDMAN, B., POUEYMIROU, W., PAPAIOANNOU, V. E., DECHIARA, T. M. & GOLDFARB, M. 1995. Requirement of FGF-4 for postimplantation mouse development. *Science,* 267**,** 246-9.

FLAHERTY, K. M., DELUCA-FLAHERTY, C. & MCKAY, D. B. 1990. Three-dimensional structure of the ATPase fragment of a 70K heat-shock cognate protein. *Nature,* 346**,** 623-8.

FLETCHER, R. B., BAKER, J. C. & HARLAND, R. M. 2006. FGF8 spliceforms mediate early mesoderm and posterior neural tissue formation in Xenopus. *Development,* 133**,** 1703-14.

FLETCHER, R. B. & HARLAND, R. M. 2008. The role of FGF signaling in the establishment and maintenance of mesodermal gene expression in Xenopus. *Dev Dyn,* 237**,** 1243-54.

FURTHAUER, M., THISSE, C. & THISSE, B. 1997. A role for FGF-8 in the dorsoventral patterning of the zebrafish gastrula. *Development,* 124**,** 4253-64.

FURTHAUER, M., VAN CELST, J., THISSE, C. & THISSE, B. 2004. Fgf signalling controls the dorsoventral patterning of the zebrafish embryo. *Development,* 131**,** 2853-64.

GALLO, G. & LETOURNEAU, P. C. 2004. Regulation of growth cone actin filaments by guidance cues. *J Neurobiol,* 58**,** 92-102.

GISSELBRECHT, S., SKEATH, J. B., DOE, C. Q. & MICHELSON, A. M. 1996. heartless encodes a fibroblast growth factor receptor (DFR1/DFGF-R2) involved in the directional migration of early mesodermal cells in the Drosophila embryo. *Genes Dev,* 10**,** 3003-17.

GOLDIN, S. N. & PAPAIOANNOU, V. E. 2003. Paracrine action of FGF4 during periimplantation development maintains trophectoderm and primitive endoderm. *Genesis,* 36**,** 40-7.

GOMEZ, A. R., LOPEZ-VAREA, A., MOLNAR, C., DE LA CALLE-MUSTIENES, E., RUIZ-GOMEZ, M., GOMEZ-SKARMETA, J. L. & DE CELIS, J. F. 2005. Conserved cross-interactions in Drosophila and Xenopus between Ras/MAPK signaling and the dual-specificity phosphatase MKP3. *Dev Dyn,* 232**,** 695-708.

GORVEL, J. P., CHAVRIER, P., ZERIAL, M. & GRUENBERG, J. 1991. rab5 controls early endosome fusion in vitro. *Cell,* 64**,** 915-25.

GREEN, J. 2002. Morphogen gradients, positional information, and Xenopus: interplay of theory and experiment. *Dev Dyn,* 225**,** 392-408.

GREEN, J. B., NEW, H. V. & SMITH, J. C. 1992. Responses of embryonic Xenopus cells to activin and FGF are separated by multiple dose thresholds and correspond to distinct axes of the mesoderm. *Cell,* 71**,** 731-9.

GREEN, J. B. & SMITH, J. C. 1991. Growth factors as morphogens: do gradients and thresholds establish body plan? *Trends Genet,* 7**,** 245-50.

GREENE, L. E. & EISENBERG, E. 1990. Dissociation of clathrin from coated vesicles by the uncoating ATPase. *J Biol Chem,* 265**,** 6682-7.

GRIFFIN, K., PATIENT, R. & HOLDER, N. 1995. Analysis of FGF function in normal and no tail zebrafish embryos reveals separate mechanisms for formation of the trunk and the tail. *Development,* 121**,** 2983-94.

GURDON, J. B. & BOURILLOT, P. Y. 2001. Morphogen gradient interpretation. *Nature,* 413**,** 797-803.

GUSTAFSON, T. & WOLPERT, L. 1967. Cellular movement and contact in sea urchin morphogenesis. *Biol Rev Camb Philos Soc,* 42**,** 442-98.

HADARI, Y. R., GOTOH, N., KOUHARA, H., LAX, I. & SCHLESSINGER, J. 2001. Critical role for the docking-protein FRS2 alpha in FGF receptor-mediated signal transduction pathways. *Proc Natl Acad Sci U S A,* 98**,** 8578-83.
HAN, C., BELENKAYA, T. Y., WANG, B. & LIN, X. 2004. Drosophila glypicans control the cell-to-cell movement of Hedgehog by a dynamin-independent process. *Development,* 131**,** 601-11.
HAN, C., YAN, D., BELENKAYA, T. Y. & LIN, X. 2005. Drosophila glypicans Dally and Dally-like shape the extracellular Wingless morphogen gradient in the wing disc. *Development,* 132**,** 667-79.
HANNAN, L. A., NEWMYER, S. L. & SCHMID, S. L. 1998. ATP- and cytosol-dependent release of adaptor proteins from clathrin-coated vesicles: A dual role for Hsc70. *Mol Biol Cell,* 9**,** 2217-29.
HARDCASTLE, Z., CHALMERS, A. D. & PAPALOPULU, N. 2000. FGF-8 stimulates neuronal differentiation through FGFR-4a and interferes with mesoderm induction in Xenopus embryos. *Curr Biol,* 10**,** 1511-4.
HASKEL-ITTAH, M., BEN-ZVI, D., BRANSKI-ARIELI, M., SCHEJTER, E. D., SHILO, B. Z. & BARKAI, N. 2012. Self-organized shuttling: generating sharp dorsoventral polarity in the early Drosophila embryo. *Cell,* 150**,** 1016-28.
HILL, A. J., TERAOKA, H., HEIDEMAN, W. & PETERSON, R. E. 2005. Zebrafish as a model vertebrate for investigating chemical toxicity. *Toxicol Sci,* 86**,** 6-19.
HINSHAW, J. E. & SCHMID, S. L. 1995. Dynamin self-assembles into rings suggesting a mechanism for coated vesicle budding. *Nature,* 374**,** 190-2.
HOCHSTRASSER, M. 2009. Origin and function of ubiquitin-like proteins. *Nature,* 458**,** 422-9.
HOLOWACZ, T. & SOKOL, S. 1999. FGF is required for posterior neural patterning but not for neural induction. *Dev Biol,* 205**,** 296-308.
HOLSTEIN, S. E., UNGEWICKELL, H. & UNGEWICKELL, E. 1996. Mechanism of clathrin basket dissociation: separate functions of protein domains of the DnaJ homologue auxilin. *J Cell Biol,* 135**,** 925-37.
HONGO, I., KENGAKU, M. & OKAMOTO, H. 1999. FGF signaling and the anterior neural induction in Xenopus. *Dev Biol,* 216**,** 561-81.
HUFNAGEL, L., KREUGER, J., COHEN, S. M. & SHRAIMAN, B. I. 2006. On the role of glypicans in the process of morphogen gradient formation. *Dev Biol,* 300**,** 512-22.
INABA, M., YAMANAKA, H. & KONDO, S. 2012. Pigment pattern formation by contact-dependent depolarization. *Science,* 335**,** 677.
ISAACS, H. V., POWNALL, M. E. & SLACK, J. M. 1994. eFGF regulates Xbra expression during Xenopus gastrulation. *EMBO J,* 13**,** 4469-81.
ISAACS, H. V., TANNAHILL, D. & SLACK, J. M. 1992. Expression of a novel FGF in the Xenopus embryo. A new candidate inducing factor for mesoderm formation and anteroposterior specification. *Development,* 114**,** 711-20.
ITOH, N. 2007. The Fgf families in humans, mice, and zebrafish: their evolutional processes and roles in development, metabolism, and disease. *Biol Pharm Bull,* 30**,** 1819-25.
JACINTO, A., WOOD, W., BALAYO, T., TURMAINE, M., MARTINEZ-ARIAS, A. & MARTIN, P. 2000. Dynamic actin-based epithelial adhesion and cell matching during Drosophila dorsal closure. *Curr Biol,* 10**,** 1420-6.
JEAN, S., MIKRYUKOV, A., TREMBLAY, M. G., BARIL, J., GUILLOU, F., BELLENFANT, S. & MOSS, T. 2010. Extended-synaptotagmin-2 mediates FGF receptor endocytosis and ERK activation in vivo. *Dev Cell,* 19**,** 426-39.
JOHNSON, D. E. & WILLIAMS, L. T. 1993. Structural and functional diversity in the FGF receptor multigene family. *Adv Cancer Res,* 60**,** 1-41.
KANAOKA, Y., KIMURA, S. H., OKAZAKI, I., IKEDA, M. & NOJIMA, H. 1997. GAK: a cyclin G associated kinase contains a tensin/auxilin-like domain. *FEBS Lett,* 402**,** 73-80.
KARP, G. C. & SOLURSH, M. 1985. Dynamic activity of the filopodia of sea urchin embryonic cells and their role in directed migration of the primary mesenchyme in vitro. *Dev Biol,* 112**,** 276-83.
KATAOKA, A. & SHIMOGORI, T. 2008. Fgf8 controls regional identity in the developing thalamus. *Development,* 135**,** 2873-81.
KAWAKAMI, Y., RODRIGUEZ-LEON, J., KOTH, C. M., BUSCHER, D., ITOH, T., RAYA, A., NG, J. K., ESTEBAN, C. R., TAKAHASHI, S., HENRIQUE, D., SCHWARZ, M. F., ASAHARA, H. & IZPISUA BELMONTE, J. C. 2003. MKP3 mediates the cellular response to FGF8 signalling in the vertebrate limb. *Nat Cell Biol,* 5**,** 513-9.
KERSZBERG, M. & WOLPERT, L. 2007. Specifying positional information in the embryo: looking beyond morphogens. *Cell,* 130**,** 205-9.
KIECKER, C. & NIEHRS, C. 2001. A morphogen gradient of Wnt/beta-catenin signalling regulates anteroposterior neural patterning in Xenopus. *Development,* 128**,** 4189-201.

KIM, S. A., HEINZE, K. G. & SCHWILLE, P. 2007. Fluorescence correlation spectroscopy in living cells. *Nat Methods,* 4**,** 963-73.
KIMMEL, C. B., BALLARD, W. W., KIMMEL, S. R., ULLMANN, B. & SCHILLING, T. F. 1995. Stages of embryonic development of the zebrafish. *Dev Dyn,* 203**,** 253-310.
KIRCHHAUSEN, T. 2012. Bending membranes. *Nat Cell Biol,* 14**,** 906-8.
KISHI, S., UCHIYAMA, J., BAUGHMAN, A. M., GOTO, T., LIN, M. C. & TSAI, S. B. 2003. The zebrafish as a vertebrate model of functional aging and very gradual senescence. *Exp Gerontol,* 38**,** 777-86.
KLOCK, A. & HERRMANN, B. G. 2002. Cloning and expression of the mouse dual-specificity mitogen-activated protein (MAP) kinase phosphatase Mkp3 during mouse embryogenesis. *Mech Dev,* 116**,** 243-7.
KORNBERG, T. B. 2012. The imperatives of context and contour for morphogen dispersion. *Biophys J,* 103**,** 2252-6.
KORNBERG, T. B. & GUHA, A. 2007. Understanding morphogen gradients: a problem of dispersion and containment. *Curr Opin Genet Dev,* 17**,** 264-71.
KOSHIDA, S., SHINYA, M., NIKAIDO, M., UENO, N., SCHULTE-MERKER, S., KUROIWA, A. & TAKEDA, H. 2002. Inhibition of BMP activity by the FGF signal promotes posterior neural development in zebrafish. *Dev Biol,* 244**,** 9-20.
KOUHARA, H., HADARI, Y. R., SPIVAK-KROIZMAN, T., SCHILLING, J., BAR-SAGI, D., LAX, I. & SCHLESSINGER, J. 1997. A lipid-anchored Grb2-binding protein that links FGF-receptor activation to the Ras/MAPK signaling pathway. *Cell,* 89**,** 693-702.
KREJCI, P., PROCHAZKOVA, J., BRYJA, V., KOZUBIK, A. & WILCOX, W. R. 2009. Molecular pathology of the fibroblast growth factor family. *Hum Mutat,* 30**,** 1245-55.
KRESS, H., STELZER, E. H., HOLZER, D., BUSS, F., GRIFFITHS, G. & ROHRBACH, A. 2007. Filopodia act as phagocytic tentacles and pull with discrete steps and a load-dependent velocity. *Proc Natl Acad Sci U S A,* 104**,** 11633-8.
KRUMLAUF, R. 1994. Hox genes in vertebrate development. *Cell,* 78**,** 191-201.
KUMANO, G., EZAL, C. & SMITH, W. C. 2001. Boundaries and functional domains in the animal/vegetal axis of Xenopus gastrula mesoderm. *Dev Biol,* 236**,** 465-77.
KUMANO, G. & SMITH, W. C. 2000. FGF signaling restricts the primary blood islands to ventral mesoderm. *Dev Biol,* 228**,** 304-14.
KUMANO, G. & SMITH, W. C. 2002. Revisions to the Xenopus gastrula fate map: implications for mesoderm induction and patterning. *Dev Dyn,* 225**,** 409-21.
LAMB, T. M. & HARLAND, R. M. 1995. Fibroblast growth factor is a direct neural inducer, which combined with noggin generates anterior-posterior neural pattern. *Development,* 121**,** 3627-36.
LANDER, A. D. 2013. How cells know where they are. *Science,* 339**,** 923-7.
LANDER, A. D., NIE, Q. & WAN, F. Y. 2002. Do morphogen gradients arise by diffusion? *Dev Cell,* 2**,** 785-96.
LEA, R., PAPALOPULU, N., AMAYA, E. & DOREY, K. 2009. Temporal and spatial expression of FGF ligands and receptors during Xenopus development. *Dev Dyn,* 238**,** 1467-79.
LECUIT, T., BROOK, W. J., NG, M., CALLEJA, M., SUN, H. & COHEN, S. M. 1996. Two distinct mechanisms for long-range patterning by Decapentaplegic in the Drosophila wing. *Nature,* 381**,** 387-93.
LEE, J. T., JR. & MCCUBREY, J. A. 2002. The Raf/MEK/ERK signal transduction cascade as a target for chemotherapeutic intervention in leukemia. *Leukemia,* 16**,** 486-507.
LEHMANN, M. J., SHERER, N. M., MARKS, C. B., PYPAERT, M. & MOTHES, W. 2005. Actin- and myosin-driven movement of viruses along filopodia precedes their entry into cells. *J Cell Biol,* 170**,** 317-25.
LEWIS, J., SLACK, J. M. & WOLPERT, L. 1977. Thresholds in development. *J Theor Biol,* 65**,** 579-90.
LIN, C. C., MELO, F. A., GHOSH, R., SUEN, K. M., STAGG, L. J., KIRKPATRICK, J., AROLD, S. T., AHMED, Z. & LADBURY, J. E. 2012. Inhibition of basal FGF receptor signaling by dimeric Grb2. *Cell,* 149**,** 1514-24.
LIN, X. 2004. Functions of heparan sulfate proteoglycans in cell signaling during development. *Development,* 131**,** 6009-21.
LITTLE, S. C. & MULLINS, M. C. 2006. Extracellular modulation of BMP activity in patterning the dorsoventral axis. *Birth Defects Res C Embryo Today,* 78**,** 224-42.
LOCKE, M. 1987. The very rapid induction of filopodia in insect cells. *Tissue Cell,* 19**,** 301-18.
LONDIN, E. R., MENTZER, L., GATES, K. P. & SIROTKIN, H. I. 2007. Expression and regulation of the zinc finger transcription factor Churchill during zebrafish development. *Gene Expr Patterns,* 7**,** 645-50.
MARTIN, G. 2001. Making a vertebrate limb: new players enter from the wings. *Bioessays,* 23**,** 865-8.

MATHIS, L., KULESA, P. M. & FRASER, S. E. 2001. FGF receptor signalling is required to maintain neural progenitors during Hensen's node progression. *Nat Cell Biol,* 3**,** 559-66.
MATSUDA, S. & SHIMMI, O. 2012. Directional transport and active retention of Dpp/BMP create wing vein patterns in Drosophila. *Dev Biol,* 366**,** 153-62.
MCGREW, L. L., HOPPLER, S. & MOON, R. T. 1997. Wnt and FGF pathways cooperatively pattern anteroposterior neural ectoderm in Xenopus. *Mech Dev,* 69**,** 105-14.
MCGREW, L. L., LAI, C. J. & MOON, R. T. 1995. Specification of the anteroposterior neural axis through synergistic interaction of the Wnt signaling cascade with noggin and follistatin. *Dev Biol,* 172**,** 337-42.
MCINTOSH, I., BELLUS, G. A. & JAB, E. W. 2000. The pleiotropic effects of fibroblast growth factor receptors in mammalian development. *Cell Struct Funct,* 25**,** 85-96.
MCKEEHAN, W. L., WANG, F. & KAN, M. 1998. The heparan sulfate-fibroblast growth factor family: diversity of structure and function. *Prog Nucleic Acid Res Mol Biol,* 59**,** 135-76.
MEYERS, E. N., LEWANDOSKI, M. & MARTIN, G. R. 1998. An Fgf8 mutant allelic series generated by Cre- and Flp-mediated recombination. *Nat Genet,* 18**,** 136-41.
MILAN, M., WEIHE, U., PEREZ, L. & COHEN, S. M. 2001. The LRR proteins capricious and Tartan mediate cell interactions during DV boundary formation in the Drosophila wing. *Cell,* 106**,** 785-94.
MILLER, J., FRASER, S. E. & MCCLAY, D. 1995. Dynamics of thin filopodia during sea urchin gastrulation. *Development,* 121**,** 2501-11.
MIURA, T., HARTMANN, D., KINBOSHI, M., KOMADA, M., ISHIBASHI, M. & SHIOTA, K. 2009. The cyst-branch difference in developing chick lung results from a different morphogen diffusion coefficient. *Mech Dev,* 126**,** 160-72.
MIZUTANI, C. M., NIE, Q., WAN, F. Y., ZHANG, Y. T., VILMOS, P., SOUSA-NEVES, R., BIER, E., MARSH, J. L. & LANDER, A. D. 2005. Formation of the BMP activity gradient in the Drosophila embryo. *Dev Cell,* 8**,** 915-24.
MOHAMMADI, M., DIONNE, C. A., LI, W., LI, N., SPIVAK, T., HONEGGER, A. M., JAYE, M. & SCHLESSINGER, J. 1992. Point mutation in FGF receptor eliminates phosphatidylinositol hydrolysis without affecting mitogenesis. *Nature,* 358**,** 681-4.
MOHAMMADI, M., MCMAHON, G., SUN, L., TANG, C., HIRTH, P., YEH, B. K., HUBBARD, S. R. & SCHLESSINGER, J. 1997. Structures of the tyrosine kinase domain of fibroblast growth factor receptor in complex with inhibitors. *Science,* 276**,** 955-60.
MOLINA, G. A., WATKINS, S. C. & TSANG, M. 2007. Generation of FGF reporter transgenic zebrafish and their utility in chemical screens. *BMC Dev Biol,* 7**,** 62.
MORGAN, E. H., MARSAGLIA, G., GIBLETT, E. R. & FINCH, C. A. 1967. A method of investigating internal iron exchange utilizing two types of transferrin. *J Lab Clin Med,* 69**,** 370-81.
MORGAN, J. R., PRASAD, K., JIN, S., AUGUSTINE, G. J. & LAFER, E. M. 2001. Uncoating of clathrin-coated vesicles in presynaptic terminals: roles for Hsc70 and auxilin. *Neuron,* 32**,** 289-300.
MORGAN, T. H. 1901. Regeneration and Liability to Injury. *Science,* 14**,** 235-48.
MOTT, N. N., CHUNG, W. C., TSAI, P. S. & PAK, T. R. 2010. Differential fibroblast growth factor 8 (FGF8)-mediated autoregulation of its cognate receptors, Fgfr1 and Fgfr3, in neuronal cell lines. *PLoS One,* 5**,** e10143.
MULLER, P., ROGERS, K. W., JORDAN, B. M., LEE, J. S., ROBSON, D., RAMANATHAN, S. & SCHIER, A. F. 2012. Differential diffusivity of Nodal and Lefty underlies a reaction-diffusion patterning system. *Science,* 336**,** 721-4.
MULLER, P., ROGERS, K. W., YU, S. R., BRAND, M. & SCHIER, A. F. 2013. Morphogen transport. *Development,* 140**,** 1621-38.
MULLER, P. & SCHIER, A. F. 2011. Extracellular movement of signaling molecules. *Dev Cell,* 21**,** 145-58.
NAHMAD, M. & STATHOPOULOS, A. 2010. Establishing positional information through gradient dynamics: a lesson from the Hedgehog signaling pathway. *Fly (Austin),* 4**,** 273-7.
NELLEN, D., BURKE, R., STRUHL, G. & BASLER, K. 1996. Direct and long-range action of a DPP morphogen gradient. *Cell,* 85**,** 357-68.
NEUMANN, C. J. & COHEN, S. M. 1997. Long-range action of Wingless organizes the dorsal-ventral axis of the Drosophila wing. *Development,* 124**,** 871-80.
NEWMYER, S. L. & SCHMID, S. L. 2001. Dominant-interfering Hsc70 mutants disrupt multiple stages of the clathrin-coated vesicle cycle in vivo. *J Cell Biol,* 152**,** 607-20.
NICHOLSON, C. & SYKOVA, E. 1998. Extracellular space structure revealed by diffusion analysis. *Trends Neurosci,* 21**,** 207-15.
NOWAK, M., MACHATE, A., YU, S. R., GUPTA, M. & BRAND, M. 2011. Interpretation of the FGF8 morphogen gradient is regulated by endocytic trafficking. *Nat Cell Biol,* 13**,** 153-8.
NUNEZ, M. T., GLASS, J., FISCHER, S., LAVIDOR, L. M., LENK, E. M. & ROBINSON, S. H. 1977. Transferrin receptors in developing murine erythroid cells. *Br J Haematol,* 36**,** 519-26.

OCTAVE, J. N., SCHNEIDER, Y. J., CRICHTON, R. R. & TROUET, A. 1981. Transferrin uptake by cultured rat embryo fibroblasts. The influence of temperature and incubation time, subcellular distribution and short-term kinetic studies. *Eur J Biochem,* 115**,** 611-8.

ORNITZ, D. M. & ITOH, N. 2001. Fibroblast growth factors. *Genome Biol,* 2**,** REVIEWS3005.

OTA, S., TONOU-FUJIMORI, N. & YAMASU, K. 2009. The roles of the FGF signal in zebrafish embryos analyzed using constitutive activation and dominant-negative suppression of different FGF receptors. *Mech Dev,* 126**,** 1-17.

PARTANEN, J., SCHWARTZ, L. & ROSSANT, J. 1998. Opposite phenotypes of hypomorphic and Y766 phosphorylation site mutations reveal a function for Fgfr1 in anteroposterior patterning of mouse embryos. *Genes Dev,* 12**,** 2332-44.

PAULSEN, M., LEGEWIE, S., EILS, R., KARAULANOV, E. & NIEHRS, C. 2011. Negative feedback in the bone morphogenetic protein 4 (BMP4) synexpression group governs its dynamic signaling range and canalizes development. *Proc Natl Acad Sci U S A,* 108**,** 10202-7.

PENG, Y., HAN, C. & AXELROD, J. D. 2012. Planar polarized protrusions break the symmetry of EGFR signaling during Drosophila bract cell fate induction. *Dev Cell,* 23**,** 507-18.

PERSAUD, A., ALBERTS, P., HAYES, M., GUETTLER, S., CLARKE, I., SICHERI, F., DIRKS, P., CIRUNA, B. & ROTIN, D. 2011. Nedd4-1 binds and ubiquitylates activated FGFR1 to control its endocytosis and function. *EMBO J,* 30**,** 3259-73.

PLACZEK, M. & FURLEY, A. 1996. Patterning cascades in the neural tube. Neural development. *Curr Biol,* 6**,** 526-9.

PLOTNIKOV, A. N., HUBBARD, S. R., SCHLESSINGER, J. & MOHAMMADI, M. 2000. Crystal structures of two FGF-FGFR complexes reveal the determinants of ligand-receptor specificity. *Cell,* 101**,** 413-24.

POWNALL, M. E., TUCKER, A. S., SLACK, J. M. & ISAACS, H. V. 1996. eFGF, Xcad3 and Hox genes form a molecular pathway that establishes the anteroposterior axis in Xenopus. *Development,* 122**,** 3881-92.

PRASAD, K., BAROUCH, W., GREENE, L. & EISENBERG, E. 1993. A protein cofactor is required for uncoating of clathrin baskets by uncoating ATPase. *J Biol Chem,* 268**,** 23758-61.

RAIBLE, F. & BRAND, M. 2001. Tight transcriptional control of the ETS domain factors Erm and Pea3 by Fgf signaling during early zebrafish development. *Mech Dev,* 107**,** 105-17.

RAMIREZ-WEBER, F. A. & KORNBERG, T. B. 1999. Cytonemes: cellular processes that project to the principal signaling center in Drosophila imaginal discs. *Cell,* 97**,** 599-607.

RAMIREZ-WEBER, F. A. & KORNBERG, T. B. 2000. Signaling reaches to new dimensions in Drosophila imaginal discs. *Cell,* 103**,** 189-92.

REIFERS, F., BOHLI, H., WALSH, E. C., CROSSLEY, P. H., STAINIER, D. Y. & BRAND, M. 1998. Fgf8 is mutated in zebrafish acerebellar (ace) mutants and is required for maintenance of midbrain-hindbrain boundary development and somitogenesis. *Development,* 125**,** 2381-95.

RENAUD, O. & SIMPSON, P. 2001. scabrous modifies epithelial cell adhesion and extends the range of lateral signalling during development of the spaced bristle pattern in Drosophila. *Dev Biol,* 240**,** 361-76.

RIBISI, S., JR., MARIANI, F. V., AAMAR, E., LAMB, T. M., FRANK, D. & HARLAND, R. M. 2000. Ras-mediated FGF signaling is required for the formation of posterior but not anterior neural tissue in Xenopus laevis. *Dev Biol,* 227**,** 183-96.

RODRIGUEZ-VICIANA, P., WARNE, P. H., DHAND, R., VANHAESEBROECK, B., GOUT, I., FRY, M. J., WATERFIELD, M. D. & DOWNWARD, J. 1994. Phosphatidylinositol-3-OH kinase as a direct target of Ras. *Nature,* 370**,** 527-32.

ROEHL, H. & NUSSLEIN-VOLHARD, C. 2001. Zebrafish pea3 and erm are general targets of FGF8 signaling. *Curr Biol,* 11**,** 503-7.

ROJAS-RIOS, P., GUERRERO, I. & GONZALEZ-REYES, A. 2012. Cytoneme-mediated delivery of hedgehog regulates the expression of bone morphogenetic proteins to maintain germline stem cells in Drosophila. *PLoS Biol,* 10**,** e1001298.

ROTTINGER, E., SAUDEMONT, A., DUBOC, V., BESNARDEAU, L., MCCLAY, D. & LEPAGE, T. 2008. FGF signals guide migration of mesenchymal cells, control skeletal morphogenesis [corrected] and regulate gastrulation during sea urchin development. *Development,* 135**,** 353-65.

ROY, S. & KORNBERG, T. B. 2011. Direct delivery mechanisms of morphogen dispersion. *Sci Signal,* 4**,** pt8.

RUSAKOV, D. A. & KULLMANN, D. M. 1998. Geometric and viscous components of the tortuosity of the extracellular space in the brain. *Proc Natl Acad Sci U S A,* 95**,** 8975-80.

RYAN, P. J., PATERNO, G. D. & GILLESPIE, L. L. 1998. Identification of phosphorylated proteins associated with the fibroblast growth factor receptor type I during early Xenopus development. *Biochem Biophys Res Commun,* 244**,** 763-7.

SATO, M. & KORNBERG, T. B. 2002. FGF is an essential mitogen and chemoattractant for the air sacs of the drosophila tracheal system. *Dev Cell,* 3**,** 195-207.

SAWALA, A., SUTCLIFFE, C. & ASHE, H. L. 2012. Multistep molecular mechanism for bone morphogenetic protein extracellular transport in the Drosophila embryo. *Proc Natl Acad Sci U S A,* 109**,** 11222-7.
SCHIER, A. F. & TALBOT, W. S. 2005. Molecular genetics of axis formation in zebrafish. *Annu Rev Genet,* 39**,** 561-613.
SCHLESSINGER, J. 2000. Cell signaling by receptor tyrosine kinases. *Cell,* 103**,** 211-25.
SCHLOSSMAN, D. M., SCHMID, S. L., BRAELL, W. A. & ROTHMAN, J. E. 1984. An enzyme that removes clathrin coats: purification of an uncoating ATPase. *J Cell Biol,* 99**,** 723-33.
SCHMID, S. L. & ROTHMAN, J. E. 1985. Two classes of binding sites for uncoating protein in clathrin triskelions. *J Biol Chem,* 260**,** 10050-6.
SCHOLPP, S. & BRAND, M. 2004. Endocytosis controls spreading and effective signaling range of Fgf8 protein. *Curr Biol,* 14**,** 1834-41.
SCHOLPP, S., LOHS, C. & BRAND, M. 2003. Engrailed and Fgf8 act synergistically to maintain the boundary between diencephalon and mesencephalon. *Development,* 130**,** 4881-93.
SETO, E. S. & BELLEN, H. J. 2006. Internalization is required for proper Wingless signaling in Drosophila melanogaster. *J Cell Biol,* 173**,** 95-106.
SHINYA, M., KOSHIDA, S., SAWADA, A., KUROIWA, A. & TAKEDA, H. 2001. Fgf signalling through MAPK cascade is required for development of the subpallial telencephalon in zebrafish embryos. *Development,* 128**,** 4153-64.
SIGISMUND, S., ARGENZIO, E., TOSONI, D., CAVALLARO, E., POLO, S. & DI FIORE, P. P. 2008. Clathrin-mediated internalization is essential for sustained EGFR signaling but dispensable for degradation. *Dev Cell,* 15**,** 209-19.
SIVE, H. L., DRAPER, B. W., HARLAND, R. M. & WEINTRAUB, H. 1990. Identification of a retinoic acid-sensitive period during primary axis formation in Xenopus laevis. *Genes Dev,* 4**,** 932-42.
SMITH, T. G., SWEETMAN, D., PATTERSON, M., KEYSE, S. M. & MUNSTERBERG, A. 2005. Feedback interactions between MKP3 and ERK MAP kinase control scleraxis expression and the specification of rib progenitors in the developing chick somite. *Development,* 132**,** 1305-14.
SOLDATI, T., SHAPIRO, A. D., SVEJSTRUP, A. B. & PFEFFER, S. R. 1994. Membrane targeting of the small GTPase Rab9 is accompanied by nucleotide exchange. *Nature,* 369**,** 76-8.
SPITSBERGEN, J. M. & KENT, M. L. 2003. The state of the art of the zebrafish model for toxicology and toxicologic pathology research--advantages and current limitations. *Toxicol Pathol,* 31 Suppl**,** 62-87.
STERN, H. M. & ZON, L. I. 2003. Cancer genetics and drug discovery in the zebrafish. *Nat Rev Cancer,* 3**,** 533-9.
STOREY, K. G., GORIELY, A., SARGENT, C. M., BROWN, J. M., BURNS, H. D., ABUD, H. M. & HEATH, J. K. 1998. Early posterior neural tissue is induced by FGF in the chick embryo. *Development,* 125**,** 473-84.
STOSCHECK, C. M. & CARPENTER, G. 1984. Characterization of the metabolic turnover of epidermal growth factor receptor protein in A-431 cells. *J Cell Physiol,* 120**,** 296-302.
STUMPF, H. F. 1966. Mechanism by which cells estimate their location within the body. *Nature,* 212**,** 430-1.
SULLIVAN, A. L., GRASSO, J. A. & WEINTRAUB, L. R. 1976. Micropinocytosis of transferrin by developing red cells: an electron-microscopic study utilizing ferritin-conjugated transferrin and ferritin-conjugated antibodies to transferrin. *Blood,* 47**,** 133-43.
SUMMERBELL, D. 1979. The zone of polarizing activity: evidence for a role in normal chick limb morphogenesis. *J Embryol Exp Morphol,* 50**,** 217-33.
SUN, X., MEYERS, E. N., LEWANDOSKI, M. & MARTIN, G. R. 1999. Targeted disruption of Fgf8 causes failure of cell migration in the gastrulating mouse embryo. *Genes Dev,* 13**,** 1834-46.
SWANEY, K. F., HUANG, C. H. & DEVREOTES, P. N. 2010. Eukaryotic chemotaxis: a network of signaling pathways controls motility, directional sensing, and polarity. *Annu Rev Biophys,* 39**,** 265-89.
TABATA, T. & TAKEI, Y. 2004. Morphogens, their identification and regulation. *Development,* 131**,** 703-12.
TAKADA, S., STARK, K. L., SHEA, M. J., VASSILEVA, G., MCMAHON, J. A. & MCMAHON, A. P. 1994. Wnt-3a regulates somite and tailbud formation in the mouse embryo. *Genes Dev,* 8**,** 174-89.
TAO, L. & NICHOLSON, C. 2004. Maximum geometrical hindrance to diffusion in brain extracellular space surrounding uniformly spaced convex cells. *J Theor Biol,* 229**,** 59-68.
THORNE, R. G., LAKKARAJU, A., RODRIGUEZ-BOULAN, E. & NICHOLSON, C. 2008. In vivo diffusion of lactoferrin in brain extracellular space is regulated by interactions with heparan sulfate. *Proc Natl Acad Sci U S A,* 105**,** 8416-21.
THORNE, R. G. & NICHOLSON, C. 2006. In vivo diffusion analysis with quantum dots and dextrans predicts the width of brain extracellular space. *Proc Natl Acad Sci U S A,* 103**,** 5567-72.
TICKLE, C., SUMMERBELL, D. & WOLPERT, L. 1975. Positional signalling and specification of digits in chick limb morphogenesis. *Nature,* 254**,** 199-202.

TRUEB, B. & STEINBERG, F. 2011. A net-like structure with pores is observed during cell fusion induced by the receptor FGFRL1. *Commun Integr Biol,* 4**,** 287-90.
TSANG, M. & DAWID, I. B. 2004. Promotion and attenuation of FGF signaling through the Ras-MAPK pathway. *Sci STKE,* 2004**,** pe17.
TURNER, N. & GROSE, R. 2010. Fibroblast growth factor signalling: from development to cancer. *Nat Rev Cancer,* 10**,** 116-29.
ULLRICH, O., HORIUCHI, H., BUCCI, C. & ZERIAL, M. 1994. Membrane association of Rab5 mediated by GDP-dissociation inhibitor and accompanied by GDP/GTP exchange. *Nature,* 368**,** 157-60.
UMEDA, A., MEYERHOLZ, A. & UNGEWICKELL, E. 2000. Identification of the universal cofactor (auxilin 2) in clathrin coat dissociation. *Eur J Cell Biol,* 79**,** 336-42.
UNGEWICKELL, E., UNGEWICKELL, H., HOLSTEIN, S. E., LINDNER, R., PRASAD, K., BAROUCH, W., MARTIN, B., GREENE, L. E. & EISENBERG, E. 1995. Role of auxilin in uncoating clathrin-coated vesicles. *Nature,* 378**,** 632-5.
VAN DER ZEE, M., STOCKHAMMER, O., VON LEVETZOW, C., NUNES DA FONSECA, R. & ROTH, S. 2006. Sog/Chordin is required for ventral-to-dorsal Dpp/BMP transport and head formation in a short germ insect. *Proc Natl Acad Sci U S A,* 103**,** 16307-12.
VASIOUKHIN, V., BAUER, C., YIN, M. & FUCHS, E. 2000. Directed actin polymerization is the driving force for epithelial cell-cell adhesion. *Cell,* 100**,** 209-19.
VILA-CARRILES, W. H., ZHOU, Z. H., BUBIEN, J. K., FULLER, C. M. & BENOS, D. J. 2007. Participation of the chaperone Hsc70 in the trafficking and functional expression of ASIC2 in glioma cells. *J Biol Chem,* 282**,** 34381-91.
WANG, J. K., XU, H., LI, H. C. & GOLDFARB, M. 1996. Broadly expressed SNT-like proteins link FGF receptor stimulation to activators of Ras. *Oncogene,* 13**,** 721-9.
WARD, J. H., KUSHNER, J. P. & KAPLAN, J. 1982. Regulation of HeLa cell transferrin receptors. *J Biol Chem,* 257**,** 10317-23.
WARTLICK, O., KICHEVA, A. & GONZALEZ-GAITAN, M. 2009. Morphogen gradient formation. *Cold Spring Harb Perspect Biol,* 1**,** a001255.
WEAVER, C. & KIMELMAN, D. 2004. Move it or lose it: axis specification in Xenopus. *Development,* 131**,** 3491-9.
WELLS, J. M. & MELTON, D. A. 2000. Early mouse endoderm is patterned by soluble factors from adjacent germ layers. *Development,* 127**,** 1563-72.
WIDBERG, C. H., NEWELL, F. S., BACHMANN, A. W., RAMNORUTH, S. N., SPELTA, M. C., WHITEHEAD, J. P., HUTLEY, L. J. & PRINS, J. B. 2009. Fibroblast growth factor receptor 1 is a key regulator of early adipogenic events in human preadipocytes. *Am J Physiol Endocrinol Metab,* 296**,** E121-31.
WIEFFER, M., MARITZEN, T. & HAUCKE, V. 2009. SnapShot: endocytic trafficking. *Cell,* 137**,** 382 e1-3.
WILKIE, A. O. 2005. Bad bones, absent smell, selfish testes: the pleiotropic consequences of human FGF receptor mutations. *Cytokine Growth Factor Rev,* 16**,** 187-203.
WIXON, J. 2000. Featured organism: Danio rerio, the zebrafish. *Yeast,* 17**,** 225-31.
WOLF, C., GERLACH, N. & SCHUH, R. 2002. Drosophila tracheal system formation involves FGF-dependent cell extensions contacting bridge-cells. *EMBO Rep,* 3**,** 563-8.
WOLPERT, L. 1969. Positional information and the spatial pattern of cellular differentiation. *J Theor Biol,* 25**,** 1-47.
WOLPERT, L. 1971. Positional information and pattern formation. *Curr Top Dev Biol,* 6**,** 183-224.
WOLPERT, L. 2009. Diffusible gradients are out - an interview with Lewis Wolpert. Interviewed by Richardson, Michael K. *Int J Dev Biol,* 53**,** 659-62.
XU, X., LI, C., TAKAHASHI, K., SLAVKIN, H. C., SHUM, L. & DENG, C. X. 1999. Murine fibroblast growth factor receptor 1alpha isoforms mediate node regression and are essential for posterior mesoderm development. *Dev Biol,* 208**,** 293-306.
YAMAGUCHI, T. P., HARPAL, K., HENKEMEYER, M. & ROSSANT, J. 1994. fgfr-1 is required for embryonic growth and mesodermal patterning during mouse gastrulation. *Genes Dev,* 8**,** 3032-44.
YAMAMOTO, Y., TAKESHITA, H. & SAWA, H. 2011. Multiple Wnts redundantly control polarity orientation in Caenorhabditis elegans epithelial stem cells. *PLoS Genet,* 7**,** e1002308.
YAN, D. & LIN, X. 2009. Shaping morphogen gradients by proteoglycans. *Cold Spring Harb Perspect Biol,* 1**,** a002493.
YIM, Y. I., SUN, T., WU, L. G., RAIMONDI, A., DE CAMILLI, P., EISENBERG, E. & GREENE, L. E. 2010. Endocytosis and clathrin-uncoating defects at synapses of auxilin knockout mice. *Proc Natl Acad Sci U S A,* 107**,** 4412-7.

YU, S. R., BURKHARDT, M., NOWAK, M., RIES, J., PETRASEK, Z., SCHOLPP, S., SCHWILLE, P. & BRAND, M. 2009. Fgf8 morphogen gradient forms by a source-sink mechanism with freely diffusing molecules. *Nature,* 461**,** 533-6.

YUSTE, R. & BONHOEFFER, T. 2004. Genesis of dendritic spines: insights from ultrastructural and imaging studies. *Nat Rev Neurosci,* 5**,** 24-34.